

## ABSTRACT

Title of Document: DESIGN AND CONSTRUCTION OF LOW POWER, PORTABLE PHOTOCATALYTIC WATER TREATMENT UNIT USING LIGHT EMITTING DIODE

Mihir K. Chokshi, Master of Science, 2006

Directed By: Dr. A. P. Davis  
Department of Civil and Environmental  
Engineering

Limited availability of mobile technology to disinfect drinking water at low cost led to the current research of using titanium dioxide ( $\text{TiO}_2$ ) photocatalysis for drinking water disinfection. New UV light emitting diodes (LEDs) have potential for application in this technology. The research was divided into three parts: immobilization of  $\text{TiO}_2$ , optimization of coating and reactor using methyl orange and investigating disinfection efficiency for *Escheriachia coli* (ATCC 25922). Thin  $\text{TiO}_2$  films supplemented with Degussa P25, coated on glass beads and calcinated at  $500^\circ\text{C}$  had  $9.9\ \mu\text{m}$  maximum and  $2\ \mu\text{m}$  average thickness,  $0.28\ \text{m}^2/\text{g}$  BET surface area and was dominated by the anatase  $\text{TiO}_2$  phase. A reactor with LEDs degraded methyl orange with a first order rate constant of  $0.39\ \text{hr}^{-1}$  and  $3\ \log_{10}$  *E. coli* removal was noted in 240 mins. With anticipated drops in LED cost, use of LEDs for  $\text{TiO}_2$  photocatalysis remains a promising disinfection technology.

DESIGN AND CONSTRUCTION OF LOW POWER, PORTABLE  
PHOTOCATALYTIC WATER TREATMENT UNIT USING LIGHT EMITTING  
DIODE

By

Mihir K. Chokshi

Thesis submitted to the Faculty of the Graduate School of the  
University of Maryland, College Park, in partial fulfillment  
of the requirements for the degree of  
Master of Science  
2006

Advisory Committee:  
Dr. Allen P. Davis, Chair  
Dr. Eric A. Seagren  
Dr. Oliver J. Hao

## Acknowledgements

I would like to acknowledge Tate Incorporated for providing financial support to the research. I would like to express my sincerest and heartfelt thanks to Dr. Allen P. Davis whose intellectual advice, discussion, comments and support were a source of encouragement during the course of this project. I would like to specially thank Dr. David Martin Ayres for his assistance throughout this work. In spite of his busy schedule, he was always glad to provide his technical help and valuable comments. I would also like to thank Dr. Eric A. Seagren and Dr. Oliver J. Hao for serving on my advisory committee. I am grateful to all my friends, members of the laboratory, and the staff of Civil and Environmental Engineering Department for their administrative support. I would like to dedicate this thesis to my family for their everlasting support, without which I would have not been able to achieve my goals.

## TABLE OF CONTENTS

LIST OF FIGURES .....	v
LIST OF TABLES.....	ix
CHAPTER 1. INTRODUCTION .....	1
CHAPTER 2. BACKGROUND .....	5
2.1. Titanium Dioxide (TiO <sub>2</sub> ) Semiconductor Photocatalysis .....	5
2.2. PCO Mechanism for Target Pollutants .....	17
2.2.1. Formaldehyde Degradation.....	17
2.2.2. Methyl Orange Degradation .....	18
2.2.3. <i>E. coliform</i> ( <i>E. coli</i> ) Degradation.....	19
CHAPTER 3. MATERIALS AND METHODS .....	20
3.1. Materials .....	20
3.2. Analytical Techniques .....	21
3.3. Methods for Preparing TiO <sub>2</sub> Sol .....	23
3.4. TiO <sub>2</sub> Coating Methods .....	24
3.4.1. Suspension Method.....	24
3.4.2. Ceramic Funnel Method .....	25
3.4.3. Ceramic Funnel Method With Etching .....	26
3.5. TiO <sub>2</sub> Coating Analysis .....	27
3.5.1. Environmental Scanning Electron Microscope (ESEM) Analysis .....	27
3.5.2. BET Surface Area Analysis .....	27
3.5.3. X- Ray Diffraction Analysis .....	28
3.5.4. Coated TiO <sub>2</sub> Mass Calculations .....	28
3.6. Experiments Analyzing Photocatalytic Efficiency .....	29
3.6.1. Formaldehyde Photodegradation Using Vertically Oriented Prototype Reactor .....	31
3.6.2. <i>E. coli</i> Photodegradation in Prototype Reactor.....	31
3.6.3. Methyl Orange Photodegradation .....	33
3.6.3.1. Methyl Orange Photodegradation Using Prototype Reactor .....	36
3.6.3.2. Methyl Orange Photodegradation Using Portable Reactor.....	36
3.6.4. <i>E. coli</i> Photodegradation Using Portable Reactor.....	42
CHAPTER 4. RESULTS AND DISCUSSION.....	44
4.1. Coating Method .....	44
4.2. Coating Characterization .....	44
4.2.1. Environmental Scanning Electron Microscope (ESEM) Analysis .....	44
4.2.2. BET Surface Area Analysis .....	49
4.2.3. X- Ray Diffraction Analysis .....	50
4.2.4. Coated TiO <sub>2</sub> Mass Calculations .....	52
4.3. Experiments Analyzing Photocatalytic Efficiency .....	54

4.3.1. Formaldehy Photodegradation Using Vertically Oriented Prototype Reactor .....	54
4.3.2. <i>E. coli</i> Degradation Using Prototype Reactor.....	56
4.3.3. Methyl Orange Photodegradation Using Horizontally Oriented Prototype Reactor .....	62
4.3.4. Methyl Orange Photodegradation Using Portable Reactor.....	71
4.3.5. <i>E. coli</i> Photodegradation Using Portable Reactor.....	79
4.4. Comparison Between Prototype and Portable PCO Reactor .....	82
CHAPTER 5. CONCLUSIONS AND RECOMMENDATIONS .....	92
APPENDIX AND DATA TABLES .....	97
REFERENCES .....	107

## LIST OF FIGURES

Figure 2.1. Primary steps involved in semiconductor photocatalysis. Values in parenthesis are for TiO <sub>2</sub> vs normal hydrogen electrode (Hoffmann et al., 1995).....	7
Figure 2.2. XRD pattern for TiO <sub>2</sub> prepared by sol gel dip coating and titanium-isopropoxide as precursor (Kim et al., 2002) .....	12
Figure 2.3. Qualitative light intensity profile in packed bed reactor (Dijkstra et al., 2001) .....	13
Figure 2.4. UV LED customized with heat sink, proprietary reflector, transparent windows to optimize the output power from LED.....	16
Figure 3.1. Flow diagram for coating of titanium dioxide on glass beads.....	25
Figure 3.2. Experimental setup for Coating of beads using ceramic funnel method.....	26
Figure 3.3. Schematic diagram of vertical packed bed PCO reactor.....	32
Figure 3.4. Packed Bed Plug Flow Reactor (Prototype Reactor) illuminated with four 15W UV tubes.....	34
Figure 3.5. Top view of column and UV tubes configuration for Prototype PCO reactor.....	35
Figure 3.6. Schematic diagram of horizontal continuous packed bed plug flow PCO reactor.....	36
Figure 3.7. Partly constructed reactor mounted with LEDs, lenses and mounting units.....	39
Figure 3.8. Portable PCO reactor with PBR connected in series with a CMFR operated as recirculating reactor using UV LEDs as illumination source.....	40

Figure 3.9. Top close-up view of portable PCO reactor with UVLED 340 and UVLED 370 placed along the sides, top and bottom to illuminate the column.....	41
Figure 3.10. Schematic diagram of horizontal continuous portable recirculating PCO reactor.....	42
Figure 4.1. Uncoated glass bead serving as reference to other ESEM micrographs of coated glass beads.....	45
Figure 4.2. Comparison of single - coated unwashed and washed beads to analyze the effect of washing beads. TiO <sub>2</sub> coatings were prepared by <i>Method 1</i> .....	45
Figure 4.3. Comparison between glass beads coated with TiO <sub>2</sub> by <i>Method 1</i> with single coating and double coating for analysis of coating uniformity.....	46
Figure 4.4. Comparing micrographs of beads coated with TiO <sub>2</sub> by two different methods to check for the uniformity in coating.....	47
Figure 4.5. The effect of supplemental TiO <sub>2</sub> (Degussa P25) powder to sol gel preparation.....	48
Figure 4.6. ESEM micrograph of cross section of a glass bead coated with <i>Mixture C</i> and <i>Method 2</i> .....	48
Figure 4.7. XRD graphs for powder prepared from Degussa P25, <i>Mixture F</i> and <i>Mixture C</i> .....	51
Figure 4.8. Formaldehyde degradation curve using vertically oriented prototype reactor and glass beads coated by with <i>Mixture C</i> by <i>Method 1</i> . pH 5.0 ± 0.2, Ionic Strength 1.72 x 10 <sup>-2</sup> M NaClO <sub>4</sub> , DO saturated with O <sub>2</sub> , data evaluated using MS Excel.....	56

Figure 4.9. Linearized data for *E. coli* photocatalytic degradation with dark and light controls in horizontally oriented prototype reactor. pH = 6.0 ± 0.2, Ionic Strength = 1.7 x 10<sup>-2</sup> M NaClO<sub>4</sub>, DO saturated with O<sub>2</sub> and data evaluated using MS Excel.....60

Figure 4.10. Photocatalytic degradation of methyl orange in horizontally oriented prototype reactor indicating a pseudo first order degradation pattern. Points indicate experimental data while lines indicate concentration calculated from first order kinetic model. pH = 6.0 ± 0.2, Ionic Strength = 1.7 x 10<sup>-2</sup> M NaClO<sub>4</sub>, DO saturated with O<sub>2</sub>, Mixture D, E and F synthesized by supplementing P25 TiO<sub>2</sub> powder.....65

Figure 4.11. Linearized graph for methyl orange degradation in horizontally oriented prototype reactor to obtain pseudo first order rate constant value for each experiment. Mixture D, E and F contains supplemental 0.5 g TiONa, 0.25 g P25 and 0.5 g P25 TiO<sub>2</sub> powder, respectively. pH = 7.0 ± 0.2, Ionic Strength = 1.7 x 10<sup>-2</sup> M NaClO<sub>4</sub>, DO saturated with O<sub>2</sub> and data evaluated using MS Excel.....66

Figure 4.12. Methyl orange degradation graph to analyze the reproducibility of TiO<sub>2</sub> synthesis (*Mixture F*) and coating (*Method 3*) method. pH = 6.0 ± 0.2, Ionic Strength = 1.72 x 10<sup>-2</sup> M NaClO<sub>4</sub>, DO saturated with O<sub>2</sub>. Each experiment was performed using freshly prepared batch of glass bead coated with *Mixture F* by *Method 3*. The photocatalytic experiment data are represented by 3 separate experiments performed under identical conditions.....69

Figure 4.13. Linearized graph for pseudo first order methyl orange degradation. pH = 6.0 ± 0.2, Ionic Strength = 1.72 x 10<sup>-2</sup> M NaClO<sub>4</sub>, DO saturated with O<sub>2</sub> and data evaluated using MS Excel. All photocatalytic experimental data have been combined to provide a first order rate constant that would fit individual experimental data sets.....70

Figure 4.14. Methyl orange degradation curve to illustrate the effect of increase in number of LEDs. pH = 6.0 ± 0.2, Ionic Strength = 1.72 x 10<sup>-2</sup> M NaClO<sub>4</sub> and DO saturated with O<sub>2</sub>.....74

Figure 4.15. Linearized graph for methyl orange degradation indicating a faster degradation with increased number of LEDs. pH = 6.0 ± 0.2, Ionic Strength = 1.72 x 10<sup>-2</sup> M NaClO<sub>4</sub> and DO saturated with O<sub>2</sub> and data evaluated using MS Excel.....74

- Figure 4.16. Experimental data for PCO of methyl orange for indirect and direct recirculation with control experiments for direct recirculation. 10.8 hr and 12.4 hr readings for photocatalytic experiment under indirect recirculation are not considered for estimating the first order rate constant. pH =  $6.0 \pm 0.2$ , Ionic Strength =  $1.72 \times 10^{-2}$  M NaClO<sub>4</sub> and DO saturated with O<sub>2</sub>.....77
- Figure 4.17. Linearized graph for pseudo first order methyl orange photocatalytic degradation. For both operating configurations, each point indicates a separate experiment performed under identical conditions. 10.8 hr and 12.4 hr readings for photocatalytic experiment under indirect recirculation are not considered for estimating the first order rate constant. pH =  $6.0 \pm 0.2$ , Ionic Strength =  $1.72 \times 10^{-2}$  M NaClO<sub>4</sub> and DO saturated with O<sub>2</sub> and data evaluated with MS Excel.....78
- Figure 4.18. *E. coli* photocatalytic degradation in portable reactor operated as batch reactor using cuvettes to pack glass beads with dark and lighted controls. pH of  $7.0 \pm 0.2$ ,  $1.7 \times 10^{-2}$  M NaClO<sub>4</sub> ionic strength and saturated DO. The data for *E. coli* photocatalytic experiments were obtained from Table 4.5 and are represented by full symbols, while the hollow symbols represent *E. coli* photocatalysis experiment data in portable reactor.....81
- Figure 4.19. Comparison of two reactors with different light sources and power inputs. The HRT (min) on x- axis is for the data of prototype reactor while the illumination time (min x 10) is for the data from the portable reactor.....89
- Figure 4.20. First order rate constant for methyl orange degradation in portable reactor operated as indirect recirculation. The rate constant values for UV LED370 operating alone are presented in parenthesis in Table 4.14.....90

## LIST OF TABLES

Table 2.1. Factors to be considered during different stages of reactor design and configuration to maximize the efficiency of PCO reactor.....	7
Table 3.1. Characteristics of Light Emitting Diodes (Roithner laser, UV LED370 and Sensor Technology, UV LED340).....	38
Table 4.1. BET surface area of glass beads uncoated, coated with <i>Mixture C</i> and <i>Method 2</i> and coated with <i>Mixture F</i> and <i>Method 3</i> . All readings are single experimental values.....	49
Table 4.2. Analysis for calculating mass of TiO <sub>2</sub> coated on the surface of glass beads using <i>Method 3</i> and TiO <sub>2</sub> prepared using <i>Mixture F</i> . Cumulative mass of beads has been measured and average and standard deviation values are obtained.....	52
Table 4.3. Formaldehyde photodegradation using vertically oriented prototype reactor and glass beads coated with <i>Method 1</i> . The values for single column experiments with 0.23 ml/min flow rate have not been recorded due to failure in connections.....	55
Table 4.4. <i>E. coli</i> degradation for vertically oriented prototype PCO reactor and glass beads coated with <i>Mixture C</i> by <i>Method 1</i> . Samples were either duplicated or triplicated. pH = 7.0 ± 0.2, Ionic Strength = 1.72 x 10 <sup>-2</sup> M NaClO <sub>4</sub> , DO saturated with O <sub>2</sub> . The values in bold represent average values of <i>E. coli</i> concentrations. C/C <sub>0</sub> is calculated based on the average values of <i>E. coli</i> concentrations.....	57
Table 4.5. Experimental data for <i>E. coli</i> photocatalytic degradation with dark and light control in the horizontally oriented prototype reactor packed with glass beads coated with <i>Mixture F</i> by <i>Method 2</i> under pH of 7.0 ± 0.2, 1.7 x 10 <sup>-2</sup> M NaClO <sub>4</sub> ionic strength and saturated DO. The values in bold represent average values of <i>E. coli</i> concentrations. C/C <sub>0</sub> is calculated based on the average values of <i>E. coli</i> concentrations.....	59
Table 4.6. Photocatalytic degradation of methyl orange over glass beads coated with different sol mixtures and coating methods in horizontally oriented	

prototype reactor. pH =  $6.0 \pm 0.2$ , Ionic Strength =  $1.72 \times 10^{-2}$  M NaClO<sub>4</sub>, DO saturated with O<sub>2</sub>.....62

Table 4.7. Pseudo first order methyl orange degradation rate constant values for different photocatalytic experiments performed in horizontally oriented prototype reactor. pH =  $6.0 \pm 0.2$ , Ionic Strength =  $1.72 \times 10^{-2}$  M NaClO<sub>4</sub>, DO saturated with O<sub>2</sub>.....64

Table 4.8. Photocatalytic degradation of methyl orange under identical experimental conditions using TiO<sub>2</sub> prepared with *Mixture F* and beads coated by *Method 3*. pH =  $6.0 \pm 0.2$ , Ionic Strength =  $1.72 \times 10^{-2}$  M NaClO<sub>4</sub> and DO saturated with O<sub>2</sub>.....68

Table 4.9. Methyl orange degradation using portable reactor with indirect recirculation to illustrate the effect of light intensity. Glass beads coated with *Method 3* and TiO<sub>2</sub> prepared by *Mixture F*, pH =  $6.0 \pm 0.2$ , Ionic Strength =  $1.72 \times 10^{-2}$  M NaClO<sub>4</sub> and DO saturated with O<sub>2</sub>.....73

Table 4.10. Photocatalytic degradation of methyl orange under identical experimental conditions using TiO<sub>2</sub> prepared with *Mixture F* and beads coated by *Method 3* for portable reactor operated as (i) indirect recirculation and (ii) direct circulation. 12 UV LED340 (operated at 100 mA each) + 16 UV LED370 (operated at 25 mA each) were used as UV light source. The direct circulation data includes data of control experiments. pH =  $6.0 \pm 0.2$ , Ionic Strength =  $1.72 \times 10^{-2}$  M NaClO<sub>4</sub> and DO saturated with O<sub>2</sub>. Each data point represents separate experiment performed under identical conditions.....75

Table 4.11. Experimental data for *E. coli* photocatalytic degradation in portable reactor with dark and light control under pH of  $7.0 \pm 0.2$ ,  $1.7 \times 10^{-2}$  M NaClO<sub>4</sub> ionic strength and saturated DO. The values in bold represent average values of *E. coli* concentrations. C/C<sub>0</sub> is calculated based on the average values of *E. coli* concentrations. Natural decay of *E. coli* is obtained from measuring the influent sample before and after the experiment was conducted. The effect of natural decay is included in the readings for the *E. coli* experiments.....79

Table 4.12. Number of photons for each type of light source for calculating the efficiency of the reactors.....84

Table 4.13. Input and output efficiencies as a function of time for prototype and portable reactor.....	85
Table 4.14. Comparison of powers and rate constants for methyl orange experiments with different UV light sources.....	86
Table 4.15. Rate constants for methyl orange degradation for portable reactor under indirect recirculation with UV LEDs operated at different input powers. Values in parenthesis represent input powers and rate constants for UV LED370 only.....	90

# CHAPTER 1

## INTRODUCTION

A reliable source of water for drinking is a necessity for all humans. Municipal water supplies are part of the permanent infrastructure that supports day-to-day life and operations. Water supplies for military operations, however, must be mobile and cannot rely on complex fixed infrastructure. Additionally, natural water supplies may be subject to severe environmental contamination through both microbial pathogens and by the presence of organic and inorganic materials, including harmful chemicals. Thus, there is a need for mobile units to purify water to adequate quality for drinking.

Among the conventional physical and chemical methods for disinfecting water, chlorination has been used over the past century as a reliable, easy and relatively cheap method of treatment. Although its bacterial inactivation effects have been proven, a great concern is that chemical risks could be enhanced due to the by-products (trihalomethane compounds) formed during the disinfection processes. Certain types of bacteria, viruses and protozoa, e.g., *Cryptosporidium*, *Gardia Lamblia*, *Legionella*, *Mycobacterium* or *Yersinia* (Dunlope et al., 2002; Kim et al., 2002) cannot be efficiently removed or degraded from water using chlorination. Thus, there is a need to use an advanced oxidation process (AOP) to generate a reliable source of water keeping the cost of operation low. AOP techniques are becoming well established for destruction of unwanted chemicals or microorganisms. Of all the AOPs, semiconductor photocatalysis has been viewed as an effective means of producing highly effective oxidant.

Semiconductor photocatalysis has been applied to variety of problems related to environmental interests in addition to water and air purification.

Semiconductors like  $\text{TiO}_2$ ,  $\text{ZnO}$ ,  $\text{Fe}_2\text{O}_3$ ,  $\text{CdS}$  and  $\text{ZnS}$  (Hoffmann et al., 1995, Mills and Le Hunte, 1997) can act as sensitizers for light induced redox reactions due to their electronic formations, which are characterized by a filled electron valence band and an empty conduction band. However, of these semiconductors  $\text{TiO}_2$  has proven to be the most suitable for photocatalysis applications.  $\text{TiO}_2$  is photocatalytically active, biologically and chemically inert, does not undergo photocorrosion and chemical corrosion and it is inexpensive.

The present work focused on achieving the following goals:

1. Developing a method to prepare catalytically-active  $\text{TiO}_2$  and immobilize it on a support media. Immobilization of catalyst on the support media in a fixed bed will allow re-use of the catalyst, increase the exposure of catalyst to light and eliminate the need of filtering  $\text{TiO}_2$  for its reuse.
2. Design and construct a low power, portable and highly efficient photocatalytic oxidation reactor using  $\text{TiO}_2$  as catalyst and ultraviolet light emitting diodes (UV LED) as the source of photons. The designed reactor will be operated as a packed bed plug flow type photocatalytic oxidation (PCO) reactor. The reactor should be able to provide treated water (treatment period not to exceed 30 min) meeting with drinking water standards (*Escheriachia coli* concentrations less than 1 colony forming unit/100 ml of treated sample as per EPA water quality standards).

This research has been divided into two major phases to achieve the goals. This first is the preparation of TiO<sub>2</sub> sol and optimization of coating on the support media to allow reuse of catalyst. Glass beads were used as support media due to following reasons:

- It is chemically and biologically inert
- High transmission of light
- Easy availability
- Inexpensive

Since the sol gel method is a relatively easy method that produces consistent TiO<sub>2</sub> sol, it were employed in producing TiO<sub>2</sub>, which were further coated onto the glass beads by a thermal immobilization process. Thermal immobilization results in quick adhering of TiO<sub>2</sub> onto the support media along with the phase change from amorphous TiO<sub>2</sub> to crystalline anatase/rutile TiO<sub>2</sub>. The PCO reactor were packed with coated glass beads to maximize the exposure of the catalyst to light and pathogens in the flowing water, but still keep the catalyst immobilized, and thus, the catalyst can be reused.

In the reactor construction second phase, two reactors were constructed with different light sources. A prototype reactor of the actual PCO reactor was constructed and illuminated with four desktop 15 watt ultraviolet tubes. This reactor was used to optimize the TiO<sub>2</sub> preparation and coating methods, while the actual portable PCO reactor was illuminated with ultraviolet LEDs emitting a specific wavelength. The LEDs in the portable reactor were configured in such a way that the total operating power of reactor was near that of an automobile battery (12 volts). This configuration of LEDs resulted in a significant decrease in power consumption as compared to conventionally used light sources.

Formaldehyde and methyl orange experiments were performed in the prototype to evaluate the photocatalytic activity of TiO<sub>2</sub> prepared by a sol gel method and coated by a thermal immobilization process. Once the data for methyl orange were analyzed, photocatalytic degradation rate constants were evaluated using various degradation rate relationships. To evaluate the development of kinetic rates of photocatalysis in the prototype reactor, experimental runs were conducted for methyl orange and *E. coli* at varying illumination times. Based on the experimental results of the *E. coli* and methyl orange experiments for the prototype PCO reactor, similar experiments will be conducted for the portable PCO reactor using methyl orange as a test chemical. An empirical relationship between the rate constants for the prototype reactor and the portable reactor were computed for methyl orange degradation experiments. The rate constant relationship and the rate constant for *E. coli* degradation in prototype reactor were used to manipulate the time required for the project goal, a 3 log<sub>10</sub> removal of *E. coli* in the portable reactor with less than 30 min of treatment time and 3 to 4 liters of drinking water.

## **CHAPTER 2**

### **BACKGROUND**

The semiconductor driven photocatalysis process has been extensively studied over the last 25 years for the removal of pathogens (Blake et al., 1999, Maness et al., 1999, Dunlop et al., 2002, Cho et al., 2003, Ibanez et al., 2003, Sun et al., 2003), organic contaminants (Smith et al., 1975, Ohko et al., 1999, Sakthivel et al., 2002, Arana et al., 2004, Bao et al., 2004), and inorganic pollutants (Vohra and Davis, 2000) in water and air. Although various types of semiconducting materials are available for the photocatalysis process, only few of them are suitable for photocatalytic processes. For a semiconductor to successfully and be environmentally useful, it must be:

1. Photocatalytically active
2. Biologically and chemically inert
3. Inexpensive
4. Workable within the near visible light / UV light spectrum
5. Reusable

#### **2.1. TITANIUM DIOXIDE (TiO<sub>2</sub>) SEMICONDUCTOR PHOTOCATALYSIS**

TiO<sub>2</sub> has two crystalline forms, anatase and rutile, with band gap energies of 3.2 eV and 3.0 eV, respectively (Blake et al., 1999). TiO<sub>2</sub> in the anatase form appears to be the most photoactive and most practical of the semiconductors for widespread use in environmental applications such as water, wastewater, hazardous waste and air treatment (Mills et al., 1997). TiO<sub>2</sub> is non-toxic, insoluble under most conditions, inexpensive,

chemically inert and absorbs UV light. Although there are many different sources of TiO<sub>2</sub>, Degussa P25 has effectively become a research standard because it has:

1. A well defined nature (i.e., typically 70:30 mixture of anatase: rutile, BET surface area of about 50 m<sup>2</sup>/g, average particle size of 30 nm)
2. Substantially higher photocatalytic activity, than most other available samples (Mills et al., 1997)

Activation of a semiconductor (TiO<sub>2</sub>) occurs when a photon with energy (wavelength  $\lambda \leq 388$  nm for TiO<sub>2</sub>) strikes the semiconductor and is absorbed. The electrons from the valence band ( $e_{vb}^-$ ) are excited to the conduction band ( $e_{cb}^-$ ), leaving an electron vacancy (hole -  $h^+$ ) behind in the valence band (Figure 2.1). Electron ( $e^-$ ) - hole ( $h^+$ ) pairs so formed can interact in 3 different ways (Halmann 1996, Hoffmann et al., 1996, Huang et al., 2000, Mills et al., 1997, Oppenlander 2002);

1. Recombine and dissipate the input energy as heat (Eq. 2.1)
2. Get trapped in metastable surface states
3. Migrate to the semiconductor surface and cause oxidation/reduction reactions by charge transfer to species adsorbed onto the semiconductor

In the absence of suitable  $e^-$  and  $h^+$  scavengers, the energy stored is dissipated within a few nanoseconds by recombination (Hoffmann et al., 1995, Linsebigler et al., 1995, Mills et al., 1997). If a suitable scavenger or surface site is available to trap the electron or hole, recombination is prevented and a subsequent redox reaction takes place.

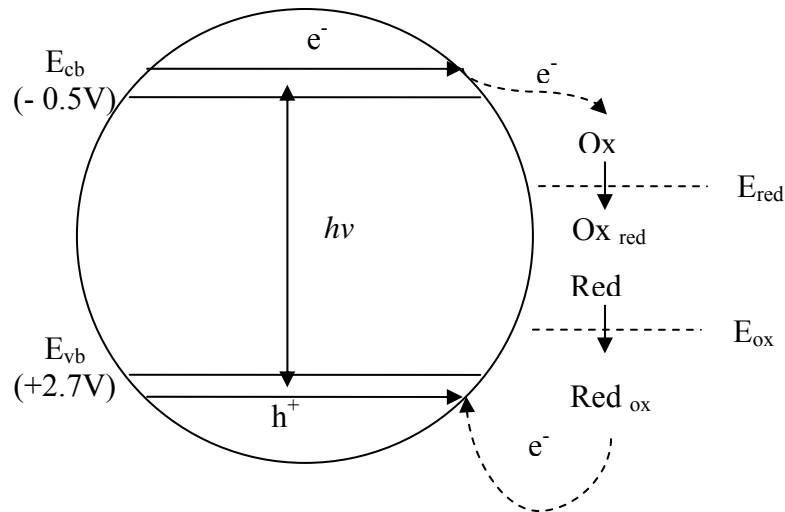
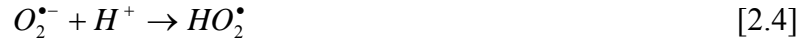
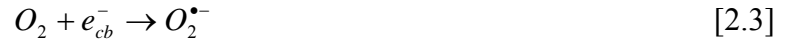


**Figure 2.1. Primary steps involved in semiconductor photocatalysis. Values in parenthesis are for TiO<sub>2</sub> vs normal hydrogen electrode (Hoffmann et al., 1995)**

The negatively charged electrons require an acceptor species to be present such that they can be scavenged and, thus, prevented from participating in deleterious  $e^- \cdot h^+$  recombination processes (Eq 2.2). Molecular oxygen (Eq 2.3) functions as an electron scavenger and thus generates superoxide ions ( $O_2^{\bullet -}$ ). The superoxide (Eq 2.4 to 2.6) can further produce hydrogen peroxide at the TiO<sub>2</sub> water interface. Hydrogen peroxide (Eq 2.7 & 2.9) in turn generates the hydroxyl radical ( $OH^{\bullet}$ ). Valence band holes (Eq 2.9) react with the surface adsorbed  $OH^-$  ions, producing  $OH^{\bullet}$ . The  $OH^{\bullet}$  radicals, being electron deficient, are very powerful oxidants and thus oxidize the organic substrate, resulting in intermediate compound formation and eventually resulting in CO<sub>2</sub> and H<sub>2</sub>O formation (Wei et al., 1994; Hoffmann et al., 1995; Lisenbigler et al., 1995; Halmann, 1996; Sunada et al., 1998; Cho et al., 2003; Sun et al., 2003).





The kinetics of photodegradation of organic pollutants sensitized by TiO<sub>2</sub>, on steady state illumination fit a Langmuir-Hinshelwood kinetic scheme (Eq 2.10) (Mills and Le Hunte 1997; Nam et al., 2002) with the rate given by:

$$\frac{dC}{dt} = -\frac{k_1 k_2 C}{1 + k_2 C} \quad [2.10]$$

where,  $k_1$  is a rate constant (mg/L-hr),  $k_2$  is a second rate constant (L/mg) and  $t$  is the illumination period (hr)

The lower limit for L-H kinetics (i.e.,  $k_2 C \ll 1$ ) corresponds to pseudo first order kinetics (Eq 2.11) while the upper limit for L-H kinetics (i.e.,  $k_2 C \gg 1$ ) corresponds to a pseudo zero order kinetic expression (Eq 2.12).

$$\frac{dC}{dt} = -k_1 \quad [2.11]$$

$$\frac{dC}{dt} = -k_1 k_2 C \quad [2.12]$$

Work done by numerous authors has attempted to understand various factors that would govern successful design and operation of a PCO reactor. Factors governing efficiency of PCO reactor are listed in Table 2.1.

**Table 2.1. Factors to be considered during different stages of reactor design and configuration to maximize the efficiency of PCO reactor**

<b>Parameter / Method</b>	<b>Importance</b>
TiO <sub>2</sub> sol preparation method	Ease of coating on support media
Support media	Adhesion, ease of coating, cost of support media, surface characteristics
Coating method	Adhesion, thickness and uniformity of TiO <sub>2</sub> coating
Calcination temperature	Crystallinity of structure and form of TiO <sub>2</sub> (anatase or rutile)
Reactor design (LED wavelength and orientation, packed bed column orientation, type of column used and size of column)	Efficiency of PCO
Experimental parameters (dissolved oxygen, pH, temperature, light intensity, initial concentration of pollutant)	Reactor optimization
Type of pollutant (pathogen, organic, inorganic chemical)	PCO efficiency changes depending on type of pollutant

Demessie et al. (1999), Ban et al. (2003) and Addamo et al. (2004) discussed different methods of preparing and coating TiO<sub>2</sub> onto support media and concluded that different methods result in differences in morphology, crystal phase, particle aggregate size and activity of the TiO<sub>2</sub> catalyst.

Leonard et al. (1999) coated TiO<sub>2</sub> powder onto 3 different support materials (glass beads, zeolite and activated charcoal) by a sonication process. With repeated use of catalyst, the change in zero order rate constant of isopropanol for the glass beads (12.0 to 12.1 mg/ l-min) was negligible as compared to that of zeolite (14.1 to 12.7 mg/ l –min) and activated charcoal (19.4 to 12.1 mg/l –min), demonstrating higher stability of coated TiO<sub>2</sub> to adhere on the surface of glass beads. The zero order rate constant values ( $k_{\text{activated charcoal}} > k_{\text{zeolite}} > k_{\text{glass beads}}$ ) for the first trial only, proves that increasing surface area of catalyst increases photocatalytic activity. A similar study done by Sakthivel et al. (2002) compared two support media (glass beads – GB, and aluminum beads - AB). The results showed that the maximum number of dye (acid brown 14) molecules adsorbed per gram of TiO<sub>2</sub>-AB ( $1.124 \times 10^{-4}$ ) was five times higher than that adsorbed per gram of TiO<sub>2</sub>-GB ( $0.207 \times 10^{-4}$ ). This indicates that the support media plays an important role by allowing the adsorbent (chemical or pathogen) to adsorb on the surface. This creates a high concentration environment around the catalyst and hence increases the degradation rate.

Guillard et al. (2002) proved that adhesion of TiO<sub>2</sub> coating onto a support media was better for sol gel coating as compared to P25 TiO<sub>2</sub> coating. Films of titanium dioxide were produced on silicon wafers, on soda lime glass and on Pyrex glass plates using different sol gel methods. The P25 TiO<sub>2</sub> coatings were easily detached upon wiping with paper and were pulled off in a single Scotch tape test, while the sol gel coatings were not damaged when wiped with several types of paper, either wet or dry or with a solvent. Films could not be removed even after 10 successive Scotch tape tests and were abraded with difficulty by fingernail.

Kim et al. (2002), Ahn et al. (2003), Hamid et al. (2003) and Lee et al. (2003) reported that varying the temperature during calcination of TiO<sub>2</sub> could change the morphology of TiO<sub>2</sub>. They found that calcination temperature between 400 °C and 600 °C would yield the anatase form of TiO<sub>2</sub>. The UV – VIS spectra of calcined TiO<sub>2</sub> thin films over a wavelength range of 300 – 1000 nm, at two catalyst concentrations of 1 M and 3 M, showed that TiO<sub>2</sub> thin films prepared at 400 °C and 600 °C had maximum transparency (60 % to 80 % for 350 – 400 nm range). X- Ray Diffraction (XRD) patterns also showed that the TiO<sub>2</sub> material calcined at 300 °C was amorphous, while TiO<sub>2</sub> calcined at 400 °C and 600 °C were mainly nano–crystalline anatase types. An increase in intensities of anatase peaks was noted as the temperature was increased from 400 °C to 600 °C, implying an improvement in crystallinity. Increasing the temperature above 800 °C would result in phase change from the anatase to the rutile form. The XRD analysis done by various authors (Burnside et al., 1998; Demessie et al., 1999; Kim et al., 2002; Hamid and Rehman, 2003; Lee et al., 2003; Ryu et al., 2003; Addamo et al., 2004; Lee et al., 2004) indicated peak anatase formation for temperatures above 400 °C, while for 300 °C; no anatase peaks were observed (Figure 2.2). For temperatures above 800 °C, rutile peaks started showing in the XRD, which indicates the start of phase change around 900 °C. Thus it can be said that for calcination, temperatures of 400 °C to 600 °C should provide adequate ratio of anatase/rutile.

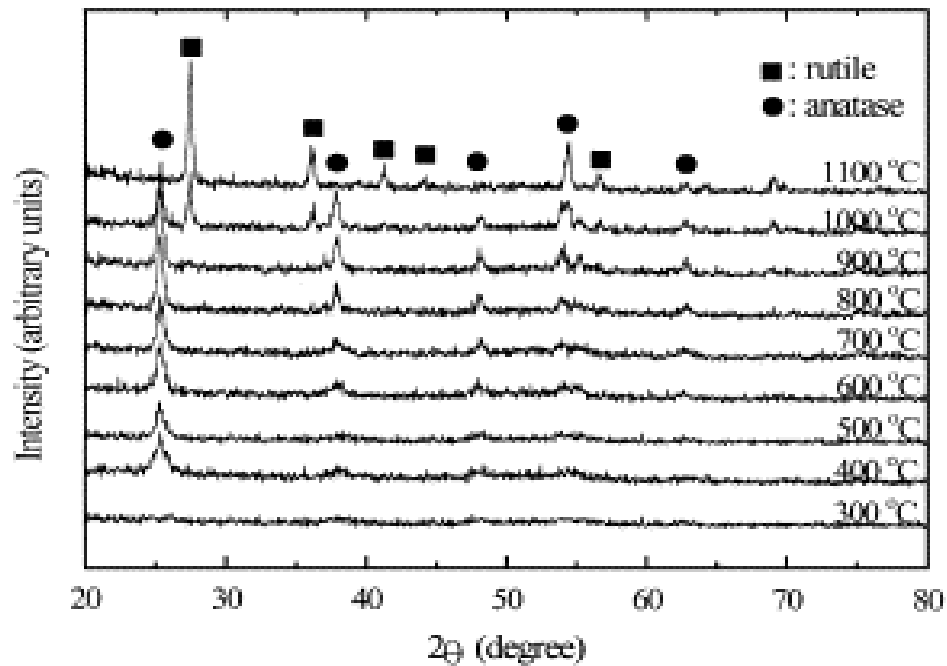


**Figure 2.2. XRD pattern for TiO<sub>2</sub> prepared by sol gel dip coating and titanium-isopropoxide as precursor (Kim et al., 2002)**

Guillard et al. (2002) examined the effects of TiO<sub>2</sub> film thickness coated on glass support media by different sol gel methods and found that photocatalytic degradation of malic acid was faster with the increase in thickness of coating, with the maximum occurring at 2 μm. Similar results were also obtained by Lee et al. (2004), where they found that the sterilization ratio  $(1 - C/C_0)$  for *G. lamblia* increased linearly up to 5 layers (200 nm per coating) of coating and there after decreased. Thus there is a linear relationship between photocatalytic activity and the thickness of coatings. The increase in thickness of coating resulting in increased photocatalytic activity could be simply attributed to the increase in the number of active sites and in the amount of photons adsorbed by TiO<sub>2</sub>, while the decrease in photocatalytic activity with increase in thickness of coating after a threshold value can be attributed to decrease in transparency of the film. Though different methods of TiO<sub>2</sub> preparation may lead to different threshold values for

the maximum thickness of coating, the thickness of coating should be enough to enhance the photodegradation capability.

Dijkstra et al. (2001) proved that in a packed bed reactor (2 mm and 1.3 mm diameter glass beads packed), the Reynolds number had no influence on the degradation rate of formic acid. Their results indicate that there would be no mass transfer limitations occurring in a packed bed reactor. From the qualitative analysis provided by Dijkstra et al. (2001), the beads situated farther away from the lamp will be irradiated with lower light intensity, therefore resulting in lower activity (Figure 2.3).

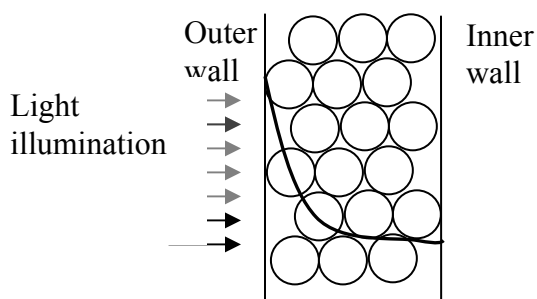


**Figure 2.3. Qualitative light intensity profile in packed bed reactor (Dijkstra et al., 2001)**

Cho et al. (2003) studied how the  $\text{OH}^\bullet$  radical, acting either independently or in collaboration with other reactive oxygen species (ROS), is related to the inactivation of *E. coli*. For experiments with air sparging plus an  $\text{OH}^\bullet$  radical scavenger (30 mM methanol) and  $\text{O}_2$  sparging plus  $\text{OH}^\bullet$  radical scavenger, 0.5 log inactivation was achieved for 90 min illumination in both the cases. The 0.5 log inactivation was due to the presence of ROS; in the presence of  $\text{OH}^\bullet$  radical scavenger, other ROS such as  $\text{O}_2^{\bullet-}$  or  $\text{H}_2\text{O}_2$  could be formed. Considerable PCO inactivation of *E. coli* occurred in the presence of oxygen (approx. 1.0 log for air sparging and 2.5 log for  $\text{O}_2$  sparging for 90 min

illumination), while in the absence of O<sub>2</sub>, no *E. coli* inactivation was achieved. These results can be used to explain that OH• are main the photooxidant for *E. coli* inactivation. Thus, more available dissolved oxygen molecules scavenge more conduction band electrons, reducing the chances of recombination reaction. The delayed Chick-Watson model [Eq 2-13] was applied to determine the concentration of OH• radical for *E. coli* inactivation. The results demonstrated a linear relationship between OH• radicals generated and *E. coli* inactivation, with 0.8 x 10<sup>-5</sup> mg-min/l OH• radical production required for a 2 log *E. coli* inactivation.

$$\log \frac{N}{N_0} = \begin{cases} 0 & \text{if } CT \leq CT_{lag} = \frac{1}{k} \log \left( \frac{N}{N_0} \right) \\ -k(CT - CT_{lag}) & \text{if } CT \geq CT_{lag} = \frac{1}{k} \log \left( \frac{N}{N_0} \right) \end{cases} \quad [2.13]$$

where, N<sub>0</sub> is the initial *E. coli* population (CFU/ml), N is the remaining *E. coli* population at time t (CFU/ml), C is the OH• concentration (mg/l), k is the inactivation rate constant with ozone (l-mg<sup>-1</sup>min<sup>-1</sup>), and T is the inactivation time (min).

Kuhn et al. (2003) found the inactivation efficiencies decreased in the order: *E. coli* > *Pseudomonas aeruginosa* > *Staphylococcus aureus* > *Enterococcus faecium* > *Candida albicans* for photocatalytic oxidation using TiO<sub>2</sub>. Since the complexity and density of the cell wall increases in the same order of precedence: *E. coli* and *P. aeruginosa* having thin and slack cell walls (gram negative), *S. aureus* and *E. faecium* having thicker and denser cell walls (gram positive), and *C. albicans* having a thick eukaryotic cell wall, the primary step in inactivation of pathogens should consists of an

attack by ROS on the cell wall, leading to puncture or inactivation. Thus the type of microorganism will greatly affect the inactivation efficiency of photocatalysis.

Sun et al. (2003) examined the effects of initial dissolved oxygen (DO) on photocatalysis, and reported that an increase in DO results in increased photocatalytic degradation rates for *E. coli*, but this phenomenon was limited to a maximum DO level of 25.25 mg/l. This limit was attributed to the fact that the TiO<sub>2</sub> semiconductor surface may become highly hydroxylated to the extent of inhibiting the adsorption of *E. coli* mass cells at the active sites for initiating or participating in the PCO oxidation reactions in presence of excess DO.

Wei et al. (1994), Dunlop et al. (2002) and Sun et al. (2003) studied the effects of initial *E. coli* concentration on the photocatalysis degradation rate (pseudo first order). Results indicated that the removal rate increases with increase in *E. coli* influent concentration. This may be due to the increase of relative adsorption availability on the TiO<sub>2</sub> surface as the probability for surface interaction would increase at high concentration.

Wei et al. (1994), Dunlop et al. (2002) and Cho et al. (2004) investigated the effects of light intensity on *E. coli* inactivation and found that the inactivation rate increases with increase in light intensity. Wei et al. (1994) found that the rate of cell kill increased proportionally with increase in light intensity, while Cho et al. (2004) found that *E. coli* inactivation rate increases with increase in light intensity, it does not increase proportionally, i.e., *E. coli* inactivation with four lamps ( $6 \times 10^{-5}$  Einstein/L-sec) was only two times more efficient than that with one lamp ( $1.5 \times 10^{-5}$  Einstein/L-sec). Thus the

proportionality would depend on the type of reactor, type and loading of  $\text{TiO}_2$ , operating conditions, etc.

With the recent development in the field of laser technology, there is a great potential for UV LEDs to become a viable source of UV light for photocatalysis. UV LEDs are small in size, long lasting and highly efficient. Their wavelength spectra are narrow and can be designed for any required peak wavelength. A UV LED is a diode, which emits UV light by combining holes and electrons on the interface of two semiconductor materials (Chen et al. 2005). The aluminum gallium nitride (AlGaN) or gallium nitride (GaN) LED chip is encapsulated in a metal glass package with UV transparent optical window (Figure 2.4).



**Figure 2.4. UV LED customized with heat sink, proprietary reflector, transparent windows to optimize the output power from LED (Sensor Electronics)**

Chen et al. (2005) explored the feasibility of using UV LED as a light source for photocatalysis of perchloroethylene (PCE) in a rectangular stainless steel gas phase reactor. They reported a 43% degradation of PCE in 64 seconds with 375 nm peak wavelength UV LEDs (Nishia, 16 LEDs with 1 mW output power) operated as a very

low (UV light output/catalyst coating area) ratio of only  $49 \mu\text{W}/\text{cm}^2$  and Degussa P25 loading of  $0.69 \text{ mg}/\text{cm}^2$ .

In short, it is possible to adopt  $\text{TiO}_2$  - sensitized photocatalysis under UV irradiation as an economical and effective disinfection technology for drinking water. Immobilizing  $\text{TiO}_2$  onto an inert support material like glass beads and packing them in a column would eliminate the need for filtration to remove the catalyst. Because UV LEDs can be operated on DC power supply and have shown to degrade PCE in air (Chen et al. 2003), the use of UV LEDs as light source for the treatment of water samples containing microorganisms can be applied.

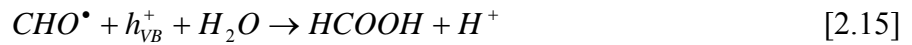
## **2.2. PCO MECHANISM FOR TARGET POLLUTANTS**

Though there is a long list of microorganisms and organic and inorganic compounds that can be removed or inactivated by photocatalysis, this work concentrated on using formaldehyde for initial study to examine photocatalytic activity of  $\text{TiO}_2$  prepared and coated on glass beads. Methyl orange (MO) was further used to optimize the reactor design and configuration to achieve maximum photocatalytic degradation rate. Finally *E. coli* was used to prove that the constructed and optimized reactor can disinfect water to the required quality for drinking.

### ***2.2.1. Formaldehyde Degradation***

Formaldehyde is fairly soluble (55% - US Environmental Protection Agency - USEPA) in water and was used as an indicator of the photocatalytic activity of  $\text{TiO}_2$  prepared by sol gel methods and coated by thermal immobilization processes. Arana et al.

(2004) reported that formaldehyde can be degraded via photocatalysis as a zero order reaction, while Christoskova et al. (2002) reported that catalytic oxidation of formaldehyde proceeds according to a pseudo first order kinetics. The degradation of formaldehyde (Eq. 2.14 to 2.17) in presence of O<sub>2</sub> was also known to proceed via radical chain reactions on the surface of coated TiO<sub>2</sub> with formic acid being an intermediate product (Ohko et al. 1998; Arana et al., 2004).



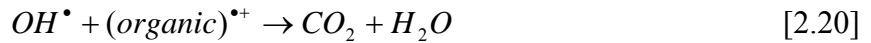
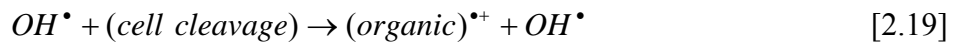
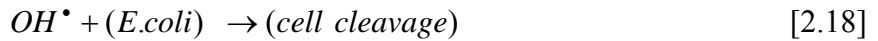
### **2.2.2. Methyl Orange Degradation**

Methyl orange is one of the most important classes of commercial dyes. It is stable to visible and near UV light and provides a useful probe for photocatalytic reactions (Brown et al., 1984; Nam et al., 2002; Bao et al., 2004). Because methyl orange turns yellow in an alkaline solution and red in acidic solution, it is easy to monitor and analyze by spectrophotometry. The mineralization, decolorization and decomposition of methyl orange over TiO<sub>2</sub> have been well studied, showing a pseudo first order degradation pattern (Bao et al., 2004)

### 2.2.3. *E. coliform* (*E. coli*) Degradation

The drinking water treatment industry uses a system of surrogate bacterial indicators in order to assess the efficiency of the disinfection process. *E. coliforms* has been the most studied microorganism. If this organism is not detected in the treated water, the water is regarded as free from fecal contamination (Dunlop et al., 2002). The USEPA has regulated that the *E. coli* concentration in drinking water should be less than 1 colony forming unit (CFU)/100 ml (USEPA). Numerous experiments have been performed with *E. coli* and photocatalysis, and thus been proven that *E. coli* inactivation is pseudo –first order (Kuhn et al., 2003; Sun et al., 2003; Dunlop et al., 2004)

It is believed that hydroxyl radicals are responsible for creating cleavages in *E. coli* and further for conversion of cleaved *E. coli* cells to dissolved organic radicals, which further undergo a chain of reactions to ultimately produce carbon dioxide (CO<sub>2</sub>) and water (H<sub>2</sub>O) (Wei et al., 1994; Lisenbigler et al., 1995; Halmann, 1996; Huang et al., 2000; Cho et al., 2003; Sun et al., 2003):



## CHAPTER 3

### MATERIALS AND METHODS

#### 3.1. MATERIALS

Titanium isopropoxide (TIP) (Fisher Scientific) was selected as precursor for hydrolysis of TiO<sub>2</sub> as it has been widely used for producing TiO<sub>2</sub> sol-gel with simple laboratory methods (Demessie et al., 1999; Kim et al., 2002; Lee et al., 2002; Ryu et al., 2003; Lee et al., 2004). Degussa AG P-25 titanium dioxide (99.5 +%, non porous, 50 m<sup>2</sup>/g, anatase/ rutile mix), isopropanol (Fisher Scientific), 1N HCl (Fisher Scientific) and deionized (DI) water (Hydro service reverse osmosis/ ion exchange apparatus Model LPRO – 20) were used along with TIP for formation of TiO<sub>2</sub> sol and the sol was then coated on glass beads (1.0 to 1.2 mm average diameter, soda-lime silica glass, Potters Industries Inc). The coated TiO<sub>2</sub> was calcined in a furnace (Fisher Scientific, Isotemp programmable muffler furnace) with a ramp heating of 5°C/min till the temperature reached 500°C, and was held at 500°C for 3 h. Adjustment in pH during the photocatalytic oxidation studies were made drop wise with 0.1 N NaOH. Formaldehyde (Fisher Scientific), methanol (Fisher Scientific) and *E. coli* (*Escherichia coli* (Migula) Castellani and Chalmers, ATCC 25922, FDA strain Seattle 1946, gram negative bacterium) have been used as influent pollutants to measure the photocatalytic activity. Whenever buffering of solution was required, it was done using a 0.1 M phosphate buffer.

The prototype reactor was built using 4 XX-15A UV tubes (Spectrolite, 365 nm peak wavelength with 1100 μW/cm<sup>2</sup> output at 25 cm for two tubes) with two tubes on

each side housed in rugged anodized aluminum with specular aluminum reflectors to ensure maximum UV irradiation. A cardboard box was used to support the reactor and two metal stands used to hold the square quartz column (1 cm x 1 cm x 30 cm, Vitrocom, Inc.) filled with glass beads. A peristaltic pump (Cole Parmer) with solid state speed controller (Masterflex) and tubing (1/16" and 1/32" diameter Viton tubing) is used to control the flow rate through the reactor.

For the construction of portable reactor, a solid base plate (Aluminum breadboard, Thorlabs), several mounting bases (BA1S, Thorlabs), post holders (PH1 and PH1, Thorlabs), posts (TR20/M, TR50/M and TR100/M, Thorlabs), pedestal pillar posts (RS12/M, RS25/M and RS50/M, Thorlabs) small V – clamps (VC1, Thorlabs), clamping forks (CF series, Thorlabs), UV LEDs (Roithner laser, 370 nm peak wavelength, 1 mW output LED and Sensor electronics, 340 nm peak wavelength, 0.5 mW output LEDs), laser mounts (SM1 series, Thorlabs), lens (BK7 with 25 mm focal point, Edmund optics), lens tubes (SM series, Thorlabs) and wires for LED power connections were employed. LEDs were mounted directly either on a circuit board or mounted on laser mounts and then fixed on the circuit board. Other components like the quartz column, peristaltic pump, speed controller, viton tubing were the same as above.

### **3.2. ANALYTICAL TECHNIQUES**

For formaldehyde measurement and calibration, fresh Nash reagent (Smith et al., 1975, Vohra et al., 2000) was prepared containing 15.0 g ammonium acetate ( $\text{NH}_4\text{OAc}$ ) and 0.2 ml acetyl acetone ( $\text{C}_5\text{H}_8\text{O}_2$ ) in DI water to make 50 ml volume. Formaldehyde standard solutions of known concentrations from 10 to 300  $\mu\text{M}$  were prepared and 5 ml

of this solution was mixed with 2 ml of Nash reagent, which was then incubated at 60°C for 30 mins. Absorbance was measured with a Baush and Lomb Spectronic 21 MV Spectrophotometer at 415 nm. Formaldehyde concentrations varying from 10 – 300 µM were used for obtaining a calibration curve. The same method was used for measurement of formaldehyde concentrations in influent and effluent samples (Smith et al., 1975; Vohra et al., 2000). Analysis was done after collecting 10 ml of the sample. The samples are filtered using 0.2 µm filters (Pall Corporation) and refrigerated in dark bottles in order to avoid any further degradation, with the storage period not exceeding 6 hr.

Methyl orange (VWR Scientific) concentration curves were obtained by measuring the absorbance of methyl orange stock solutions with concentration 5 – 50 mg/L at pH 6 and  $1.7 \times 10^{-2}$  M NaClO<sub>4</sub>. Absorbance of methyl orange stock solution was measured with a Baush and Lomb Spectronic 21 MV Spectrophotometer at 510 nm wavelength (Brown et.al., 1984). The calibration chart was used to calculate the influent and effluent concentrations of methyl orange for various experiments performed.

For *E. coli* measurements in influent and effluent water, freeze dried *E. coli* cultures were grown aerobically in BD Broth (Difco) at pH 7.0 and 35 °C for 48 hr and refrigerated for further use, with stock cultures transferred at a regular interval. Nutrient broth was autoclaved at 121 °C for 15 min before use at pH of 7.0 and ionic strength of  $1.7 \times 10^{-2}$  M NaClO<sub>4</sub>. Serial dilutions were carried out in 9 ml tubes containing DI water at pH 7 and  $1.7 \times 10^{-2}$  M NaClO<sub>4</sub> to achieve *E. coli* concentration of  $10^4$  -  $10^6$  CFU/ 100 ml. The initial and final samples were plated onto BD agar (Difco), strictly following the Standard Plate Count (SPC) method (Eaton et al., 1995). When the samples were treated for higher HRTs (>30 min), the Membrane Filtration Method (MFM) (Eaton et al., 1995)

was used to measure *E. coli* counts. For this method, 10 ml samples were collected and passed through a 0.45  $\mu\text{M}$  filter (Pall Corporation). The filter was placed over adsorbent pad (Pal Corporation) with nutrient agar. The plates were incubated at 35 °C for 48 hr and colony forming units (CFUs) were visually identified using a colony counter and reported as average CFUs/100 ml. All samples were duplicated/ triplicated except for MFM. All apparatus was sterilized at 121°C for 15 min, or were washed with at least 20% bleach for 10 mins to provide rapid decontamination.

### **3.3. METHODS FOR PREPARING TiO<sub>2</sub> SOL**

TiO<sub>2</sub> was synthesized using sol gel method, with titanium (IV) isopropoxide as its precursor. TiO<sub>2</sub> sol was prepared by adding 25 ml of isopropanol to a 50 ml beaker containing 3.6 ml of TIP. This mixture was stirred vigorously for 10 min using a magnetic stirrer. Subsequently, 7.3 ml of 1 N HCl was added after adding 0.9 ml of DI water and the mixture was rigorously stirred for 2 hr with the flask sealed with Parafilm to avoid any loss of isopropanol and/or water by evaporation during mixing (Dagan and Tomkiewics, 1993; Demessie et al., 1999; Kim et al., 2002; Hamid and Rehman, 2003). This mixture has a molar ratio of TIP: isopropanol: H<sub>2</sub>O: HCl of 1:27:5:20 (designated as mixture C). Similarly other sols with molar ratios 1:27:5:10 and 1:27:5:15 (designated as A and B, respectively) were prepared. The sols produced with molar ratios A and B were thick and highly viscous. The glass beads coated by using these molar ratios were not coated evenly and indicated flakes of coating. Sol produced from molar ratio C was less viscous and produced a transparent TiO<sub>2</sub> coating surface. Furthermore three additional sols were produced with molar ratios 1:27:5:20, but with an addition of 0.25 g of TiONa

(Millennium Inorganic Chemicals formally known as SCM Chemicals), 0.25 g and 0.5 g of TiO<sub>2</sub> (Degussa, P25) and designated as mixtures D, E and F, respectively. The additional TiO<sub>2</sub> powder that was added to sols was assumed to help in increasing the photocatalytic activity by increasing catalyst loading and surface area.

Glass beads are thoroughly washed with 0.1 N HCl prior to coating to etch the surface of glass beads, so that when the sol dries, titanium dioxide attaches well on the surface. By thoroughly washing beads with acid, impurities on the surface are removed which would hinder the binding of titanium dioxide (Sakthivel et al., 2002). After washing, the glass beads are dried completely before suspending them in sol to avoid change in the molar ratio of TIP: Water. The glass beads are coated via different methods and SEM micrographs are taken in order to compare the coating patterns.

### **3.4. TiO<sub>2</sub> COATING METHODS**

#### ***3.4.1. Suspension Method***

In this method the ratio of the mass of beads (grams) to the volume of sol (milliliter) was kept constant at 2; so as to completely submerge the glass beads in sol (Kim et al., 2002; Sakthivel et al., 2002; Lee et al., 2004). Figure 3.1 describes the entire process of coating TiO<sub>2</sub> onto the glass beads. After initial preparation of sol and mixing it for 2 hrs and preparation of glass beads, the required amount of sol and glass beads are mixed in a beaker in such a way that the beads are submerged in sol. The mixture was then allowed to dry for 24 hr to produce an amorphous TiO<sub>2</sub> thin film on the glass substrate, which was then converted to a microcrystalline TiO<sub>2</sub> after heating in air at 500°C for 3 hours. After heating the beads are allowed to cool to room temperature and

then washed thoroughly with deionized water. The beads can now be either used for experiments if uniformly coated or another coat may be applied. Samples are obtained from single and double coats to check the uniformity of coating achieved.

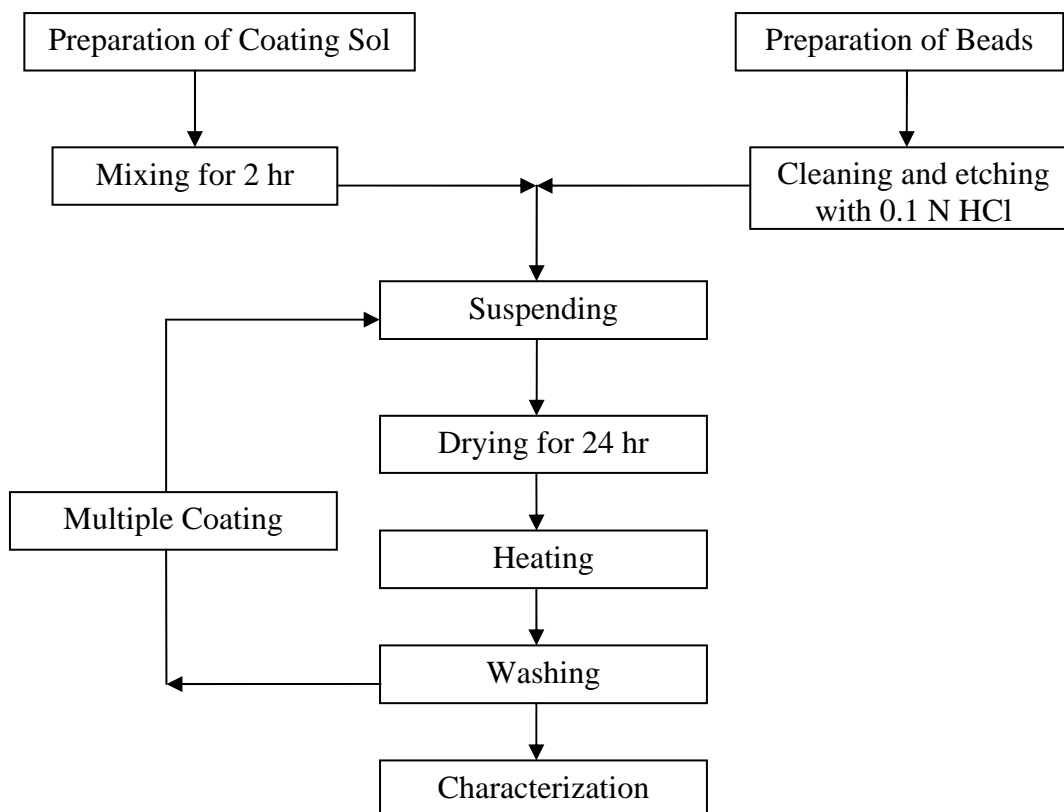


**Figure 3.1. Flow diagram for coating of titanium dioxide on glass beads**

### 3.4.2. Ceramic Funnel Method

Characterization indicated that at least two coats are required to completely cover the surface of glass beads using *Method 1*. Also, since this method takes almost 3 days to produce a batch of beads, a newer method to reduce the drying period of the sol was used. Figure 3.2 describes the experimental setup, where the glass beads are filled in a hollow ceramic funnel and  $\text{TiO}_2$  sol was poured in the funnel until the beads are

completely submerged in sol. Hot air was allowed to flow through the funnel packed with beads suspended in sol until the solution evaporates. This process of adding sol in parts was repeated 3 to 4 times, which resulted in the total volume of sol used equal to the mass of beads to be coated (3 – 4 times results in 70 g of beads coated by 70 ml of sol). The beads are transferred to a furnace and heated at a 5 °C/min ramp up to 500 °C, and held at this temperature for 2 h. Subsequently they are allowed to cool at room temperature and then washed thoroughly with DI water.

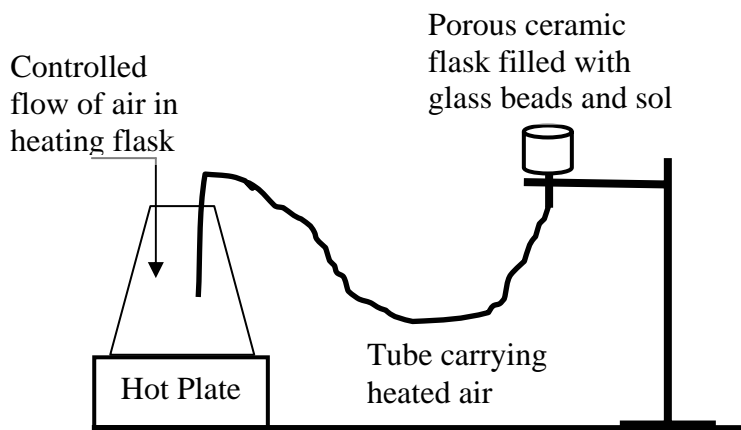


**Figure 3.2. Experimental setup for Coating of beads using ceramic funnel method**

### ***3.4.3. Ceramic Funnel Method With Etching***

In selected cases, glass beads were coated via *Method 2*, and after the beads were cooled to room temperature they were etched with dilute 0.1 N HCl, followed by washing thoroughly with DI water (Nakato et al., 1995). This process helped in roughening the catalyst surface and removing loosely bound TiO<sub>2</sub>. Method 3 was also used for coating beads prepared by sol mixtures D, E and F and further tested for photocatalytic activity.

### 3.5. TiO<sub>2</sub> COATING ANALYSIS

The glass beads coated using various sol mixtures and by different methods were analyzed by Environmental Scanning Electron Microscope (ESEM, Electroscan E3, Philips), BET surface area analyzer (Nova 2100), X-Ray Diffraction (XRD, Siemens D5000) and mass of TiO<sub>2</sub> coated on the glass beads measurement using precision balance (Mettler Toledo).

#### 3.5.1. Environmental Scanning Electron Microscope (ESEM) Analysis

ESEM analysis was done using an Electroscan E3 (Philips) for uncoated glass beads and glass beads coated with *Mixture C* by *Method 1* (washed and unwashed with DI, single and double coat). Also this procedure was used for comparing the uniformity of coating done by *Methods 1, 2* and *3*, showing the effect of supplemental TiO<sub>2</sub> added during sol gel synthesis process and calculating the thickness of coating.

#### 3.5.2. BET Surface Area Analysis

The BET surface area was determined for four different samples in Nova 2100 BET surface area analyzer, i.e., uncoated beads, glass beads coated by *Mixture C* by *Method 2*, glass beads coated with *Mixture F* by *Method 3*, and glass beads coated with *Mixture F* by *Method 3* used for photocatalytic experiment and gently washed with DI water. The procedure for operating NOVA 2100 BET analyzer is explained in brief below:

1. Plug vacuum pump, open the nitrogen gas tank and turn on the instrument
2. Weigh sample and put it in the degas station

3. Start degassing and continue for 45 mins at 100 °C, unload degasser and weight the sample again
4. If the weight measure before and after degassing is significantly different, degasses again
5. Otherwise proceed to analysis, by placing the sample in analysis station
6. Fill reservoir with liquid nitrogen and start the analysis
7. The instrument will display the results once the analysis is over
8. Switch off the instrument, vacuum pump and nitrogen gas tank

### ***3.5.3. X- Ray Diffraction Analysis***

The XRD analysis (Siemens D5000) for glass beads coated with TiO<sub>2</sub> did not provide any possible peaks, so the XRD analysis was done for powder prepared from *Mixture C*, *Mixture F* and Degussa P25, all calcinated at 500 °C with 5 °C/min of ramp heating. The X-ray diffraction pattern was obtained by measuring in the 2θ range between 20° and 80°, with a step size of 0.1°.

### ***3.5.4. Coated TiO<sub>2</sub> Mass Calculations***

The mass of TiO<sub>2</sub> coated on glass beads was found by measuring the difference between the cumulative mass of uncoated glass beads as a function of the number of beads and the cumulative mass of glass beads coated with *Mixture F* by *Method 3* as a function of number of beads using a precision balance (Mettler Toledo). Before measuring the weight of beads, the beads were placed overnight in oven at 100 °C to dry

them completely. The data was further used to estimate a possible thickness of the coating.

### **3.6. EXPERIMENTS ANALYZING PHOTOCATALYTIC EFFICIENCY**

The photocatalytic oxidation (PCO) experiments were conducted in different types of reactor configurations based on the progress of work. Once TiO<sub>2</sub> was successfully coated onto the glass beads, the evaluation of photocatalytic activity of coated TiO<sub>2</sub> was required. In order to evaluate the TiO<sub>2</sub> catalyst activity, photodegradation experiments were performed using formaldehyde, methyl orange and *E. coli*.

A rough experiment was performed using a round flask (250 ml volume), with an initial formaldehyde concentration of 100 µM. The reactor was loaded with 200 g/L of glass beads coated with *Mixture C* by *Method 1*, which were kept in suspension by rigorous stirring using a magnetic stirrer. The reactor was illuminated with four 15W UV tubes. Due to the attrition caused by magnetic stirrer on the glass beads, loss of coating was observed after each experiment and thus, a change in reactor configuration was required. A new reactor with a packed bed column was employed.

TiO<sub>2</sub> coated glass beads were packed in a cylindrical or square column and the column was placed vertically in one configuration and horizontally in another. A peristaltic pump was used to control various flow rates through the column. All the connections were sealed with Parafilm to avoid any leakage and the column was connected to the influent tank by Viton tubing. Parafilm was covered by aluminum foil to avoid splitting of parafilm due to the effects of UV directly or indirectly through heat.

The flow rate through the column was measured by measuring the volume of sample collected over a period of time. The packed bed volume of the column was calculated from the difference between the volume of the empty reactor and the volume of glass beads packed in the reactor. To cross check the volume of the packed bed reactor, the column was packed with glass beads and was filled using a graduated cylinder with DI water until the fluid started overflowing. The volume poured in the column was measured as the difference in the volumes in the graduated cylinder. The error in the values was less than 5%. The hydraulic retention time (HRT) of column is the time a given fluid element takes to pass through the packed column and was calculated by dividing the reactor packed bed volume by the measured flow rate.

The influent sample was constantly mixed using a magnetic stirrer and the pH of influent samples was maintained at 5.0 (formaldehyde), 6.0 (methyl orange) or 7.0 (*E. coli*)  $\pm 0.2$  with 0.1 N HCl and 0.1 N NaOH. The ionic strength was maintained at  $1.7 \times 10^{-2}$  M NaClO<sub>4</sub> and the initial temperature averaged  $25 \pm 2$  °C. A continuous flow of oxygen was maintained in the influent tank throughout the experiment to achieve saturation of dissolved oxygen. Since oxygen plays an important role of preventing electron-hole recombination reaction, it is very important to keep the influent sample saturated with oxygen. All apparatus components were washed with DI water and oven dried or autoclaved to avoid any contamination. The column was illuminated from all directions to avoid any possibility of limitation of light intensity as explained by Dijkstra et al. (2001). Experiments with controls; (i) UV and column packed with uncoated glass beads and (ii) No UV with column packed with glass beads coated with *Mixture F* by *Method 3*, were conducted. Each reactor was equipped with an external aluminum foil

cover to avoid UV loss. All the readings for the experiments performed were taken after at least 1.5 – 2.0 HRTs to reach steady state conditions.

### ***3.6.1. Formaldehyde Photodegradation Using Vertically Oriented Prototype Reactor***

The vertically oriented packed bed plug flow type reactor (Figure 3.3) is equipped with a circular glass column filled with glass beads coated with TiO<sub>2</sub> sol *Mixture C* by *Method 1*. Uncoated samples of the same beads were used for controls. Occasionally two columns were connected in series to increase the total HRT of the reactor. The column was placed in a vertical orientation with influent entering the column from the bottom and the effluent being collected from the top of column. The column was illuminated using four 15W UV tubes; the influent sample was saturated with oxygen; the pH was held at  $5.0 \pm 0.2$  and ionic strength was  $1.7 \times 10^{-2}$  M NaClO<sub>4</sub>.

### ***3.6.2. E. coli Photodegradation in Prototype Reactor***

The formaldehyde experiments provided proof of coated TiO<sub>2</sub> as photocatalytically active. Experiments with *E. coli* were performed for check of the disinfection efficiency of the reactor shown in Figure 3.3. The column was packed with glass beads coated with TiO<sub>2</sub> sol *Mixture C* using *Method 1* and was loaded with  $10^5 - 10^7$  CFU/100 ml of initial *E. coli*. The pH of influent sample was maintained at  $7.0 \pm 0.2$  and ionic strength of solution was maintained at  $1.7 \times 10^{-2}$  M NaClO<sub>4</sub>. All parts of the apparatus were disinfected by washing in at least 20% bleach for 10 min or sterilized by autoclaving before using to avoid any external contamination.

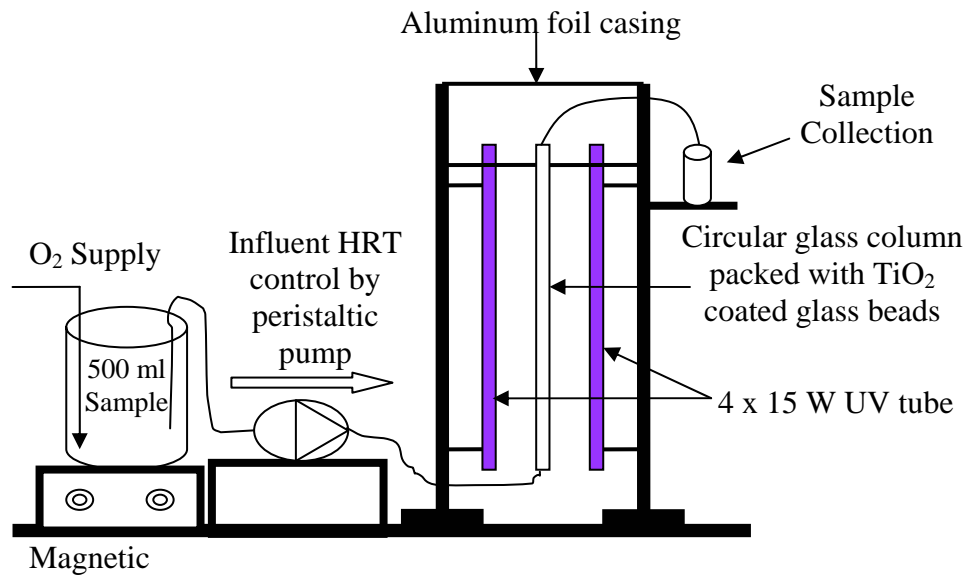


**Figure 3.3. Schematic diagram of vertical packed bed PCO reactor**

The vertical orientation of reactor being unstable and also caused higher hydraulic pressure which further resulted in rupture of seals. Therefore, the reactor was oriented horizontally for further experiments. Our goals were to use LEDs, which would be more like individual focused point sources as compared to the dispersed UV tubes, using a square quartz column instead of circular column, which would provide more surface area to be illuminated for the LEDs.

The prototype reactor experiments were performed at  $7.0 \pm 0.2$  pH,  $1.7 \times 10^{-2}$  M NaClO<sub>4</sub> ionic strength, saturated DO and an initial *E. coli* of  $10^5 - 10^7$  CFU/100 ml. Dark and lighted controls were also performed to indicate the effect of photocatalysis on disinfection. The reactor is shown in Figures 3.4 through 3.6.

### **3.6.3. Methyl Orange Photodegradation**

After a rigorous construction and optimization phase, a final prototype reactor configuration was achieved, shown in Figure 3.4. The reactor was oriented horizontally with a square quartz column packed with glass beads coated with *Mixture C, D, E or F* by *Method 2 or 3* and illuminated with four 15W UV tubes. The temperature of the reactor was maintained between  $25 \pm 5$  °C by passing air over the column and UV tubes. Figure 3.5 shows the top view of the column held in between the UV tubes. The distance between the column and UV tubes was kept at 2 -3 cm so as to avoid any dark patches in the column and to prevent loss of light. The glass beads were packed in the quartz column and sealed using square polyvinyl caps (Caplugs).

Methyl orange has been often used as a reliable model pollutant in photocatalytic reactor research. Since methyl orange turns yellow in an alkaline solution and red in acidic solution, it is also suitable for monitoring the photodegradation process (Brown et al., 1984; Nam et.al., 2002; Bao et.al., 2004). The influent and effluent pH was maintained at  $6.0 \pm 0.2$  with 0.1 N HCl and 0.1 N NaOH. Since the total volume of acid, base used was less than 5 ml (for influent tank) and 1 ml (for effluent samples); it did not affect the concentration of methyl orange. The ionic strength of the solution was fixed at  $1.7 \times 10^{-2}$  M NaClO<sub>4</sub>, with influent concentration of methyl orange between 15 mg/L and 30 mg/L.

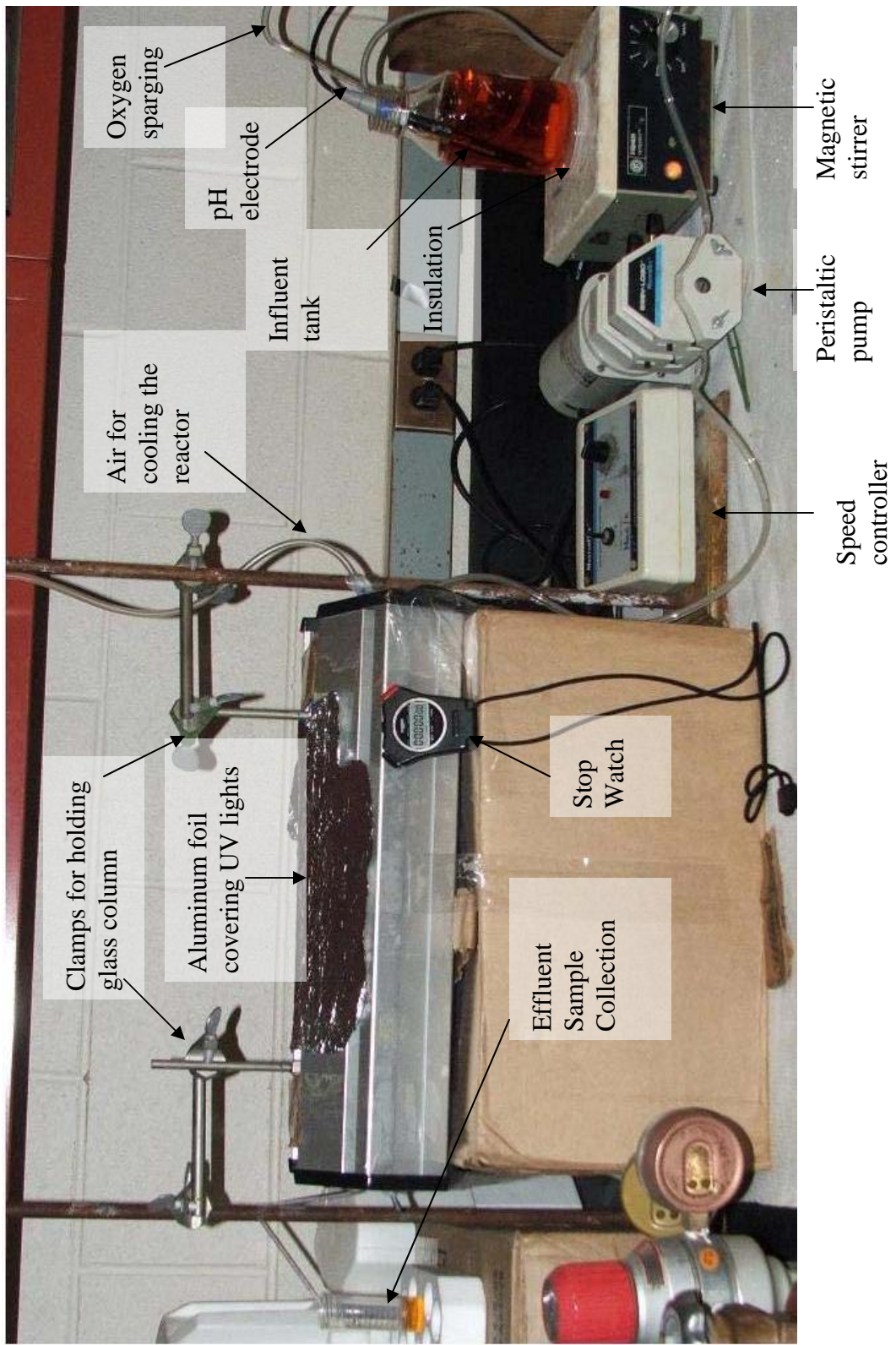


**Figure 3.4. Packed Bed Plug Flow Reactor (Prototype Reactor) illuminated with four 15W UV tubes**

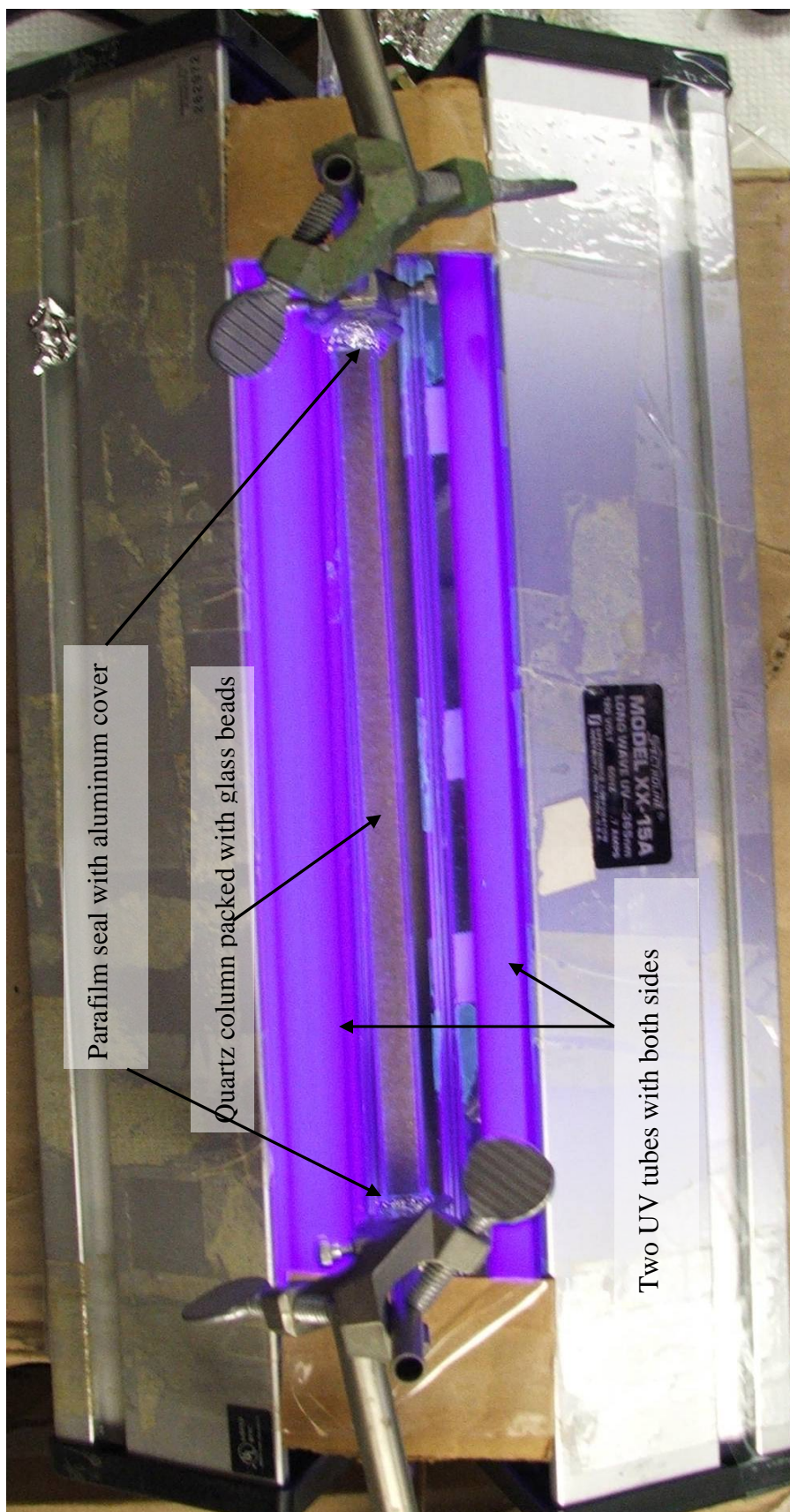
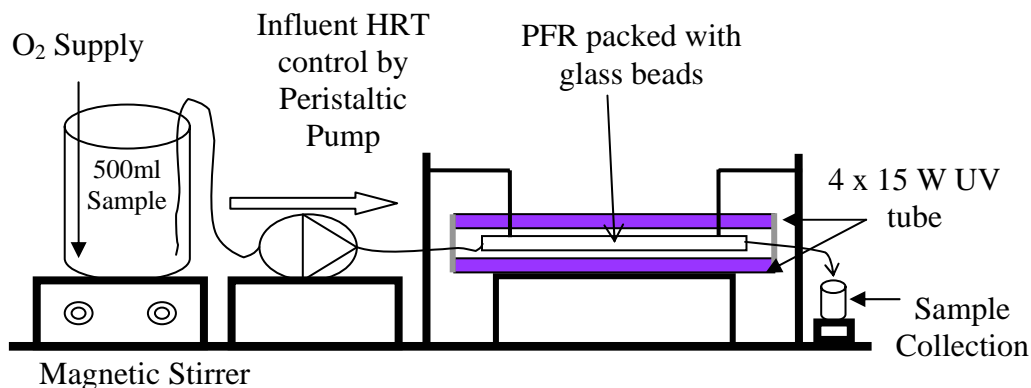


Figure 3.5. Top view of column and UV tubes configuration for Prototype PCO reactor

### 3.6.3.1. Methyl Orange Photodegradation Using Prototype Reactor

Figure 3.6 shows the experimental setup for methyl orange experiments using 4 x 15 W UV tubes. For different experiments the column was packed with glass beads coated with TiO<sub>2</sub> prepared from TiO<sub>2</sub> sol *Mixtures C, D, E and F* by *Method 2 or 3*. Experiments were performed for different HRTs to evaluate the photocatalytic oxidation kinetics. Data were also analyzed for the reproducibility of TiO<sub>2</sub> coating method and to check the loss of TiO<sub>2</sub> coating by using the catalyst for prolonged periods of time. An experiment to check the loss of coating after the photocatalytic experiment was performed where beads were removed from the column and washed gently with DI water for various HRTs.



**Figure 3.6. Schematic diagram of horizontal continuous packed bed plug flow PCO reactor**

### 3.6.3.2. Methyl Orange Photodegradation Using Portable Reactor

After the design and testing of the reactor with UV tubes was successfully carried out, design of the portable reactor with UV LEDs was done. The design constituted of using a base plate for providing a even base to mount different components, combinations

of LEDs as UV sources, a DC power supply (Agilent E 3646A), lenses (Edmund Optics Inc.) and focusing units (Thorlabs Inc.) to focus incident light from top, bottom and sides of the column to concentrate the incident light (Figure 3.7). The lenses (BK7 material) used for focusing the UV lights were not UV coated and thus caused reduced transmission through the lenses (80% to 50% for a wavelength range of 375 nm to 350 nm - Edmund optics). Due to the loss of light to such a great extent, the design was changed and the column was directly illuminated by LEDs (340 nm or/and 370 nm wavelength) placed less than 1 cm away from the outer surface of column (Figure 3.9). Due to the limitations of HRT through new reactor using it as flow through reactor (0.15 ml/min – minimum achievable flow rate), the reactor was operated as a batch type recirculating reactor to have longer illumination period.

Two different configurations were designed to work as recirculating reactors. Initially a packed bed reactor (PBR) and mixed storage reactor (MSR) were connected in a series recirculating configuration (Figure 3.8). Once a steady flow rate through the packed bed reactor was maintained, the influent tube was connected with the MSR to operate the system as a batch type recirculating system. Since minimal mixing through the length of reactor is expected, the column filled with glass beads behaves like a plug flow PBR. The effluent collecting reactor is mixed using a magnetic stirrer and the flow coming in and going out of the reactor are constant, therefore the reactor behaves like a MSR. In the MSR there is no reaction occurring but only dilution of effluent occurs. The total combined volume to be treated in a single batch was 21 ml and the volume in the MSR was been kept constant at 5 ml, while the total volume of sample undergoing photocatalytic oxidation in PBR is 6.15 ml. As the reactor was a combination of PBR and

MSR, the mathematics became very complex for deriving the equation for rate constant. Since only the PBR is illuminated degradation occurs in the PBR, while in the MSR only dilution of the effluent occurs with the PBR effluent. The degradation kinetics should be assumed to follow usual photocatalytic degradation kinetics of Langmuir – Hinshelwood (Dijkstra et al., 2001).

The second configuration consisted of only the PBR operated as a recirculating reactor, with other operating conditions remaining the same. Once the flow rate was maintained at  $0.35 \pm 0.5$  ml/min, the column outlet was connected to the inlet tube and the UV LEDs were powered. The total volume of the reactor was decreased from 21 ml to 16 ml. Since only the PBR is operated in a recirculated configuration, the degradation kinetics should also follow the lower limit of Langmuir – Hinshelwood kinetics, i.e., pseudo first order kinetics, as seen for the prototype reactor.

Due to comparatively high power input for UV LED 340 (0.5 watts input power), the LEDs were placed in metal sockets which would absorb the heat generated due to the power dissipation and the LEDs were cooled by passing air over them. The UV LEDs were operated at fixed input currents with UV LED 340 operated at 100 mA each, while the UV LED 370 were operated at 15 mA or 25 mA each based on the progress of work. The operating characteristics of two UV LEDs used are given in Table 3.1.

**Table 3.1. Characteristics of Light Emitting Diodes (Roithner laser, UV LED370 and Sensor Technology, UV LED340)**

Type of LED	Power dissipation (mW)	Output power (mW)	Operating current (mA)	Half angle (degree)
UV LED340	150 @ 30 mA	0.5 @ 20 mA	100	30°
UV LED370	60 @ 15 mA	1.0 @ 10 mA	25	110°

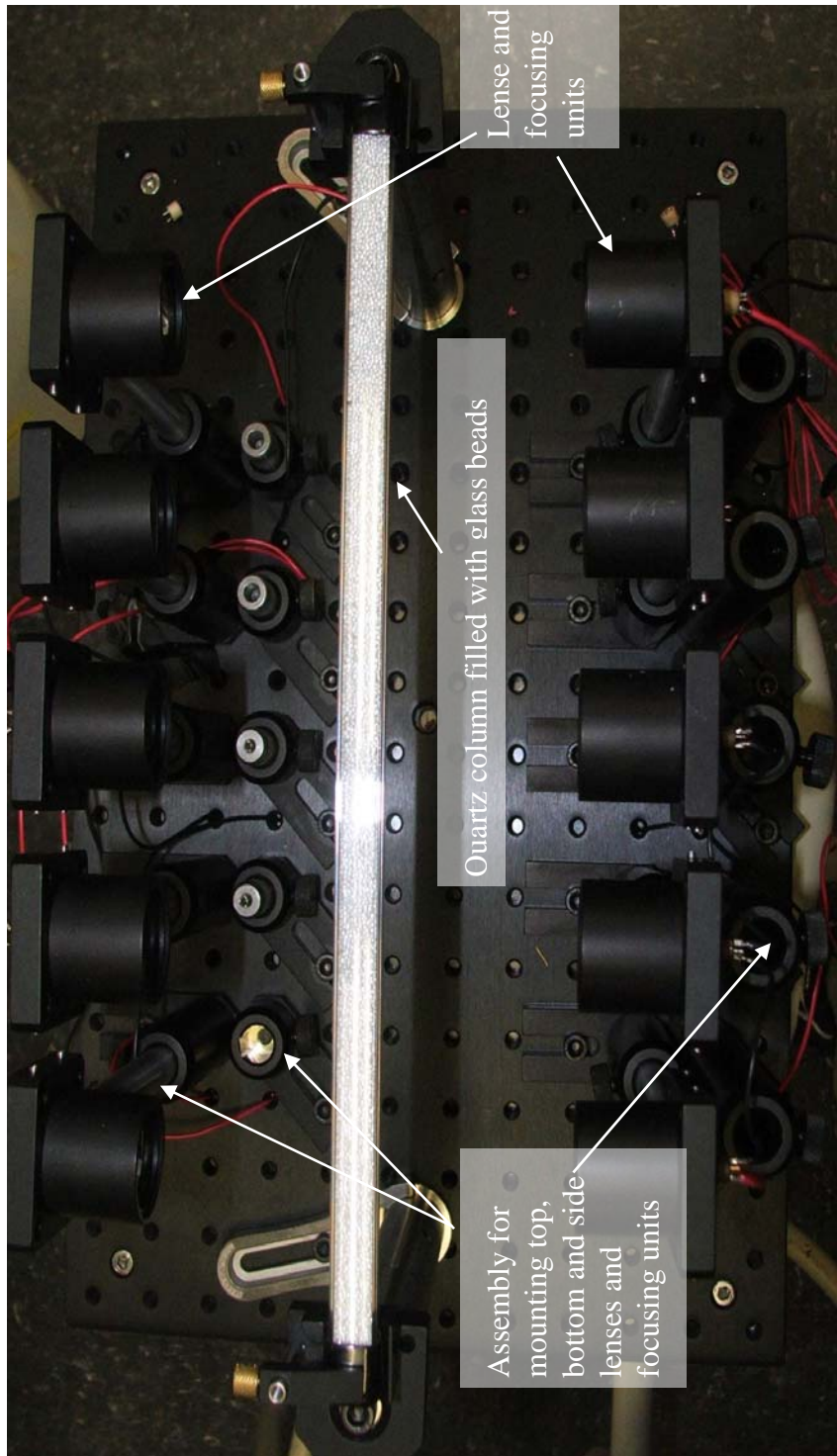


**Figure 3.7. Partly constructed reactor mounted with LEDs, lenses and mounting units**

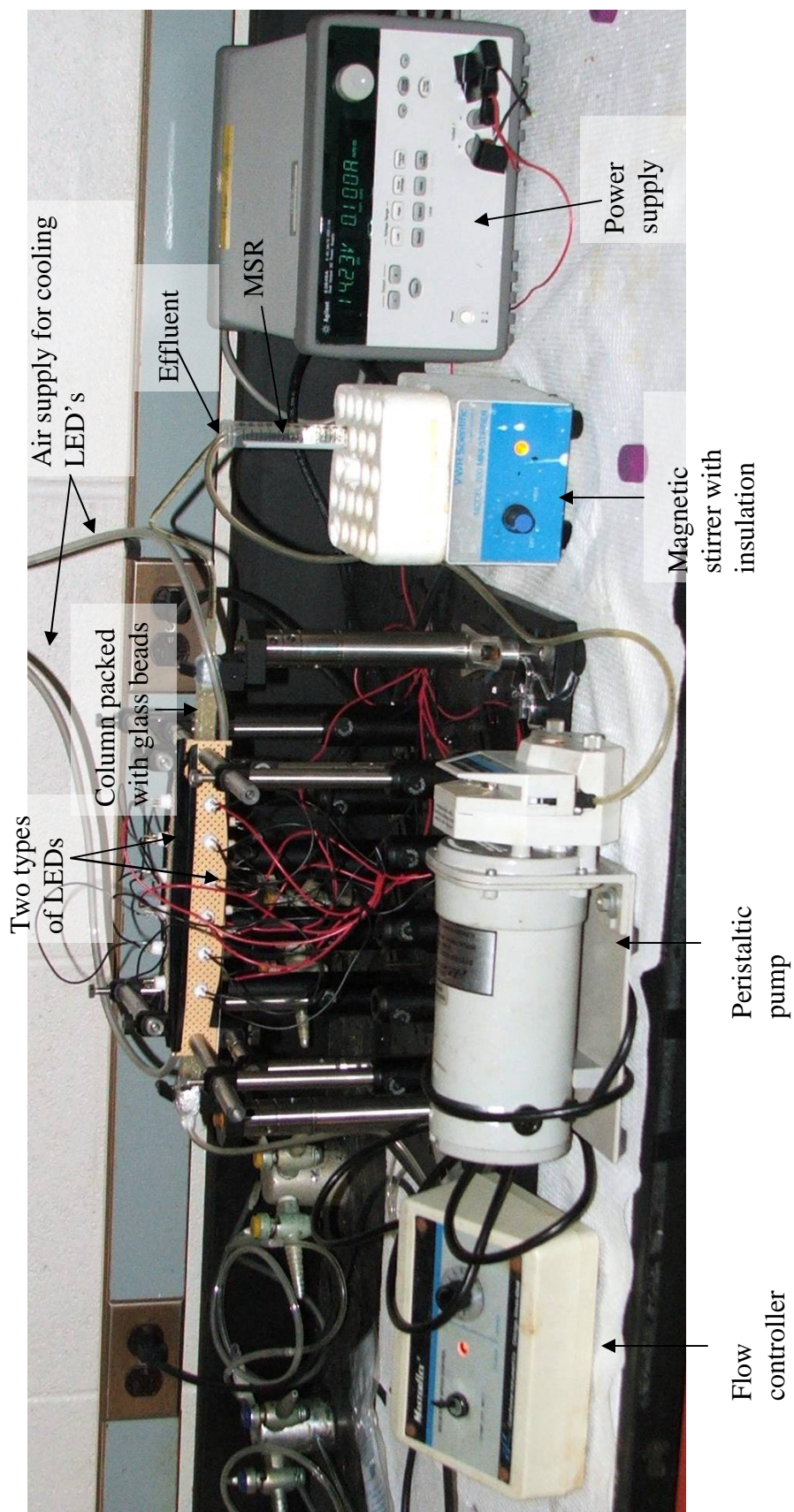


**Figure 3.8. Portable PCO reactor with PBR connected in series with a MFR operated as recirculating reactor using UV LEDs as illumination source**

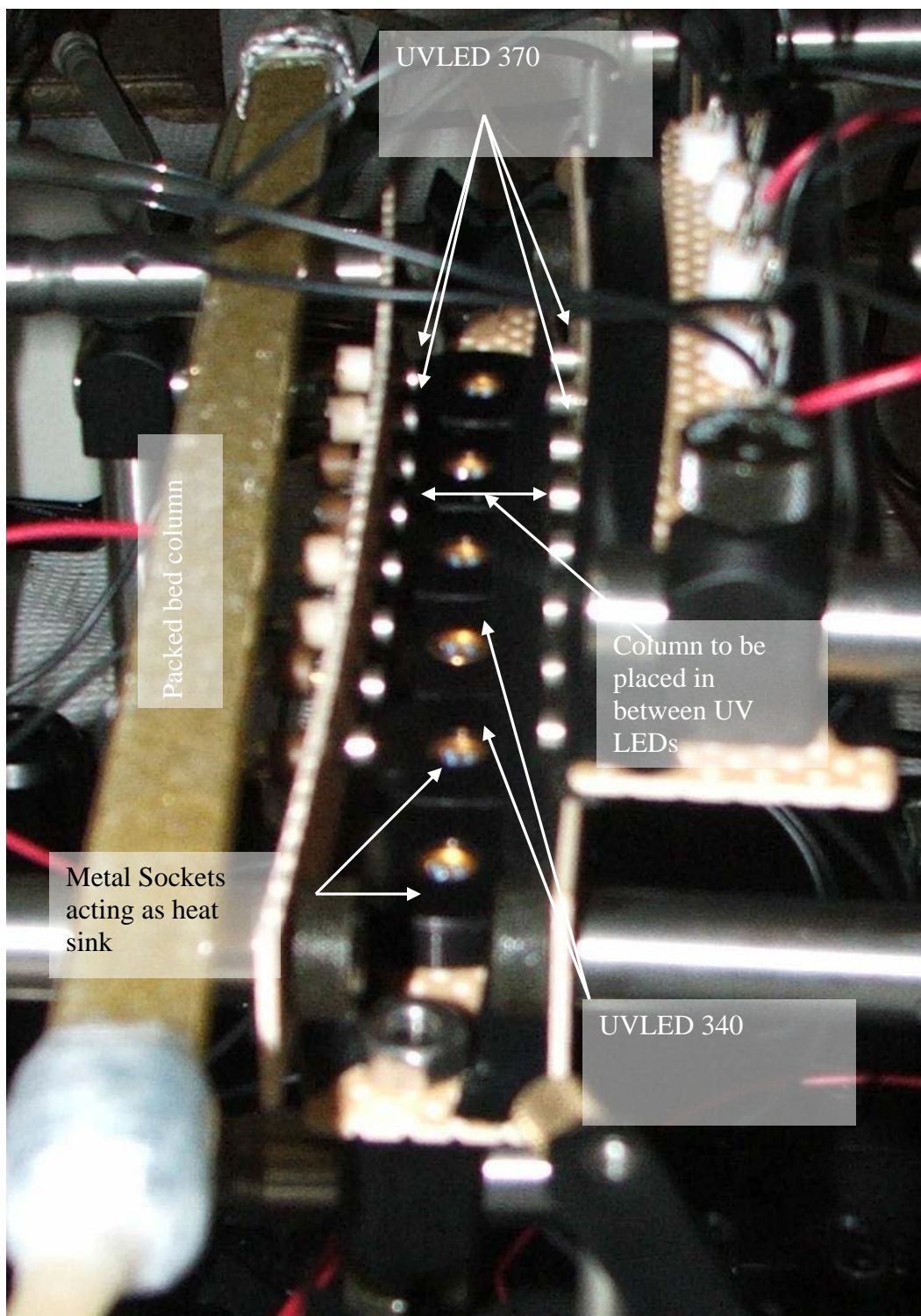


**Figure 3.9. Top close-up view of portable PCO reactor with UVLED 340 and UVLED 370 placed along the sides, top and bottom to illuminate the column**

Figure 3.10 represents a schematic diagram for the both the configuration where the PBR and MFR are connected in series and the PBR with direct recirculation. The second configuration can be obtained by removing the MFR and connecting the outlet from PBR to the inlet of PBR, shown in Figure 3.10. The column was packed with beads coated with TiO<sub>2</sub> prepared from sol *Mixture F* by *Method 3*. Experiments were performed with a combination of UV LEDs for different operation periods to evaluate the photocatalytic degradation rates.

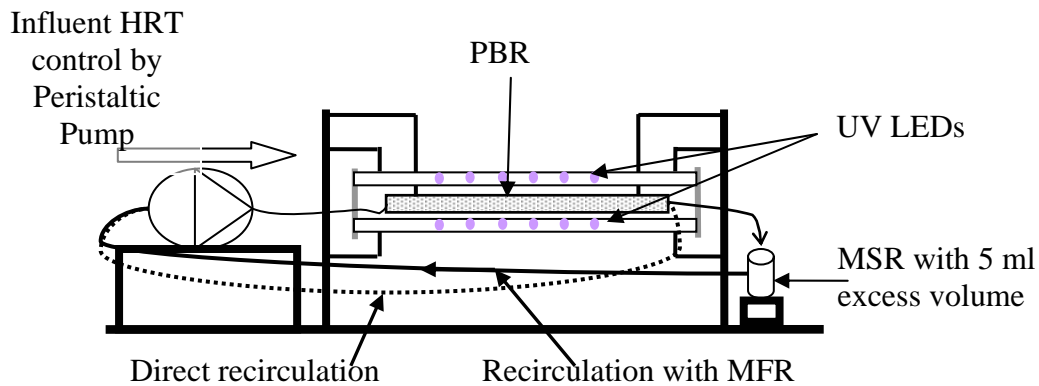


**Figure 3.10. Schematic diagram of horizontal continuous portable recirculating PCO reactor using two different configurations**

#### ***3.6.4. E. Coli Photodegradation Using Portable Reactor***

With the portable reactor designed as a direct recirculating reactor, experiments for *E. coli* were performed in the portable reactor with pH = 7.0 ± 0.2, ionic strength = 1.7 x 10<sup>-2</sup> M NaClO<sub>4</sub> and DO saturated with oxygen (Figure 3.10). Control experiments performed with the portable reactor did not yield consistent results. There could have been number of reasons due to which the consistency of experiments was not achieved.

But to prove that LEDs can be used as a viable source of UV light for water disinfection, two quartz cuvettes were filled with glass beads and water sample, and sealed with parafilm. The cuvettes were placed in the LED configuration shown in Figure 3.9 and illuminated for 5 hrs. The total volume of sample treated in each quartz cuvette was 1.8 ml, and once the experiments were over the glass beads were transferred to a sterile test tube and 1.8 ml sterile water was added to the test tube. The sample was then shaken gently to mix the water sample and detach any *E. coli* colony from the surface of glass beads, if attached. The samples were then plated as per the standard plate count technique. Dark and lighted control experiments were also performed to prove the photocatalytic effect of the UV LED light source.

## CHAPTER 4

### RESULTS AND DISCUSSION

#### 4.1. COATING METHOD

The suspension method required 24 hrs to provide a single layer of coat. The ceramic funnel method was used to reduce the coating time to less than 3 hrs and to make the process efficient by maximizing the use of sol gel. Etching of glass beads was done to remove loosely attached TiO<sub>2</sub> particles (P25), which would otherwise be washed out over prolonged period of use in PCO. Etching of coated beads would also result in roughening of the surface and thus result in higher number of active sites for reaction.

#### 4.2. COATING CHARACTERIZATION

##### 4.2.1. *Environmental Scanning Electron Microscope (ESEM) Analysis*

ESEM was used to take micrographs of coated and uncoated glass beads to compare different coating methods, the uniformity of coating and thickness of coating. An ESEM micrograph of an uncoated glass bead is shown in Figure 4.1. Comparing Figure 4.1 with other coating micrographs will help in identifying the bead coating characteristics.

ESEM micrographs of the glass beads coated using *Method 1*, are shown in Figures 4.2 and 4.3. Figure 4.2.a shows unwashed beads and Figure 4.2.b shows washed (with DI) beads; Figure 4.3.a shows beads with single coating and Figure 4.3.b shows beads with two coatings.

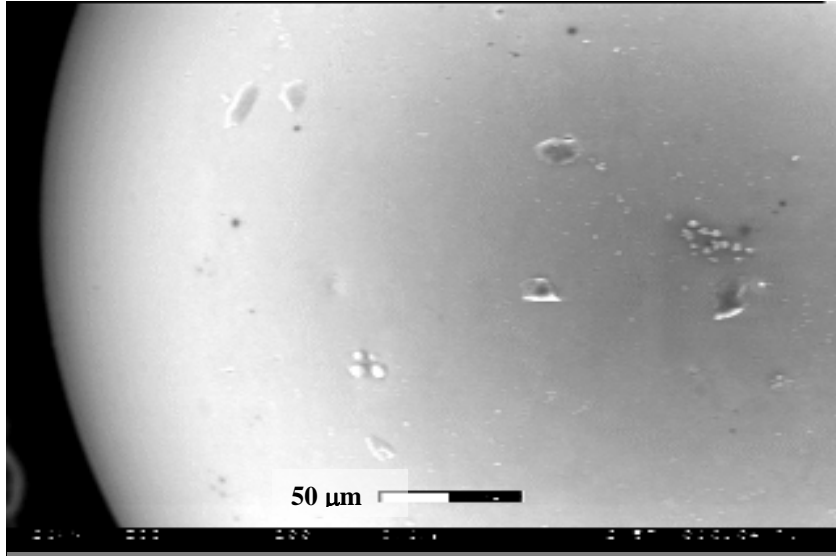


**Figure 4.1. Uncoated glass beads serving as reference to other ESEM micrographs of coated glass bead**

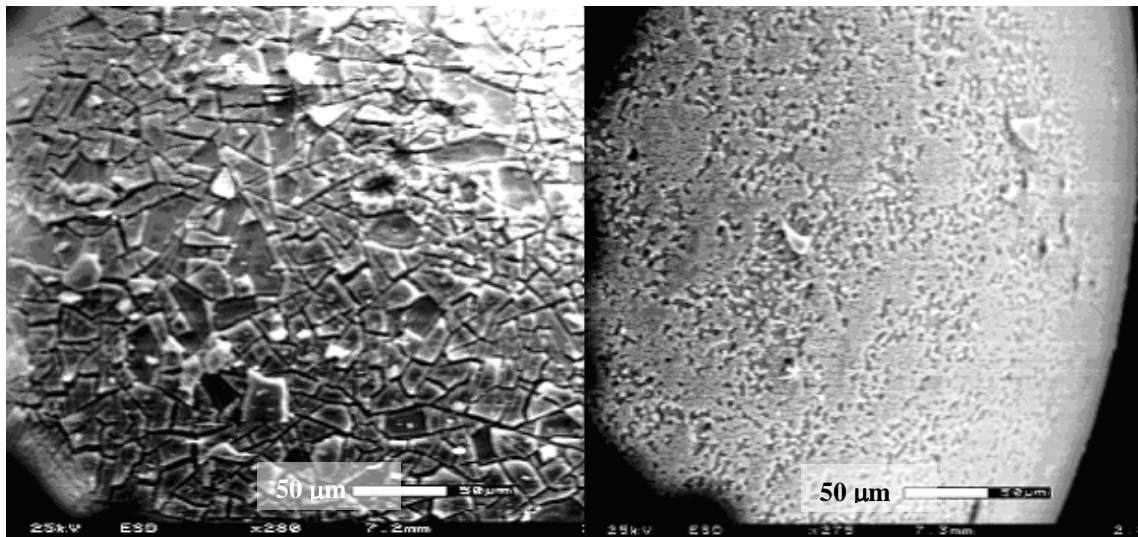


**Figure 4.2.a. Unwashed Beads**

**Figure 4.2.b. Washed beads**

**Figure 4.2. Comparison of single - coated unwashed and washed beads to analyze the effect of washing beads. TiO<sub>2</sub> coatings were prepared by *Method 1*.**

Looking at Figure 4.1 and Figure 4.2, the glass beads appear to be coated with TiO<sub>2</sub> in the latter. Comparing Figures 4.2.a and 4.2.b, it can be seen that the surface of the coating on glass beads which are not washed is uneven with flakes of TiO<sub>2</sub> weakly

attached to the glass surface. This flaky coating was removed when thoroughly washed with water, as seen in Figure 4.2.b.

Comparison of Figures 4.3.a and 4.3.a shows that the additional layering produces significant difference between coating patterns on the glass beads. In Figure 4.3.a, the surface was not as smooth as can be seen in Figure 4.3.b with two coating layers. Thus, it was concluded that two layers of  $\text{TiO}_2$  are to be applied in order to have complete and smooth coating on the glass beads surface.

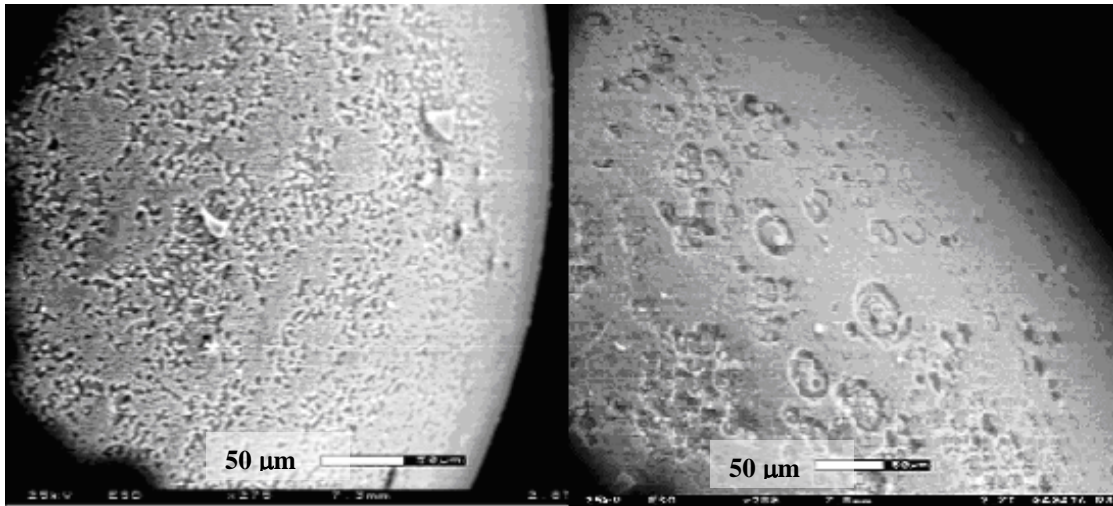


**Figure 4.3.a. Single Coat**

**Figure 4.3.b. Double Coat**

**Figure 4.3. Comparison between glass beads coated with  $\text{TiO}_2$  by *Method 1* with single coating and double coating for analysis of coating uniformity**

Due to the long time required for coating the glass beads, a more mature method (*Method 2*) was evolved from the previous experiments. In this method, due to rapid drying by hot air, the total process time from producing sol to washing of coated glass beads was reduced to 6 to 8 hr from nearly 3 days. Along with saving of process time, the process remains simple since after the sol was dried, the ceramic funnel was directly

placed in an oven for calcination. Thus, even if the beads agglomerate after drying, they are easily separated after calcination.

Comparison of the two micrographs in Figures 4.4.a and 4.4.b shows some difference in the uniformity of coating. Figure 4.4.2 shows glass beads coated with *Mixture C* by *Method 2* which seems to be more uniform with lesser irregularities. Thus, by using the newer method, along with increase in uniformity of coating, the total time for coating process was reduced to less than 6 hr.

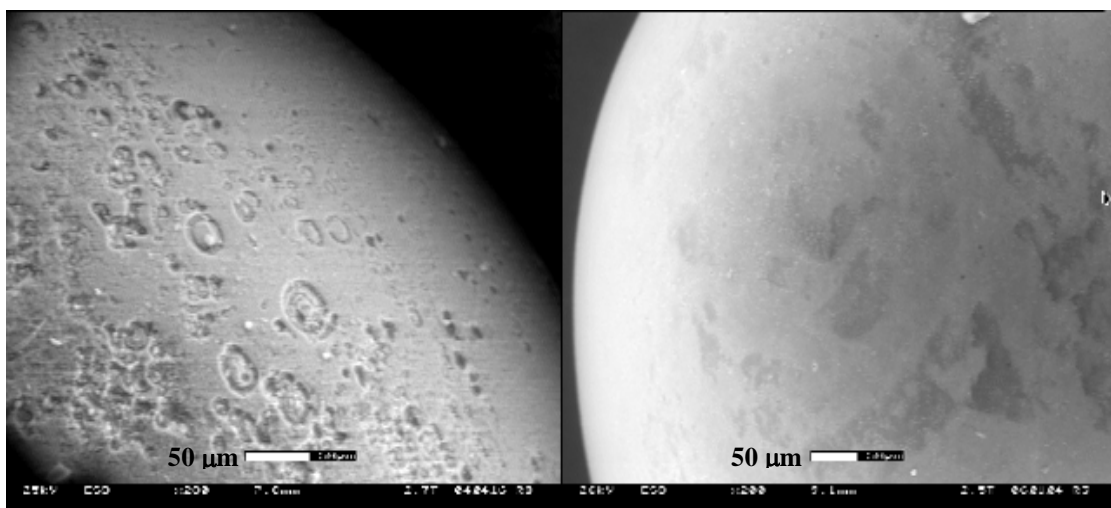


**Figure 4.4.a. Bead coated with *Method 1*, double coat**

**Figure 4.4.b. Beads coated with *Method 2*, three coats**

**Figure 4.4. Comparing micrographs of beads coated with TiO<sub>2</sub> by two different methods to check for the uniformity in coating**

Figure 4.5.a again shows the glass beads coated with TiO<sub>2</sub> prepared (*Mixture C*) without supplemental TiO<sub>2</sub> powder (Degussa P25) by *Method 2*. The bright white dots in Figure 4.5.b result from the supplemental TiO<sub>2</sub> powder attached to the glass beads coated by *Method 3*, added during sol gel preparation (*Mixture F*). Thus, this attached TiO<sub>2</sub> powder should assist in increasing the specific surface area and roughness of the catalyst, which in turn was expected to enhance the rate of the photocatalytic reaction.

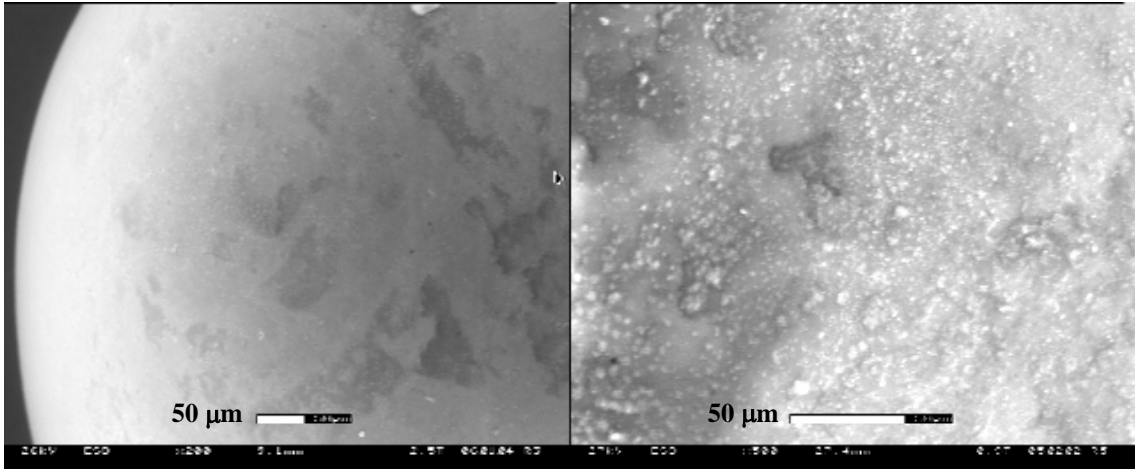


**Figure 4.5.a. Beads coated with Mixture C by Method 2**

**Figure 4.5.b. Beads coated with Mixture F by Method 3**

**Figure 4.5. The effect of supplemental TiO<sub>2</sub> (Degussa P25) powder to sol gel preparation**

A cross section of a glass bead coated with *Mixture C* by *Method 2* was analyzed under ESEM. Figure 4.6 shows the cross section of a coated glass bead. The coating thickness varies as seen in Figure 4.6.a, with 9.9 µm as maximum thickness of coating as measured by ESEM (Figure 4.6.b).

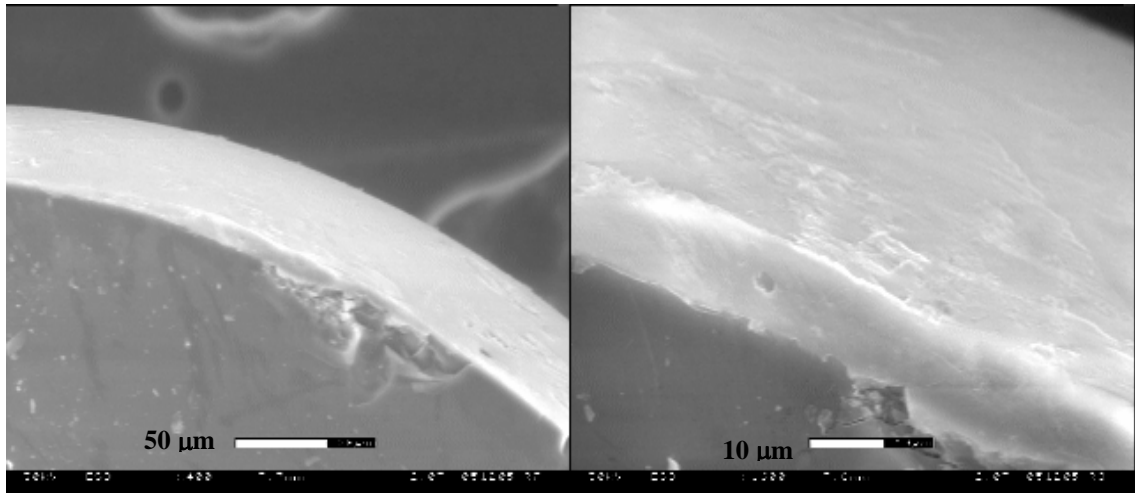


**Figure 4.6.a. Cross section showing varying thickness**

**Figure 4.6.b. Cross section showing maximum thickness of 9.9 µm**

**Figure 4.6. ESEM micrograph of cross section of a glass bead coated with Mixture C and Method 2.**

#### 4.2.2. BET Surface Area Analysis

The BET surface areas were found for uncoated beads, beads coated with sol gel *Mixture C* and *Method 2*, beads coated with sol gel *Mixture F* and *Method 3* and beads coated with sol gel *Mixture F* and *Method 3* used once for a photocatalytic experiment.

Table 4.1 below presents the BET surface area values for the four different cases.

**Table 4.1. BET surface area of glass beads uncoated, coated with *Mixture C* and *Method 2* and coated with *Mixture F* and *Method 3*.**

Type of Beads	BET Surface Area (m <sup>2</sup> /g)
Uncoated Beads	0.005
Beads Coated with <i>Mixture C</i> and <i>Method 2</i>	0.091
Beads Coated with <i>Mixture F</i> and <i>Method 3</i>	0.284
Beads Coated with <i>Mixture F</i> and <i>Method 3</i> and used once for a photocatalysis experiment	0.200

From Table 4.1, it can be seen that the BET surface area of coated beads increases by a factor of 2 (Beads Coated with *Mixture C* and *Method 2*) and 55 (Beads Coated with *Mixture F* and *Method 3*) as compared to the uncoated beads. This increase in surface area can be attributed to the TiO<sub>2</sub> coating (with and without supplemental TiO<sub>2</sub> powder) which results in a porous and rough surface. Thus the increase in surface area should help in increasing catalyst exposure to UV which in turn would increase the chances of photocatalytic reaction. The BET surface area of glass beads which have been used once for photocatalytic experiment as compared to the ones which have not been used decreases by 25%, indicating a loss of attached TiO<sub>2</sub>. Kim et al. (2002b) found that glass beads (6 mm) coated with TiO<sub>2</sub> by submerging the beads into the TiO<sub>2</sub> solution was gradually removed and resulted in complete loss after 100 hr of flowing water through

the glass beads in a packed bed reactor. A similar effect could have also resulted in decrease in the BET surface area and thereafter reduced photocatalytic efficiency.

#### **4.2.3. X- Ray Diffraction Analysis**

The XRD analysis of powder prepared from *Mixture C* and *Method 2*, *Mixture F* and *Method 3*, and Degussa P25 calcinated at 500 °C with 5 °C/min of ramp heating is shown in Figure 4.7. The XRD pattern for TiO<sub>2</sub> prepared from *Mixture C* and *Method 2* predominantly indicates the anatase phase of TiO<sub>2</sub> with a sharp peak at 25 °C, which is the major peak for the anatase structure. The XRD pattern for *Mixture F* prepared by *Method 3* shows a combination of P25 and *Mixture C* with predominance of the anatase phase. Since the mass of TiO<sub>2</sub> due to sol gel is 2.0 g, while 0.5 g of P25 is added, the *Mixture F* is dominated by TiO<sub>2</sub> due to sol gel, which has been characterized by a dominated anatase phase. The XRD patterns observed by Demessie et al. (1999), Kim et al. (2002a), Hamid and Rehman (2003) and Lee et al. (2003) were similar to the XRD patterns observed for *Mixture C*, i.e., well-crystallized anatase type TiO<sub>2</sub>.

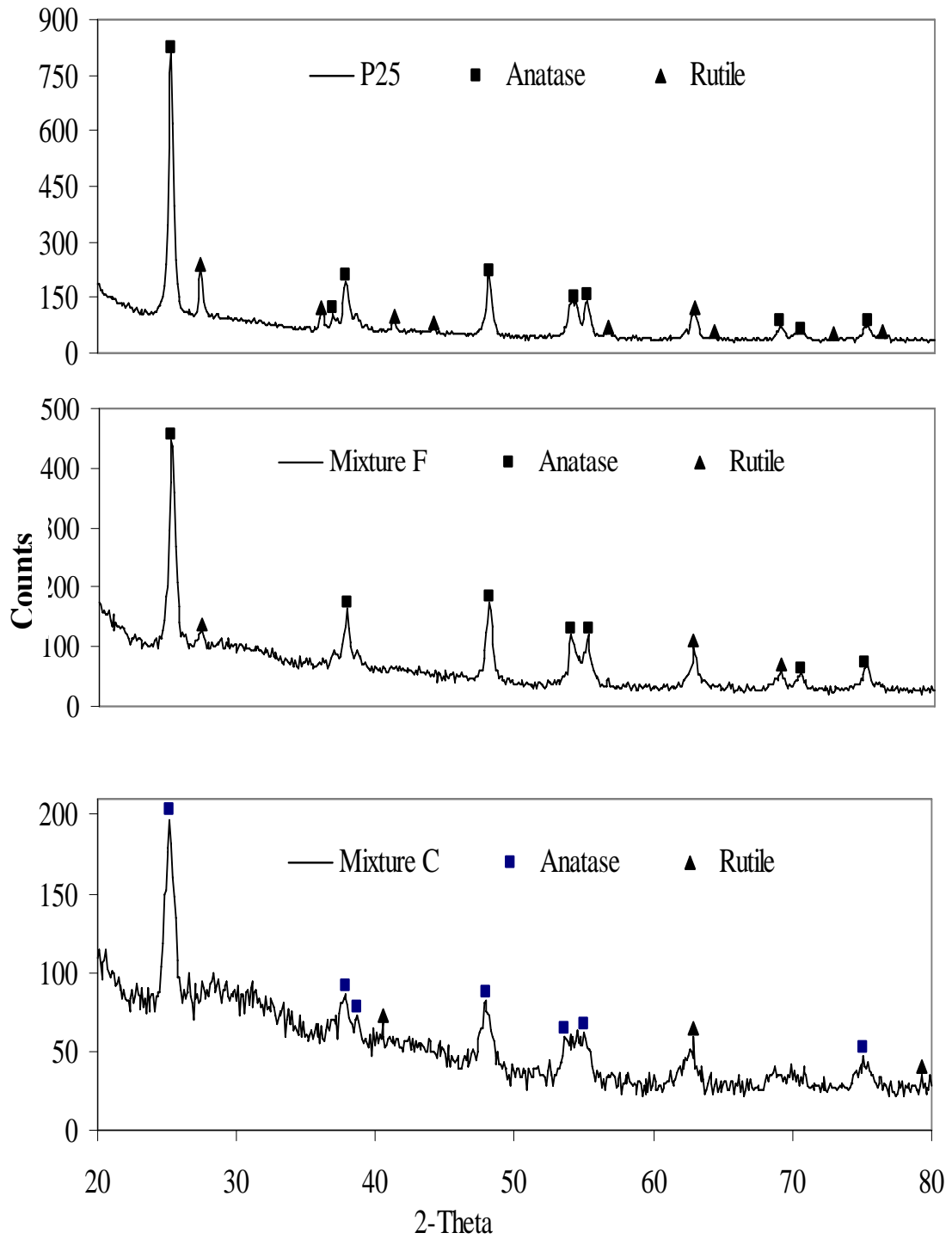


**Figure 4.7. XRD graphs for powder prepared from Degussa P25, *Mixture F* and *Mixture C***

#### 4.2.4. Coated TiO<sub>2</sub> Mass Calculations

Uncoated and coated glass beads were washed with DI water and oven dried at 100 °C before they were weighed on a precision balance (Mettler Toledo Precision Balance) and a cumulative mass/number of beads ratio was obtained. Table 4.2 shows the data for calculating the mass of TiO<sub>2</sub> coated onto the glass beads.

**Table 4.2. Analysis for calculating mass of TiO<sub>2</sub> coated on the surface of glass beads using Method 3 and TiO<sub>2</sub> prepared using Mixture F. Cumulative mass of beads has been measured and average and standard deviation values are obtained.**

Number of Beads	Mass of Uncoated Glass Beads (g)	Mass of Uncoated Glass Bead (g/bead)	Mass of Glass Beads with TiO <sub>2</sub> +Sol (g)	Mass of Coated Glass Bead (g/bead)
50	0.0924	0.001848	0.0955	0.00191
100	0.1834	0.00182	0.184	0.00177
200	0.3617	0.001783	0.3629	0.001789
300	0.5373	0.001756	0.5442	0.001813
400	0.7199	0.001826	0.7258	0.001816
500	0.9016	0.001817	0.913	0.001872
550	1.0813	0.001797	1.1054	0.001924
650	1.1754	0.001882	1.1995	0.001882
<b>Average</b>		<b>0.001816</b>		<b>0.001847</b>
<b>Standard Deviation</b>		<b>0.000036</b>		<b>0.000054</b>
<b>Difference = TiO<sub>2</sub> mass/ glass bead</b>				<b>3.1 x 10<sup>-5</sup> g/bead</b>
<b>Mass of glass beads in column (measured), M<sub>gb</sub></b>				<b>46 ± 1 g</b>
<b>Number of glass beads in column, N<sub>gb</sub> = M<sub>gb</sub>/Difference</b>				<b>25205 ± 1005</b>
<b>TiO<sub>2</sub> loaded in the column = N<sub>gb</sub> x Difference</b>				<b>0.78 ± 0.03 g</b>

The mass of uncoated bead is 0.001816 ± 0.000036 g/bead (Table 4.2), while that of the coated bead is 0.001847 ± 0.000054 g/bead. Therefore, the mass of TiO<sub>2</sub> coated on the surface of the glass bead packed in the column averages 3.1 x 10<sup>-5</sup> g/bead.

Another separate set of calculations were performed to cross check this value of mass of coated TiO<sub>2</sub> where, after coating the glass beads, the powdered TiO<sub>2</sub> which was not attached to glass beads was collected from the ceramic funnel and from the DI water used for washing beads. The mass of powder TiO<sub>2</sub> measured was  $1.0 \pm 0.1$  g. In this preparation, 70 ml of sol gel synthesis *Mixture F* was prepared by mixing 7.5 ml of TIP to 52 ml of Isopropanol, 18 ml of 1N HCl and 2 ml of DI water. This volumetric ratio should provide 0.025 moles (2 g) of TiO<sub>2</sub>. Thus, a total of 2.5 g (sol + P25) is used to coat 70 g of beads, while the summation of mass of TiO<sub>2</sub> actually coated on 70 g of glass beads ( $1.19 \pm 0.14$  g) and the uncoated powder ( $1.0 \pm 0.1$  g) is  $2.19 \pm 0.15$  g. Thus, about  $87 \pm 6\%$  of TiO<sub>2</sub> is recovered. The addition of 0.5 g Degussa P25, would fractionally add to the mass of TiO<sub>2</sub> coated on the surface of glass beads.

Based on the assumption that all the beads are coated evenly, the mass of TiO<sub>2</sub> coated on the glass beads can be further used to approximate the thickness of coating. The diameter of the glass beads varies between 1.0 to 1.2 mm (Potters Inc.). Taking an average diameter of 1.1 mm of uncoated bead and  $4.0 \text{ g/cm}^3$  as the density of TiO<sub>2</sub> (3.84 – 4.26, Fisher Scientific), the thickness of the coating is calculated as  $2.0 \pm 0.1 \text{ }\mu\text{m}$  as compared to  $9.9 \text{ }\mu\text{m}$  found using ESEM.

Using the BET surface area for glass beads coated with *Mixture F* by *Method 3* and the total mass of TiO<sub>2</sub> coated on the beads, the surface area covered by a unit mass of TiO<sub>2</sub> loaded can be calculated. The BET surface area equals  $0.284 \text{ m}^2/\text{g}$ . Since the mass of TiO<sub>2</sub> loaded is  $3.1 \times 10^{-5} \text{ g/bead}$  and the bead mass is  $0.001847 \pm 5.4 \times 10^{-5} \text{ g/bead}$ , the area covered per gram of loaded TiO<sub>2</sub> equals  $16.9 \pm 1.0 \text{ m}^2/\text{g}$  of TiO<sub>2</sub>. For the glass beads coated with *Mixture C* by *Method 2*, the BET surface area is  $0.09 \text{ m}^2/\text{g}$  of beads. Thus,

the area covered per gram of loaded TiO<sub>2</sub> equals  $5.0 \pm 0.3 \text{ m}^2/\text{g}$  of TiO<sub>2</sub>. The two values of area covered per mass of coated TiO<sub>2</sub> for two different methods indicate that the latter method would have an increased number of active sites.

### **4.3. EXPERIMENTS ANALYZING PHOTOCATALYTIC EFFICIENCY**

The results of various experiments performed were analyzed to check (i) the photocatalytic activity of coated TiO<sub>2</sub>, (ii) the consistency of the coating method, (iii) loss of coating due to repeated use of catalyst, (iv) disinfection efficiency and (v) relationships between two reactors to show the effects of light source on the pollutant removal efficiency

#### ***4.3.1. Formaldehyde Photodegradation Using Vertically Oriented Prototype Reactor***

Initially, formaldehyde was used to confirm the photocatalytic activity of coated TiO<sub>2</sub>. The glass beads used as supporting media were coated with *Mixture C* by *Method 1*. For the control run with uncoated glass beads, two columns were connected in series with a flow rate of 0.35 ml/min from each column to give a total HRT of 60 min and loaded with formaldehyde concentration of 77  $\mu\text{M}$ , pH  $5.0 \pm 0.2$ , ionic strength  $1.7 \times 10^{-2}$  M NaClO<sub>4</sub> and sample saturated with O<sub>2</sub>. The experiment yielded no significant degradation of formaldehyde (76  $\mu\text{M}$  effluent concentration). Formaldehyde degradation experimental results are shown in Table 4.3, using the vertically oriented prototype reactor with a circular column. The data set shows each point as an individual sample measurement for the same experiment taken after at least 1.5 – 2 HRTs, so as to achieve steady state conditions.

**Table 4.3. Formaldehyde photodegradation using vertically oriented prototype reactor and glass beads coated with Method 1. The values for single column experiments with 0.23 ml/min flow rate have not been recorded due to failure in connections.**

Flow Rate Q (ml/ min)	Single Column				Double Column			
		Formaldehyde Concentration				Formaldehyde Concentration		
	HRT t = V/Q (min)	Initial Conc. C <sub>0</sub> (μM)	Final Conc. C (μM)	C-C <sub>0</sub> (μM)	HRT t = V/Q (min)	Initial Conc. C <sub>0</sub> (μM)	Final Conc. C (μM)	C-C <sub>0</sub> (μM)
0.23	46	-	-	-	92	135	95.4	-39.6
0.23	46	-	-	-	92	143	97.1	-45.9
0.23	46	-	-	-	92	136	89.6	-46.4
0.28	38	150	132	-18	76	143	100	-33
0.28	38	150	128	-22	76	143	113	-30
0.28	38	150	130	-20	76	143	107	-36

Due to slight difference in the influent concentration ( $C_0$ ), a graph of ( $C - C_0$ ) as a function of HRT ( $\bar{t}$ ) (Figure 4.8) is plotted. The formaldehyde degradation data show a straight line relationship, which resembles zero order degradation, as seen by Arana et al. (2004) for formaldehyde degradation using suspended Degussa P25 as catalyst in a 250 ml glass vessel reactor at pH 5.0. The rate constant for formaldehyde degradation based on a zero order reaction can be found by:

$$C = C_0 - k\bar{t} \quad [4.1]$$

where,  $k$  is the zero order rate constant ( $\mu\text{M}/\text{min}$ ),  $\bar{t}$  is the hydraulic retention time (min),  $C$  is the concentration of formaldehyde at time  $\bar{t}$  ( $\mu\text{M}$ ) and  $C_0$  is the initial concentration of formaldehyde ( $\mu\text{M}$ ).

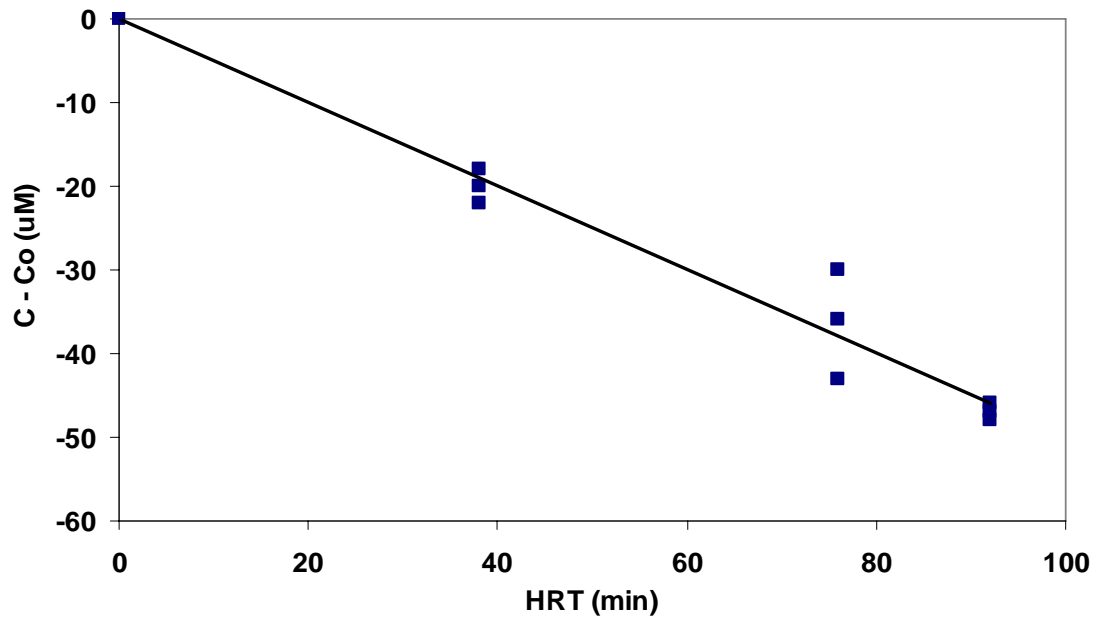


**Figure 4.8. Formaldehyde degradation curve using vertically oriented prototype reactor and glass beads coated by with *Mixture C* by *Method 1*. pH  $5.0 \pm 0.2$ , ionic strength  $1.72 \times 10^{-2}$  M NaClO<sub>4</sub>, DO saturated with O<sub>2</sub>, data evaluated using MS Excel.**

Data fitting was carried out using MS Excel and Eq. 4.1 to calculate a zero order degradation rate constant ( $k$ ) of  $0.5 \mu\text{M}/\text{min}$  and  $R^2 = 0.952$ . The formaldehyde degradation rate constant can be used to indicate the photoactivity of coated TiO<sub>2</sub> on glass beads. Thus based on these results, similar experiments were conducted to evaluate degradation of *E. coli*.

#### **4.3.2. *E. coli* Degradation Using Prototype Reactor**

*E. coli* degradation was carried out in a vertically oriented packed bed plug flow reactor. The circular column was packed with glass bead coated with *Mixture C* by *Method 1*. The pH was kept at  $7.0 \pm 0.2$ , ionic strength =  $1.7 \times 10^{-2}$  M NaClO<sub>4</sub> and DO saturated with oxygen. Table 4.4 shows the bactericidal activity of TiO<sub>2</sub> photocatalyst and confirms that it was possible to deactivate this bacterium. From Table 4.4, a

reduction in number of CFU/100 ml of *E. coli* was seen, indicating photocatalytic disinfection. Disinfection requires killing and inactivation of bacteria; the goal of this research is to achieve a reduction of 3-5 log<sub>10</sub> units within 30 min of treatment period. A 5 log<sub>10</sub> reduction is considered as an acceptable disinfection (Kuhn et al., 2003), while in our case the maximum degradation seen was 2.28 log<sub>10</sub> removal in 35 mins.

Various factors like catalyst contact surface area, incident light intensity and dissolved oxygen have to be considered to increase the efficiency of the process. If the data are critically analyzed, the readings seem to be somewhat inconsistent (for the same effluent, sample duplicates or triplicates yield different results), which may be due to human error encountered while counting CFUs.

**Table 4.4. *E. coli* degradation for vertically oriented prototype PCO reactor and glass beads coated with Mixture C by Method 1. Samples were either duplicated or triplicated. pH = 7.0 ± 0.2, Ionic Strength = 1.72 x 10<sup>-2</sup> M NaClO<sub>4</sub>, DO saturated with O<sub>2</sub>. The values in bold represent average values of *E. coli* concentrations based on number of replicates. C/C<sub>0</sub> is calculated based on the average values of *E. coli* concentrations**

Flow Rate (ml/min)	HRT (min)	<i>E. coli</i> concentration		C/C <sub>0</sub>	Log (C/Co)
		Initial Conc. C <sub>0</sub> (CFU/100 ml)	Final Conc. C (CFU/100 ml)		
0.37	29	2.0 x 10 <sup>5</sup>	1.3 x 10 <sup>4</sup>	7.0 x 10 <sup>-2</sup>	-1.15
		3.5 x 10 <sup>5</sup>	1.1 x 10 <sup>4</sup>		
		1.5 x 10 <sup>5</sup>	1.8 x 10 <sup>4</sup>		
		<b>2.0 x 10<sup>5</sup></b>	<b>1.4 x 10<sup>4</sup></b>		
0.33	32	1.5 x 10 <sup>6</sup>	7.5 x 10 <sup>4</sup>	6.1 x 10 <sup>-2</sup>	-1.22
		3.7 x 10 <sup>6</sup>	1.3 x 10 <sup>5</sup>		
		1.3 x 10 <sup>6</sup>	2.0 x 10 <sup>5</sup>		
		3.7 x 10 <sup>6</sup>	2.0 x 10 <sup>5</sup>		
		<b>2.5 x 10<sup>6</sup></b>	<b>1.5 x 10<sup>5</sup></b>		

<b>Table 4.4. (Continued) Experimental data for <i>E. coli</i> photocatalytic degradation in vertically oriented prototype reactor</b>					
<b>Flow Rate (ml/min)</b>	<b>HRT (min)</b>	<b><i>E. coli</i> concentration</b>		<b>C/C<sub>0</sub></b>	<b>Log (C/C<sub>0</sub>)</b>
		<b>Initial Conc. C<sub>0</sub> (CFU/100 ml)</b>	<b>Final Conc. C (CFU/100 ml)</b>		
0.31	34	1.0 x 10 <sup>5</sup>	8.4 x 10 <sup>3</sup>	4.4 x 10 <sup>-2</sup>	-1.35
		2.3 x 10 <sup>5</sup>	7.8 x 10 <sup>3</sup>		
		2.7 x 10 <sup>5</sup>	8.5 x 10 <sup>3</sup>		
		2.1 x 10 <sup>5</sup>	9.0 x 10 <sup>3</sup>		
		<b>1.9 x 10<sup>5</sup></b>	<b>8.4 x 10<sup>3</sup></b>		
0.30	35	1.1 x 10 <sup>6</sup>	6.8 x 10 <sup>4</sup>	5.8 x 10 <sup>-2</sup>	-1.24
		1.3 x 10 <sup>6</sup>	7.0 x 10 <sup>4</sup>		
		<b>1.2 x 10<sup>6</sup></b>	<b>6.9 x 10<sup>4</sup></b>		
0.30	35	4.0 x 10 <sup>6</sup>	2.1 x 10 <sup>4</sup>	5.2 x 10 <sup>-3</sup>	-2.28
		4.0 x 10 <sup>6</sup>	2.2 x 10 <sup>4</sup>		
		<b>4.0 x 10<sup>6</sup></b>	<b>2.1 x 10<sup>4</sup></b>		

Once the prototype reactor was used to optimize the coating method and sol preparation using methyl orange as target pollutant, *E. coli* experiments were again conducted to check the disinfection efficiency of the optimized reactor. The experiments were performed under similar conditions as explained in *Experiment 2*. Table 4.5 presents the data for experiments performed for the optimized reactor with glass beads coated with *Mixture F* by *Method 3*.

Based on the results obtained by Dunlop et al. (2002), Cho et al. (2003) and Sun et al. (2003), the photocatalysis of *E. coli* is characterized by pseudo first order kinetic behavior. Due to different input concentrations, it would be awkward to plot *E. coli* concentration as a function of HRT, so a linearized plot of (C/C<sub>0</sub>) as a function of HRT should provide a pseudo first order kinetic fit.

$$C = C_0 \exp^{-k\tau} \quad [4.2]$$

where,  $k$  is the first order rate constant ( $\text{min}^{-1}$ ) and  $\bar{t}$  is the hydraulic retention time (min),  $C_0$  and  $C$  being the initial and final concentration of *E. coli* (CFU/100 ml).

**Table 4.5. Experimental data for *E. coli* photocatalytic degradation with dark and light control in the horizontally oriented prototype reactor packed with glass beads coated with *Mixture F* by *Method 2* under pH of  $7.0 \pm 0.2$ ,  $1.7 \times 10^{-2}$  M  $\text{NaClO}_4$  ionic strength and saturated DO. The values in bold represent average values of *E. coli* concentrations.  $C/C_0$  is calculated based on the average values of *E. coli* concentrations**

Flow Rate (ml/min)	HRT (min)	<i>E. coli</i> Concentration		$C/C_0$	Log ( $C/C_0$ )
		Initial Conc. $C_0$ (CFU/100 ml)	Final Conc. $C$ (CFU/100 ml)		
DARK CONTROL					
0.89	12.1	$9.5 \times 10^6$	$6.8 \times 10^5$	$6.8 \times 10^{-1}$	-0.17
		$1.1 \times 10^6$	$7.2 \times 10^5$		
		<b><math>1.0 \times 10^6</math></b>	<b><math>7.0 \times 10^5</math></b>		
0.42	25.7	$9.5 \times 10^5$	$8.5 \times 10^5$	$8.1 \times 10^{-1}$	-0.09
		$1.1 \times 10^6$	$8.1 \times 10^5$		
		<b><math>1.0 \times 10^6</math></b>	<b><math>8.3 \times 10^5</math></b>		
0.40	27.0	$2.2 \times 10^5$	$1.5 \times 10^5$	$9.0 \times 10^{-1}$	-0.05
		$2.8 \times 10^5$	$3.0 \times 10^5$		
		<b><math>2.5 \times 10^5</math></b>	<b><math>2.2 \times 10^5</math></b>		
LIGHTED CONTROL					
0.60	18.0	$3.0 \times 10^6$	$5.5 \times 10^5$	$1.3 \times 10^{-1}$	-0.89
		$4.0 \times 10^6$	$3.5 \times 10^5$		
		<b><math>3.5 \times 10^6</math></b>	<b><math>4.5 \times 10^5</math></b>		
0.49	22.0	$6.0 \times 10^6$	$8.5 \times 10^5$	$1.2 \times 10^{-1}$	-0.92
		$8.0 \times 10^6$	$8.0 \times 10^5$		
		-	$9.0 \times 10^5$		
0.36	30	$3.0 \times 10^6$	$2.0 \times 10^5$	$5.7 \times 10^{-1}$	-1.24
		$4.0 \times 10^6$	$2.0 \times 10^5$		
		<b><math>3.5 \times 10^6</math></b>	<b><math>2.0 \times 10^5</math></b>		
PHOTOCATALYSIS					
0.86	12.5	$2.6 \times 10^6$	$1.0 \times 10^6$	$3.2 \times 10^{-1}$	-0.49
		$2.8 \times 10^6$	$7.5 \times 10^5$		
		<b><math>2.7 \times 10^6</math></b>	<b><math>8.7 \times 10^5</math></b>		
0.71	15.2	$8.3 \times 10^6$	$1.5 \times 10^6$	$1.9 \times 10^{-1}$	-0.73
		$8.7 \times 10^6$	$1.6 \times 10^6$		
		<b><math>8.5 \times 10^6</math></b>	<b><math>1.6 \times 10^6</math></b>		

<b>Table 4.5. (continued) Experimental data for <i>E. coli</i> photocatalytic degradation in horizontally oriented prototype reactor</b>					
<b>Flow Rate (ml/min)</b>	<b>HRT (min)</b>	<b><i>E. coli</i> Concentration</b>		<b>C/C<sub>0</sub></b>	<b>Log (C/C<sub>0</sub>)</b>
		<b>Initial Conc. C<sub>0</sub> (CFU/100 ml)</b>	<b>Final Conc. C (CFU/100 ml)</b>		
0.55	19.5	3.5 x 10 <sup>6</sup>	2.0 x 10 <sup>4</sup>	6.3 x 10 <sup>-3</sup>	-2.20
		4.5 x 10 <sup>6</sup>	3.0 x 10 <sup>4</sup>		
		<b>4.0 x 10<sup>6</sup></b>	<b>2.5 x 10<sup>4</sup></b>		
0.46	23.3	3.0 x 10 <sup>6</sup>	1.0 x 10 <sup>4</sup>	2.8 x 10 <sup>-4</sup>	-2.56
		5.0 x 10 <sup>6</sup>	1.2 x 10 <sup>4</sup>		
		<b>4.0 x 10<sup>6</sup></b>	<b>1.1 x 10<sup>4</sup></b>		
0.42	25.7	1.1 x 10 <sup>7</sup>	3.0 x 10 <sup>4</sup>	3.3 x 10 <sup>-3</sup>	-2.48
		1.3 x 10 <sup>7</sup>	5.0 x 10 <sup>4</sup>		
		<b>1.2 x 10<sup>7</sup></b>	<b>4.0 x 10<sup>4</sup></b>		
0.41	26.3	3.0 x 10 <sup>6</sup>	4.0 x 10 <sup>3</sup>	1.1 x 10 <sup>-3</sup>	-2.95
		5.0 x 10 <sup>6</sup>	5.0 x 10 <sup>3</sup>		
		<b>4.0 x 10<sup>6</sup></b>	<b>4.5 x 10<sup>3</sup></b>		
0.35	30.9	1.1 x 10 <sup>7</sup>	1.5 x 10 <sup>4</sup>	1.3 x 10 <sup>-3</sup>	-2.95
		1.3 x 10 <sup>7</sup>	1.2 x 10 <sup>4</sup>		
		<b>1.2 x 10<sup>7</sup></b>	<b>1.3 x 10<sup>4</sup></b>		
0.34	31.7	5.6 x 10 <sup>5</sup>	5.0 x 10 <sup>2</sup>	1.1 x 10 <sup>-3</sup>	-2.97
		6.0 x 10 <sup>5</sup>	7.0 x 10 <sup>2</sup>		
		-	6.5 x 10 <sup>2</sup>		
		<b>5.8 x 10<sup>5</sup></b>	<b>6.2 x 10<sup>2</sup></b>		
0.25	43.2	1.2 x 10 <sup>7</sup>	3.4 x 10 <sup>2</sup>	2.8 x 10 <sup>-5</sup>	-4.56
		1.4 x 10 <sup>7</sup>	-		
		<b>1.3 x 10<sup>7</sup></b>	<b>3.4 x 10<sup>2</sup></b>		

Figure 4.9 presents the linearized plot for *E. coli* photocatalytic degradation as a function of HRT. Following an initial lag phase in the first 10 min (as also seen by Dunlop et al. (2002) and Cho et al. (2003)), the rate of disinfection followed pseudo first order kinetics, as also seen by Kuhn et al. (2003) and Kim et al. (2002b). The pseudo first order rate constant for the photocatalytic experiment was found to be 0.29 min<sup>-1</sup>, while for the light control experiment the rate was 0.066 min<sup>-1</sup> and for dark control experiments the removal was less than 0.2 log<sub>10</sub> after 27 mins of HRT.

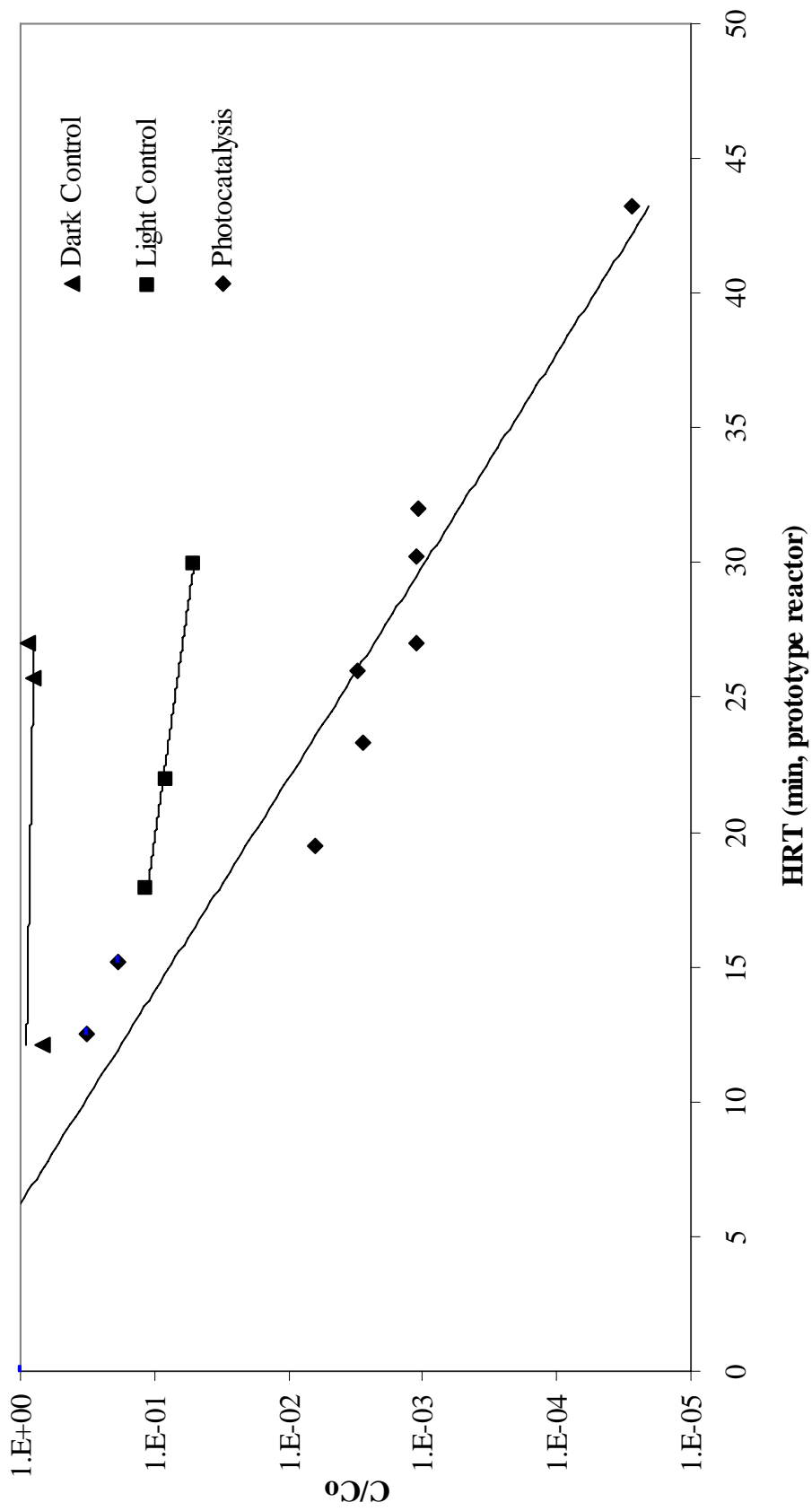


**Figure 4-9. Linearized data for *E. coli* photocatalytic degradation with dark and light controls in horizontally oriented prototype reactor. pH = 6.0 ± 0.2, Ionic Strength = 1.7 x 10<sup>-2</sup> M NaClO<sub>4</sub>, DO saturated with O<sub>2</sub> and data evaluated using MS Excel.**

### 4.3.3. Methyl Orange Photodegradation Using Horizontally Oriented Prototype

#### Reactor

To modify the reactor and increase the efficiency of the PCO, degradation of methyl orange was performed to examine the different factors which can affect the process. Table 4.6 shows data for various experiments performed for methyl orange degradation and the efficiencies for the 5 different experimental sets are compared. A remarkable change in fractional degradation ( $1-C/C_0$ ) between the experiments performed without supplemental  $TiO_2$  (i.e., *Mixture C* and *Method 2*; 34% for 20 min HRT) and with the supplement  $TiO_2$  powder (i.e., *Mixture F* and *Method 3*; 78% for 20 min HRT) to the sol gel synthesis was seen. These results indicate that addition of  $TiO_2$  P25 powder increases the PCO rate, which may be attributed to the increased surface area and the roughness of coating.

**Table 4.6. Photocatalytic degradation of methyl orange over glass beads coated with different sol mixtures and coating methods in horizontally oriented prototype reactor. pH =  $6.0 \pm 0.2$ , Ionic Strength =  $1.72 \times 10^{-2}$  M  $NaClO_4$ , DO saturated with  $O_2$ .**

Flow Rate (ml/min)	HRT (min)	Methyl Orange Concentration		C/C <sub>0</sub>
		Initial Conc. C <sub>0</sub> (mg/L)	Final Conc. C (mg/L)	
<i>Mixture C and Method 2</i>				
2.50	4.5	31.3	28.9	0.92
0.91	12.4	31.3	23.9	0.77
0.50	22.6	31.3	21.6	0.69
0.50	22.6	31.3	20.8	0.66
0.45	25.1	31.3	19.7	0.63
0.45	25.1	31.3	19.1	0.61
0.20	56.5	31.3	12.7	0.41
<i>Mixture C and Method 2</i>				
1.47	7.4	20.3	17.5	0.86
1.32	8.2	20.3	17.2	0.84
0.53	21.5	20.5	13.6	0.66

<b>Table 4.6. (continued) Photocatalytic degradation of methyl orange in horizontally oriented prototype reactor</b>				
<b>Flow Rate (ml/min)</b>	<b>HRT (min)</b>	<b>Methyl Orange Concentration</b>		<b>C/C<sub>0</sub></b>
		<b>Initial Conc. C<sub>0</sub> (mg/L)</b>	<b>Final Conc. C (mg/L)</b>	
0.53	21.5	20.5	13.8	0.67
0.47	24.1	20.5	12.6	0.62
0.47	24.1	20.5	12.2	0.60
0.15	74.6	20.3	7.2	0.36
<i>Mixture E and Method 3</i>				
0.81	14.0	28.9	28.9	0.55
0.81	14.0	28.9	16.0	0.55
0.41	27.8	28.9	15.9	0.22
0.41	27.8	28.9	6.30	0.22
<i>Mixture D and Method 3</i>				
0.73	15.5	30.1	15.9	1.00
0.73	15.5	30.1	16.2	0.53
0.54	20.9	30.1	10.5	0.54
0.54	20.9	30.1	10.5	0.35
0.50	22.6	30.1	8.80	0.35
0.16	70.5	30.1	1.00	0.29
<i>Mixture F and Method 3</i>				
0.96	11.8	32.7	21.9	0.67
0.96	11.8	32.7	18.7	0.57
0.75	15.1	32.7	13.1	0.40
0.75	15.1	32.7	13.4	0.41
0.52	21.9	32.7	7.20	0.22
0.52	21.9	32.7	8.50	0.26
<i>Mixture F and Method 3 – Glass beads reused</i>				
1.54	7.0	28	24.9	0.89
0.54	20.0	28	16.9	0.61
0.41	26.3	28	14.6	0.52
0.31	35.0	28	10.3	0.37

These data are plotted in Figure 4.10. It can be seen that when sample was illuminated, an initial fast degradation occurred, followed by a steady decay, as also seen by Nam et al. (2002) and Bao et al. (2004) for methyl orange degradation.

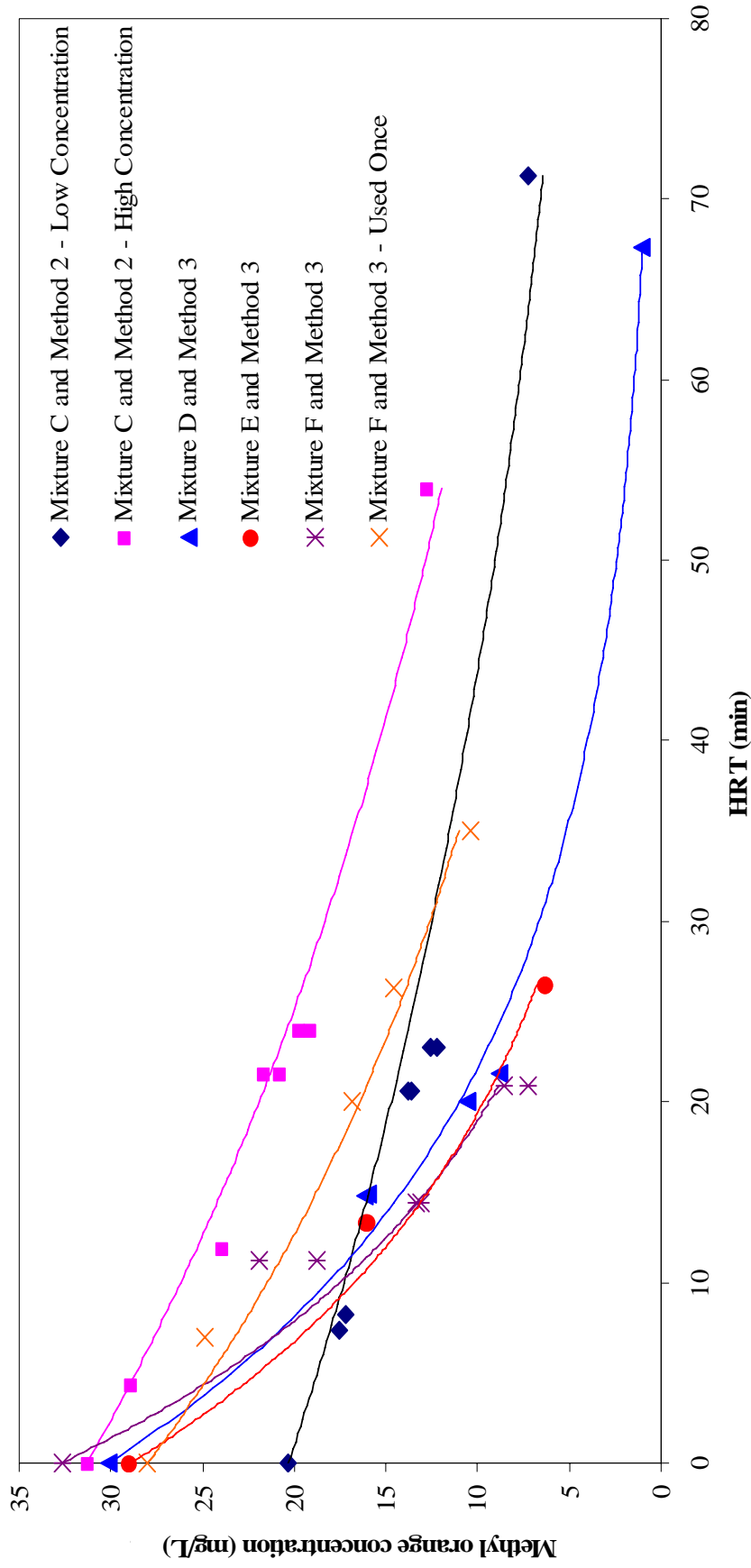


Figure 4.10. Photocatalytic degradation of methyl orange in horizontally oriented prototype reactor indicating a pseudo first order degradation pattern. Points indicate experimental data while lines indicate concentration calculated from first order kinetic model. pH =  $6.0 \pm 0.2$ , Ionic Strength =  $1.7 \times 10^{-2}$  M NaClO<sub>4</sub>, DO saturated with O<sub>2</sub>, Mixture D, E and F synthesized by supplementing P25 TiO<sub>2</sub> powder.

Thus, the photodegradation of methyl orange in water can be described according to Figure 4.10 as pseudo first order degradation. The first order degradation rate constant can be found by using following equation:

$$C = C_0 \exp(-k\bar{t}) \quad [4.3]$$

Based on Eq. 4.3, a pseudo –first order linearized graph can be plotted for  $\log C/C_0$  as a function of HRT ( $\bar{t}$ ), as shown in Figure 4.11. The values of rate constant ( $k$ ) are listed in Table 4.7 with their respective  $R^2$  values (obtained using MS Excel).

**Table 4.7. Pseudo first order methyl orange degradation rate constant values for different photocatalytic experiments performed in horizontally oriented prototype reactor. pH = 6.0 ± 0.2, Ionic Strength = 1.72 x 10<sup>-2</sup> M NaClO<sub>4</sub>, DO saturated with O<sub>2</sub>.**

Method	k (min <sup>-1</sup> )	R <sup>2</sup>
<i>Mixture C and Method 2 – Low Concentration</i>	0.016	0.9134
<i>Mixture C and Method 2 – High Concentration</i>	0.018	0.9754
<i>Mixture D and Method 3</i>	0.050	0.9926
<i>Mixture E and Method 3</i>	0.055	0.9730
<i>Mixture F and Method 3</i>	0.062	0.9078
<i>Mixture F and Method 3 – Reused after one photocatalytic experiment</i>	0.027	0.9818

From Table 4.7, it can be seen that the first order rate constant values for *Mixture F and Method 3* is greater by a factor of 3.5 as compared to that of *Mixture C and Method 2*. If the 3 experiments with Mixtures D, E and F are compared, it can be seen that there has been an incremental change in the rate constant values, but the values are marginally different and can be easily affected by the number of readings taken while calculating the rate constant.

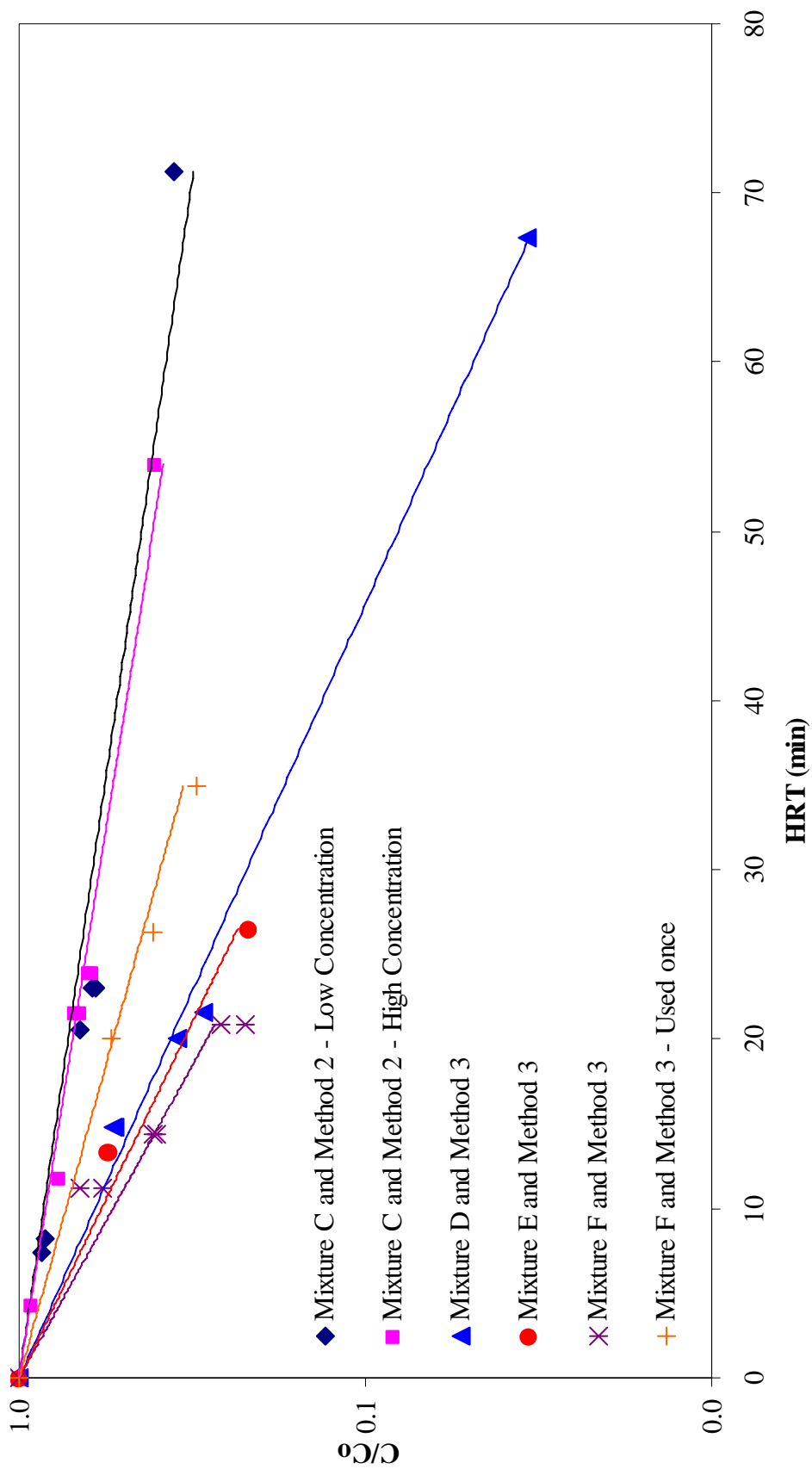


Figure 4.11. Linearized graph for methyl orange degradation in horizontally oriented prototype reactor to obtain pseudo first order rate constant value for each experiment. Mixture D, E and F contains supplemental 0.5 g TiONa, 0.25 g P25 and 0.5 g P25 TiO<sub>2</sub> powder, respectively. pH = 6.0 ± 0.2, Ionic Strength = 1.7 x 10<sup>-2</sup> M NaClO<sub>4</sub>, DO saturated with O<sub>2</sub> and data evaluated

Over many years of research, P25 has been found to be the most photocatalytic active form of TiO<sub>2</sub> (Mills and Le Hunte, 1997; Lee et al., 2002; Bao et al., 2004). Thus, the increase in photocatalytic activity can be attributed to the supplemental P25 TiO<sub>2</sub> added during sol gel synthesis, which not only is photocatalytically active but also helps in increasing the total TiO<sub>2</sub> surface area.

The results obtained from the BET experiments indicate a reduced BET surface area (by a factor of 1.4) for glass beads which have been used once as compared to the glass beads which have not been used before for photocatalytic experiment. To illustrate that the coated TiO<sub>2</sub> gets etched from the surface of glass beads not due to photocatalysis but due to the abrasion created while packing, unpacking the column and washing them with DI water, similar methyl orange experiments were conducted at various HRTs. Data for the experiment are presented in Table 4.6 and are plotted in Figure 4.10. Figure 4.11 gives linearized data for  $C/C_0$  as a function of HRT and the slope of the line provide the rate constant, which was equal to  $0.027 \text{ min}^{-1}$ , calculated using MS Excel. Thus, the first order rate constant decreased by a factor of 1.8 for the used glass beads as compared to the unused glass beads coated with *Mixture F* by *Method 3*.

To examine the reproducibility of coated TiO<sub>2</sub> experiments in the prototype PCO reactor, several experiments were performed using separate batches of glass beads coated with *Mixture F* and *Method 3* for each experiment. The results for the experiments are given in Table 4.8 and plotted in Figure 4.12. Since methyl orange degradation has been described as a first order reaction, the data can be further linearized to predict a first order rate constant (Figure 4.13). Except for one experiment (32.7 mg/L), all experiments were performed with initial concentration of  $30.5 \pm 0.2 \text{ mg/L}$ . Therefore the combined rate

constant was calculated by using influent concentration of 30.5 mg/L for all the three data sets. Figure 4.12 shows that the first order kinetic model (Eq. 4.3) gives a good fit to the experimental data and the value of rate constant from the linearized graph was found to be  $0.05 \text{ min}^{-1}$  with an  $R^2$  value of 0.9248, indicating a good fit to the data.

**Table 4.8. Photocatalytic degradation of methyl orange under identical experimental conditions using  $\text{TiO}_2$  prepared with *Mixture F* and beads coated by *Method 3*.  $\text{pH} = 6.0 \pm 0.2$ , Ionic Strength =  $1.72 \times 10^{-2} \text{ M NaClO}_4$  and DO saturated with  $\text{O}_2$ .**

Flow rate (ml/min)	HRT (min)	Methyl orange concentration		C/C <sub>0</sub>
		Initial Conc. C <sub>0</sub> (mg/L)	Final Conc. C (mg/L)	
DARK CONTROL				
0.74	15	30.6	30.6	1.00
0.46	23	30.6	30.5	1.00
0.37	29	30.6	30.5	1.00
0.26	41	30.6	30.5	1.00
LIGHT CONTROL				
0.78	14	30.8	30.4	0.99
0.34	32	30.8	29.7	0.96
0.28	39	30.8	29.5	0.96
0.25	43	30.8	29.4	0.95
PHOTOCATALYSIS BATCH -1				
0.96	11.2	32.7	21.9	0.67
0.96	11.2	32.7	18.7	0.57
0.75	14.4	32.7	13.1	0.40
0.75	14.4	32.7	13.4	0.41
0.52	20.9	32.7	7.2	0.22
0.52	20.9	32.7	8.5	0.26
PHOTOCATALYSIS BATCH -2				
2.22	5	30.7	25.3	0.82
0.90	12	30.7	18.3	0.60
0.55	19	30.7	12.5	0.41
0.39	27	30.7	5.9	0.19
0.30	36	30.7	3.6	0.12
0.14	75	30.7	1.1	0.04
PHOTOCATALYSIS BATCH -3				
1.30	8	30.2	21.9	0.72
0.80	13	30.2	16.9	0.56
0.50	21	30.2	13.5	0.45

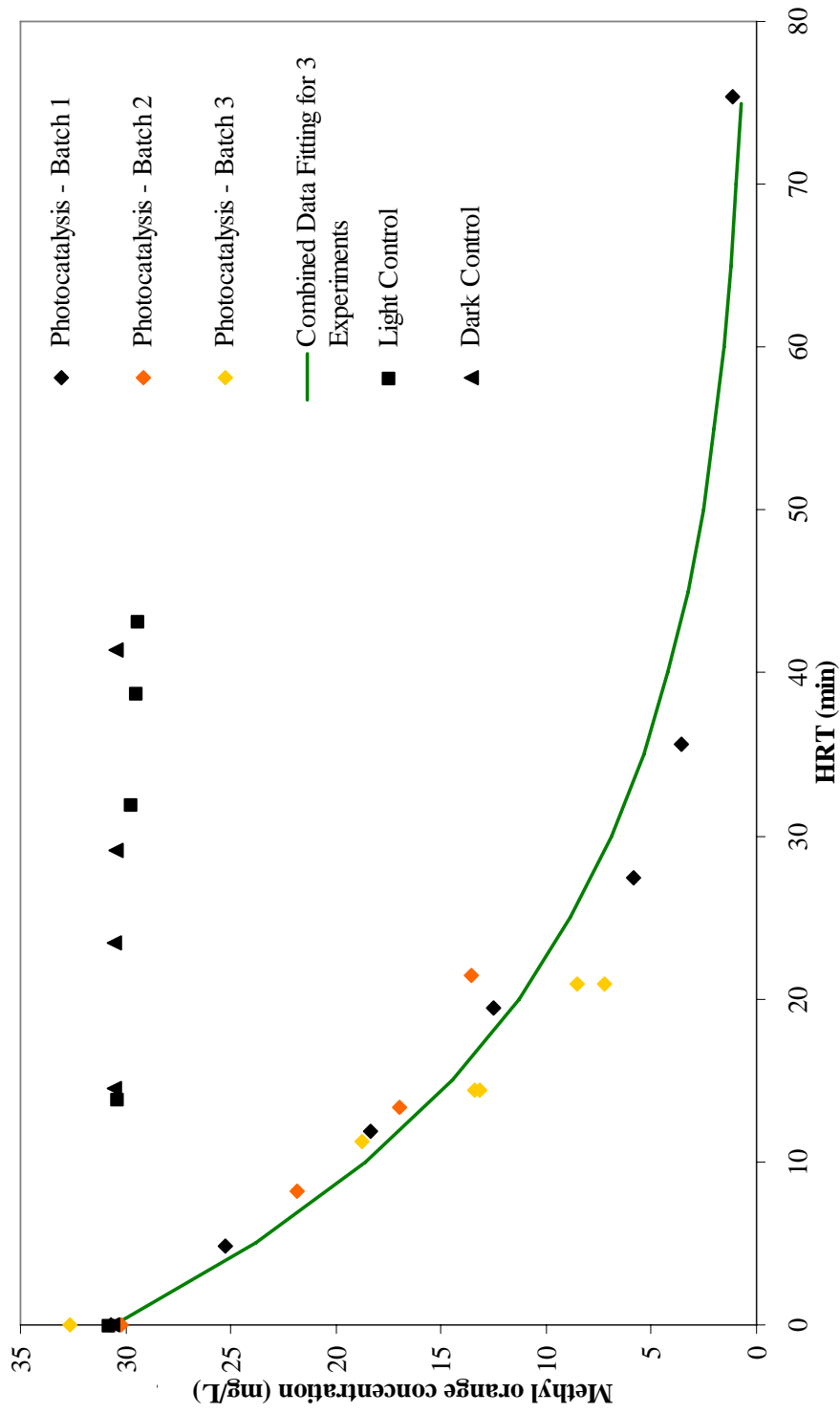


**Figure 4.12. Methyl orange degradation graph to analyze the reproducibility of TiO<sub>2</sub> synthesis (*Mixture F*) and coating (*Method 3*) method. pH = 6.0 ± 0.2, Ionic Strength = 1.72 x 10<sup>-2</sup> M NaClO<sub>4</sub>, DO saturated with O<sub>2</sub>. Each experiment was performed using freshly prepared batch of glass bead coated with *Mixture F* by *Method 3*. The photocatalytic experiment data are represented by 3 separate experiments performed under identical conditions**

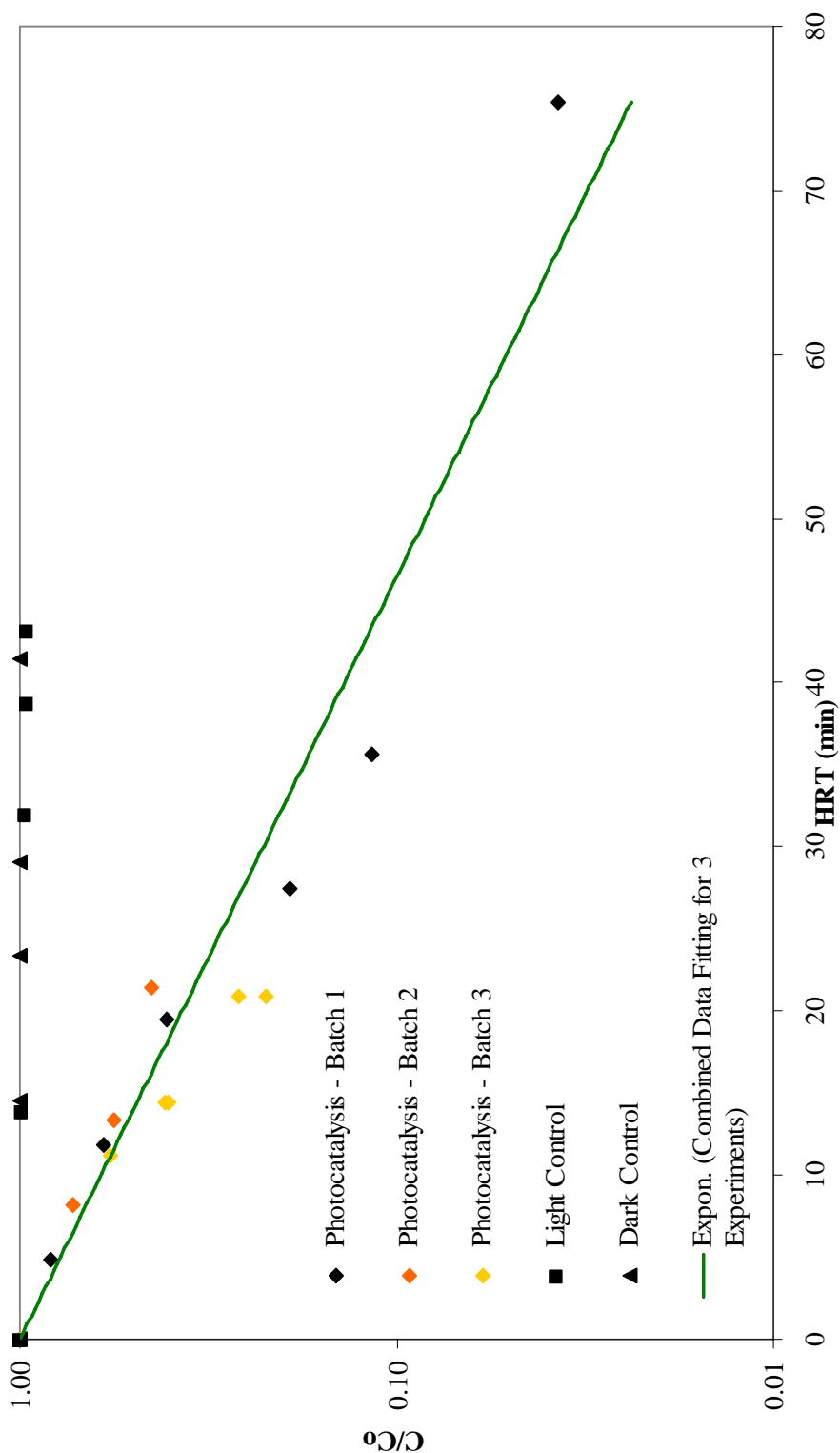


**Figure 4.13. Linearized graph for pseudo first order methyl orange degradation. pH = 6.0 ± 0.2, Ionic Strength = 1.72 x 10<sup>-2</sup> M NaClO<sub>4</sub>, DO saturated with O<sub>2</sub>. All photocatalytic experimental data have been combined to provide a first order rate constant that would fit individual experimental data sets.**

Results for the control experiments showed negligible (UV alone, TiO<sub>2</sub> alone) or no removal (glass beads coated with *Mixture F* by *Method 3*) of methyl orange.

Comparing the combined rate constant ( $0.050 \text{ min}^{-1}$ ) obtained from Figure 4.13 with the individual rate constants for the 3 experiments with glass beads coated with *Mixture F* and *Method 3*, the rate constants vary from  $0.065 \text{ min}^{-1}$  ( $R^2 = 0.9632$ ) to  $0.039 \text{ min}^{-1}$  ( $R^2 = 0.9881$ ). To calculate the rate constants (for  $0.039$  and  $0.065 \text{ min}^{-1}$ ) only 3 HRT values were used in the experiment, which can produce some inaccuracy. For batch 2, the experiment with more data, the rate constant value  $0.048 \text{ min}^{-1}$  ( $R^2 = 0.9509$ ) is very close to the combined rate constant  $0.05 \text{ min}^{-1}$  ( $R^2 = 0.9248$ ).

Thus, it can be concluded that supplementing  $\text{TiO}_2$  powder during the sol gel synthesis process not only increases BET surface area by a factor of 1.4 but also results in increased roughness on the coated surface as observed in the ESEM micrograph (Figure 4.5) and an increase in the first order methyl orange degradation rate by a factor of 1.6.

#### **4.3.4. Methyl Orange Photodegradation Using Portable Reactor**

The experimental results of methyl orange degradation in the prototype PCO reactor indicated that supplementation of  $\text{TiO}_2$  powder into the sol gel synthesis process enhances the photocatalytic degradation. A batch of beads prepared by using sol gel *Mixture F* and coating *Method 3* was packed in the square quartz column and placed in the portable LED reactor. The column was operated as a packed bed plug flow reactor while a small mixed reactor (5 ml) was connected in series with the packed bed column (Figure 3.10). The combined reactor was operated as a recirculating batch reactor with a flow rate of  $0.35 \pm 0.5 \text{ ml/min}$ .

Experiments performed with two combinations of LEDs: (i) 12 UV LED340 operating at 100 mA with 6 on each side with 3 LEDs in series each, and (ii) 12 UV

LED340 operating at 100 mA + 12 UV LED370 operating at 15 mA each, with 6 UV LED340 on the sides and 6 UV LED370 on top and bottom with 3 LEDs in series on each side. Methyl orange degradation results are provided in Table 4.9. The experimental condition in both experiments performed remained the same, i.e. pH =  $6.0 \pm 0.2$ , ionic strength =  $1.7 \times 10^{-2}$  M NaClO<sub>4</sub> and DO saturated with oxygen.

The actual illumination period in this reactor is the time that a sample is exposed to illumination during the whole experiment. Thus, the actual illumination period is the ratio of the total amount of sample circulating through the reactor (i.e., sum of sample volume in PCO reactor, mixed storage reactor and tubing) and the volume of sample under the illuminated portion (i.e., 6.15 ml), multiplied by the total illumination period. Thus, for the reactor operated as indirect recirculation, the actual illumination period will be 3.4 times less than the clock time (i.e., the total volume of sample through the reactor of 21 ml divided by 6.15 ml as the illuminated volume of sample). For the reactor operated as direct recirculation, the ratio would be 2.6 times less than the actual clock time (i.e., 16 ml as the total volume divided by 6.15 ml as the illuminated volume).

A relationship can be seen between the increase in number of LEDs (input power) and the amount of methyl orange degraded, i.e., compare experimental conditions 1 and 2 (Table 4.9). It can be seen (Figure 4.14) that with the increase in the number of LEDs in experiment 2 to twice the number in experiment 1, almost twice the amount of methyl orange can be degraded in same time. Due to the small number of data points, either a zero order or a first order kinetic model can be used to fit the data. Since it is known that methyl orange degradation follows first order kinetics (Nam et al., 2002, Bao et al., 2004, Section 4.3.3), the data can be linearized to find a rate constant for both experimental

sets. The rate constant evaluated for experiment 1 was found out to be  $0.12 \text{ hr}^{-1}$  and for experiment 2 the rate constant was  $0.20 \text{ hr}^{-1}$  with the  $R^2$  values of 0.9597 and 0.9928, respectively (Figure 4.15). The difference between the two rate constants can be attributed to the effect of increased light intensity.

**Table 4.9. Methyl orange degradation using portable reactor with indirect recirculation to illustrate the effect of light intensity. Glass beads coated with Method 3 and  $\text{TiO}_2$  prepared by Mixture F,  $\text{pH} = 6.0 \pm 0.2$ , Ionic Strength =  $1.72 \times 10^{-2} \text{ M NaClO}_4$  and DO saturated with  $\text{O}_2$ .**

Conditions	Input Power (W)	Experimental Time (hr)	Actual illumination period (hr)	Methyl orange concentration (mg/L)		C/C <sub>0</sub>
				Initial conc. C <sub>0</sub>	Final conc. C	
12 UV LED340 @ 100 mA each	6.0	0	0	16.3	16.3	1.00
		6	1.8	16.3	13.8	0.85
		8	2.4	16.3	11.9	0.73
		10	2.9	16.3	11.7	0.72
12 UV LED340 @ 100 mA + 12 UV LED370 @ 15 mA each	6.6	0	0	16.3	16.3	1.00
		6	1.8	16.3	11.9	0.73
		8	2.4	16.3	10.1	0.62
		10	2.9	16.3	8.90	0.55

Further experiments were performed in the portable reactor with indirect recirculation (i.e., using mixed storage reactor) and direct recirculation (i.e., no storage). For both experiments 12 UV LED340 (operating at 100 mA each, 6.0 W input power) and 16 UV LED370 (operating at 25 mA each, 1.4 W input power) were used as the light sources and the data for those experiments are provided in Table 4.10.

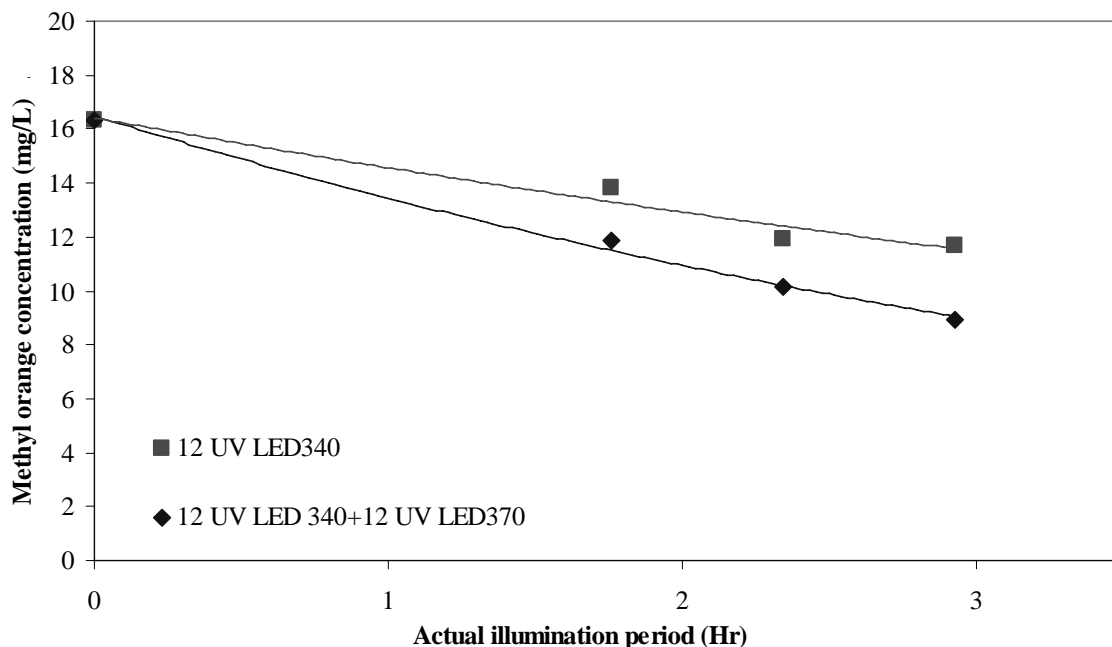


**Figure 4.14. Methyl orange degradation curve to illustrate the effect of increase in number of LEDs. pH =  $6.0 \pm 0.2$ , Ionic Strength =  $1.72 \times 10^{-2}$  M  $\text{NaClO}_4$  and DO saturated with  $\text{O}_2$ .**

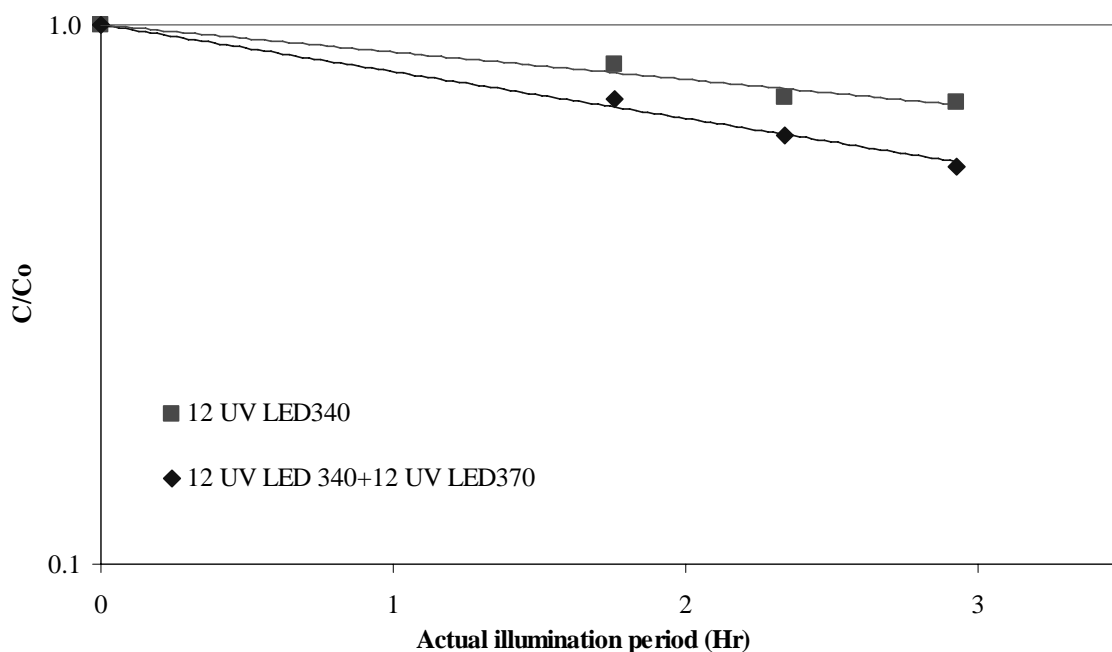


**Figure 4.15. Linearized graph for methyl orange degradation indicating a faster degradation with increased number of LEDs. pH =  $6.0 \pm 0.2$ , Ionic Strength =  $1.72 \times 10^{-2}$  M  $\text{NaClO}_4$  and DO saturated with  $\text{O}_2$  and data evaluated using MS Excel.**

**Table 4.10. Photocatalytic degradation of methyl orange under identical experimental conditions using TiO<sub>2</sub> prepared with *Mixture F* and beads coated by *Method 3* for portable reactor operated as (i) indirect recirculation and (ii) direct circulation. 12 UV LED340 (operated at 100 mA each) + 16 UV LED370 (operated at 25 mA each) were used as UV light source. The direct circulation data includes data of control experiments. pH = 6.0 ± 0.2, Ionic Strength = 1.72 x 10<sup>-2</sup> M NaClO<sub>4</sub> and DO saturated with O<sub>2</sub>. Each data point represents separate experiment performed under identical conditions.**

Illumination period (Hr)	Actual illumination period (Hr)	Methyl orange concentration		C/Co
		Initial Conc. C <sub>0</sub> (mg/L)	Final Conc. C (mg/L)	
PHOTOCATALYSIS – INDIRECT RECIRCULATION				
10	2.9	30.7	17.1	0.56
15	4.4	30.7	12.9	0.42
20	5.9	30.7	9.3	0.30
25	7.3	30.7	5.2	0.17
30	8.8	30.7	2.6	0.08
35	10.3	30.7	0.3	0.01
40	11.7	30.7	0.2	0.01
DARK CONTROL – DIRECT RECIRCULATION				
5	2.1	30.7	30.6	1.00
10	4.1	30.7	30.5	1.00
15	6.2	30.7	30.4	0.99
LIGHT CONTROL – DIRECT RECIRCULATION				
5	2.1	31.1	30.7	0.98
10	4.1	31.1	30.4	0.98
15	6.2	31.1	30.3	0.97
PHOTOCATALYSIS – DIRECT RECIRCULATION				
2.5	1.0	29.5	19.4	0.66
5	2.1	29.5	13.0	0.44
7.5	3.1	29.5	10.1	0.34
10	4.1	29.5	7.1	0.24
12.5	5.1	29.5	4.0	0.13
15	6.2	29.5	2.2	0.07

The concentration of methyl orange as a function of actual illumination period is plotted in Figure 4.16. The data for photocatalysis with direct recirculation should follow a pseudo first order degradation as the only reaction that takes place is in the illuminated area of the PCO reactor and it has been shown to follow first order kinetics in the

prototype reactor. For indirect recirculation, the graph shows that the rate is somewhere between zero and first order, and would be difficult to be reliably determined. Since there is only dilution occurring in the mixed storage reactor, the rate becomes slower for the reactor when operated as indirect recirculation. The reason the portable reactor was initially configured to operate with indirect recirculation was to saturate the effluent again with DO, but in doing so the sample in the mixed storage reactor started evaporating. After trial and error data fitting using a L-H model, the data for the experiment with the indirect recirculation did not fit, and after not considering the 10.8 hr and 12.4 hr readings for data fitting, a first order kinetic model fit the data fairly well, as shown in Figure 4.17.

The rate constant for methyl orange photocatalysis in portable reactor operated under indirect recirculation was  $0.24 \text{ hr}^{-1}$  with an  $R^2$  value of 0.9418, while for the reactor operated under direct recirculation yielded a rate constant of  $0.39 \text{ hr}^{-1}$  with an  $R^2$  value of 0.9815. Thus, the degradation rate obtained for portable reactor operated as direct recirculation can be compared to the prototype reactor using the experimental data and calculating the number of photons each reactor uses to achieve the given degradation rate.

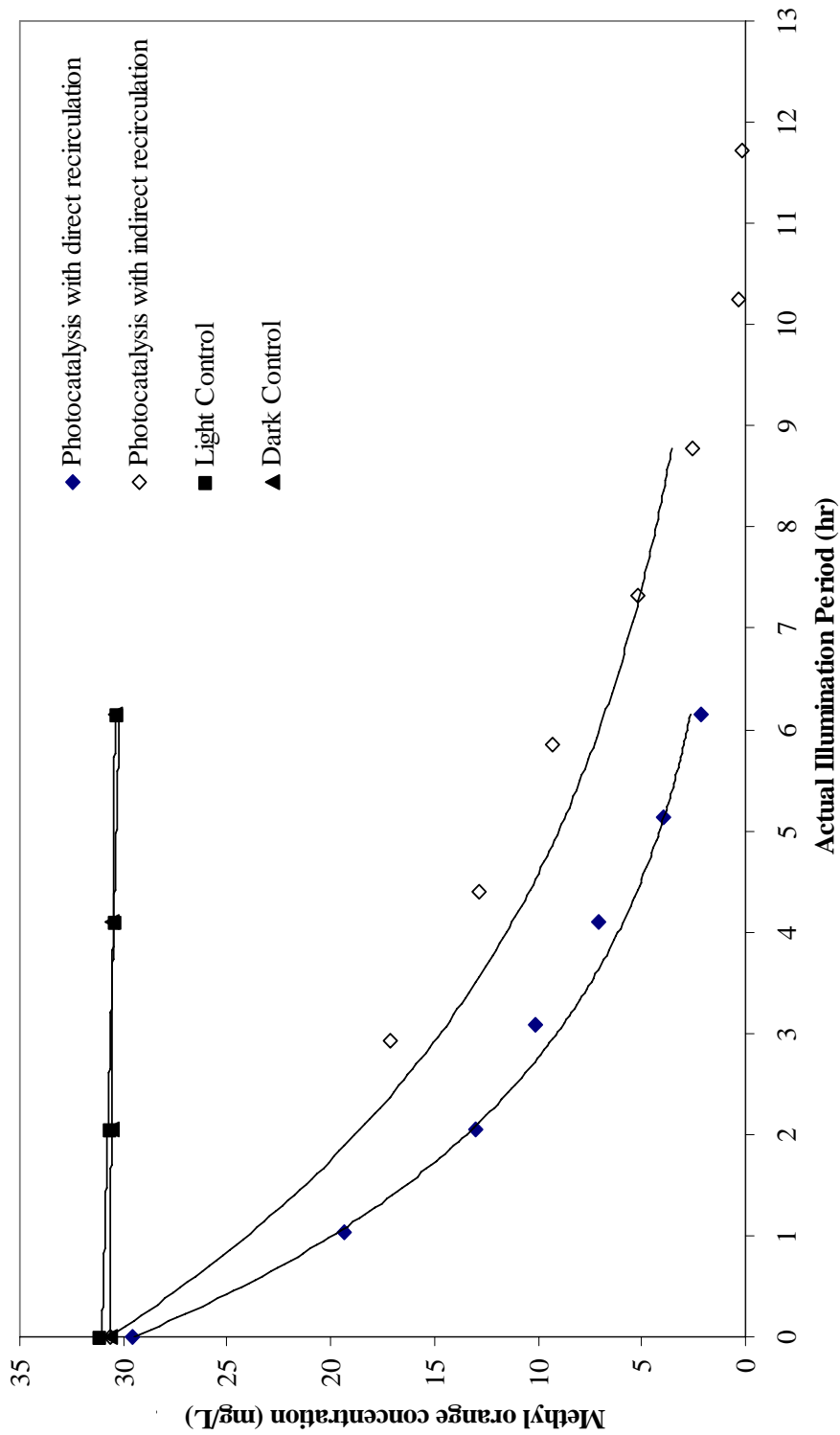


Figure 4.16. Experimental data for PCO of methyl orange for indirect and direct recirculation with control experiments for direct recirculation. 10.8 hr and 12.4 hr readings for photocatalytic experiment under indirect recirculation are not considered for estimating the first order rate constant. pH =  $6.0 \pm 0.2$ , Ionic Strength =  $1.72 \times 10^{-2}$  M NaClO<sub>4</sub> and DO saturated with O<sub>2</sub> and data evaluated using MS Excel.

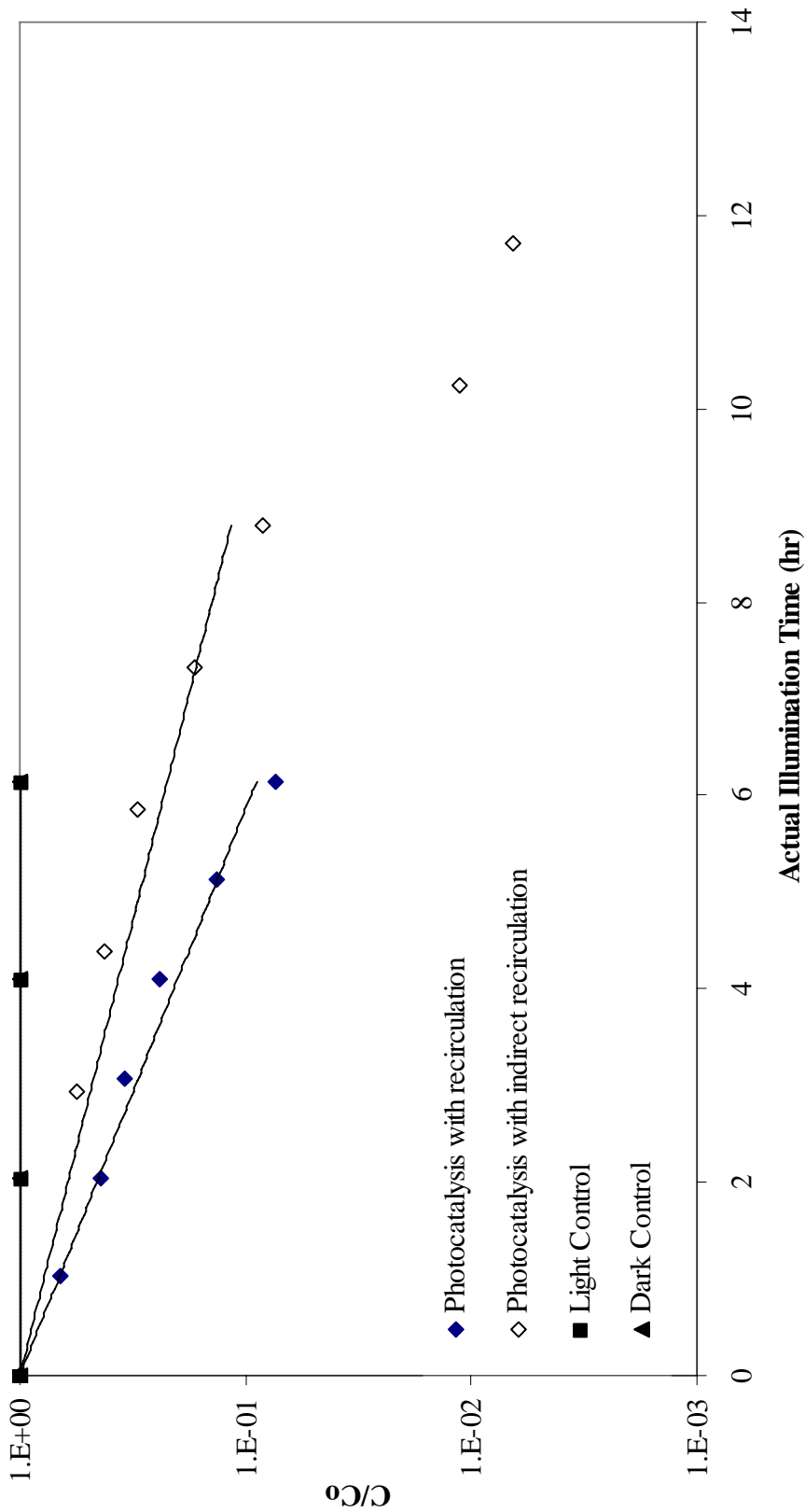


Figure 4.17. Linearized graph for pseudo first order methyl orange photocatalytic degradation. For both operating configurations, each point indicates a separate experiment performed under identical conditions. 10.8 hr and 12.4 hr readings for photocatalytic experiment under indirect recirculation are not considered for estimating the first order rate constant.  $\text{pH} = 6.0 \pm 0.2$ , Ionic Strength =  $1.72 \times 10^{-2}$  M  $\text{NaClO}_4$  and DO saturated with  $\text{O}_2$  and data evaluated with MS Excel.

#### 4.3.5. *E. coli* Photodegradation Using Portable Reactor

Based on the results of methyl orange experiments in the direct recirculation portable reactor and the *E. coli* experiments in the prototype reactor, *E. coli* photocatalytic degradation in the portable reactor under direct recirculation configuration was examined. The results for some of the control experiments in the direct recirculation system indicated higher than 3 log<sub>10</sub> removal of *E. coli* apparently due to removal by filtration, while for some experiments the results indicated growth of more than 2 log<sub>10</sub> *E. coli*. Due to such inconsistency in the results, instead of packing coated glass beads in a column and using a flow through system, glass beads were packed in two quartz cuvettes and photocatalysis experiments for batch systems were performed. The results of the photocatalytic experiments are presented in Table 4.11.

An average of 0.28 log<sub>10</sub> removal of *E. coli* was recorded due to natural decay. The *E. coli* die over 5 hrs of treatment period without undergoing any type of reaction, which can be possibly due to lack of nutrients. The natural decay of *E. coli* occurs in all the experiments and the results indicated included the degradation due to natural decay. In Figure 4.18, a 30 min HRT was required for a 3 log<sub>10</sub> removal in the prototype reactor (data obtained from Table 4.5). Assuming that the *E. coli* degradation in the portable reactor will follow the same first order kinetics, 3 log<sub>10</sub> removal requires an illumination period of 240 min.

**Table 4.11. Experimental data for *E. coli* photocatalytic degradation in portable reactor with dark and light control under pH of  $7.0 \pm 0.2$ ,  $1.7 \times 10^{-2}$  M  $\text{NaClO}_4$  ionic strength and saturated DO. The values in bold represent average values of *E. coli* concentrations.  $C/C_0$  is calculated based on the average values of *E. coli* concentrations. Natural decay of *E. coli* is obtained from measuring the influent sample before and after the experiment was conducted. The effect of natural decay is included in the readings for the *E. coli* experiments.**

Actual illumination period (min)	<i>E. coli</i> Concentration		$C/C_0$	Log ( $C/C_0$ )
	Initial Conc. $C_0$ (CFU/100 ml)	Final Conc. $C$ (CFU/100 ml)		
NATURAL DECAY				
0	$7.0 \times 10^6$	$4.0 \times 10^6$	$5.2 \times 10^{-1}$	-0.29
	$7.5 \times 10^6$	$3.5 \times 10^6$		
	<b><math>7.3 \times 10^6</math></b>	<b><math>3.8 \times 10^6</math></b>		
0	$1.3 \times 10^7$	$5.5 \times 10^6$	$5.4 \times 10^{-1}$	-0.27
	$1.4 \times 10^7$	$9.0 \times 10^6$		
	<b><math>1.4 \times 10^7</math></b>	<b><math>7.3 \times 10^6</math></b>		
DARK CONTROL				
0	$7.0 \times 10^6$	$1.1 \times 10^6$	$1.6 \times 10^{-1}$	-0.80
	$8.0 \times 10^6$	$1.2 \times 10^6$		
	<b><math>7.5 \times 10^6</math></b>	<b><math>1.2 \times 10^6</math></b>		
0	$7.0 \times 10^6$	$8.0 \times 10^5$	$1.1 \times 10^{-1}$	-0.95
	$8.0 \times 10^6$	$9.0 \times 10^5$		
	<b><math>7.5 \times 10^6</math></b>	<b><math>8.5 \times 10^5</math></b>		
LIGHT CONTROL				
300	$6.0 \times 10^6$	$1.0 \times 10^4$	$3.1 \times 10^{-3}$	-2.51
	$8.0 \times 10^6$	$3.3 \times 10^4$		
	<b><math>7.0 \times 10^6</math></b>	<b><math>2.2 \times 10^4</math></b>		
300	$6.0 \times 10^6$	$8.0 \times 10^4$	$1.1 \times 10^{-2}$	-1.94
	$8.0 \times 10^6$			
	<b><math>7.0 \times 10^6</math></b>	<b><math>8.0 \times 10^4</math></b>		
PHOTOCATALYSIS				
300	$4.0 \times 10^6$	$4.0 \times 10^2$	$1.1 \times 10^{-4}$	-3.95
	$3.2 \times 10^6$			
	<b><math>3.6 \times 10^6</math></b>	<b><math>4.0 \times 10^2</math></b>		
300	$4.0 \times 10^6$	$8.0 \times 10^2$	$2.2 \times 10^{-4}$	-3.65
	$3.2 \times 10^6$			
	<b><math>3.6 \times 10^6</math></b>	<b><math>8.0 \times 10^2</math></b>		

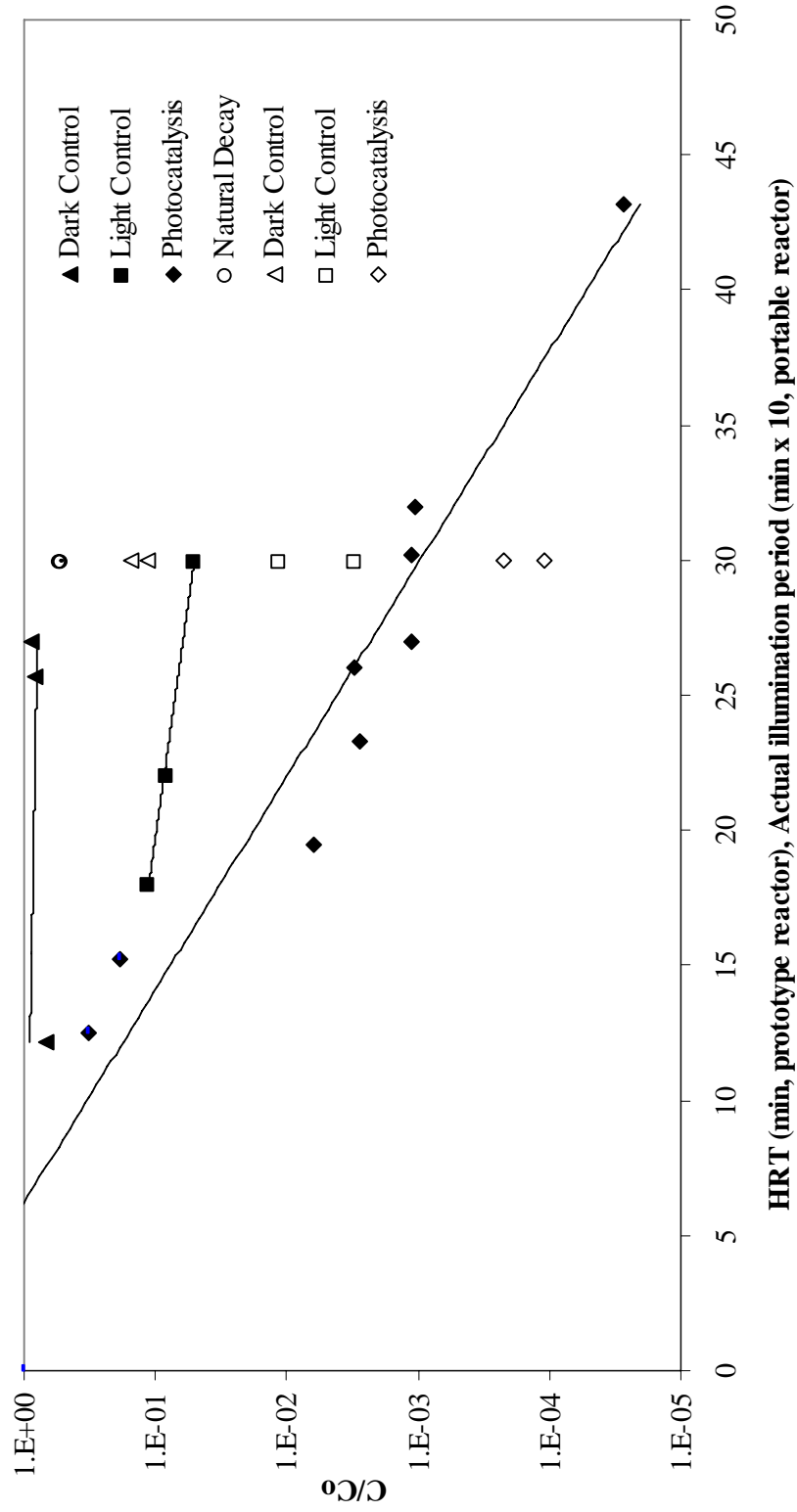


Figure 4.18. *E. coli* photocatalytic degradation in portable reactor operated as batch reactor using cuvettes to pack glass beads with dark and lighted controls. pH of  $7.0 \pm 0.2$ ,  $1.7 \times 10^{-2}$  M NaClO<sub>4</sub> ionic strength and saturated DO. The data for *E. coli* photocatalytic experiments were obtained from Table 4.5 and are represented by full symbols, while the empty symbols represent *E. coli* photocatalysis experiment data in portable reactor.

The major difference to achieve a 3 log<sub>10</sub> removal was space time (i.e., 30 min vs 240 min), which has also been seen by Chen et al. (2005), where perchloroethylene was degraded in air for two different light sources (i.e., 16 UV LED375 operating at 1 mW each resulted in 43% PCE conversion in 64 s, and 300 mW black light resulted in 90% PCE conversion in 8 s). Even though the time required for a 3 log<sub>10</sub> *E. coli* removal in the portable reactor is not satisfactory, the results prove that it is possible to use LEDs as light source for photocatalysis as a technology to disinfect drinking water.

#### **4.4. COMPARISON BETWEEN PROTOTYPE AND PORTABLE PCO REACTOR**

Using the data obtained from the prototype reactor experiments for methyl orange and the portable reactor under direct recirculation experiments, along with various assumptions, a relationship between input power, output power and methyl orange degradation can be obtained. The generalized assumptions for obtaining these relationships are:

1. All the photons emitted from the LED or the UV tube as calculated as being absorbed at the TiO<sub>2</sub> surface and result in e<sup>-</sup> and h<sup>+</sup>, which further result in generation of OH<sup>•</sup>
2. Each OH<sup>•</sup> generated degrades one molecule of methyl orange
3. The output power of LED and UV tubes calculated is correct

Thus using the energy wavelength relationship, and using the actual input or output power for LEDs or UV tubes, the number of photons per unit time can be calculated as (Stumm and Morgan, 1996):

$$E_{Theoretical} = hc / \lambda \quad [4.4]$$

where,  $E_{Theoretical}$  is the energy of a photon (Watt-sec/photon),  $h$  is Plank's constant ( $6.6 \times 10^{-34}$  W-sec<sup>2</sup>),  $c$  is the velocity of light in vacuum ( $3 \times 10^8$  m/sec) and  $\lambda$  is the wavelength of light (m).

$P_{Actual}$  is the input or output power for LEDs or UV lights. The input power for UV LEDs is straight forward to calculate since it is the current at which they were operated multiplied by the operating voltage. The total input power for LEDs was 1.4 W for UV LED 370 and 6.0 W for UV LED 340, while the output power calculated by linearly increasing the values given in Table 3.1, for UV LED 370 was calculated as 0.04 W and for UV LED 340 as 0.03 W. The input power for each UV tube was 15 W (i.e., 60 W total, Spectronics Corp.), while the output power for a set of two UV tubes radiating a dispersed light (i.e., 320 nm to 400 nm, peak wavelength 365 nm) is  $1100 \mu\text{W}/\text{cm}^2$ , at a distance of 25 cm (Spectronics Corp.). Assuming that the UV tubes radiate light radially with 365 nm as a single wavelength, at 25 cm distance the total output power of two UV tubes would be 7.77 W ( $1100 \mu\text{W}/\text{cm}^2 \times \pi \times 45 \text{ cm} \times 50 \text{ cm}$ , intensity  $\times$  surface area of cylinder of 45 cm length and 25 cm diameter). Thus at a distance of 2.5 cm (i.e., at the column surface) the light intensity would be  $0.011 \text{ W}/\text{cm}^2$  ( $7.77 \text{ W} / \pi \times 45 \text{ cm} \times 5 \text{ cm}$ ). Now, assuming that the column face parallel to the UV tubes receives twice the light that the column faces that are perpendicular to the UV tubes, each face receives 0.275 W (i.e.,  $0.011 \text{ W}/\text{cm}^2 \times 25 \text{ cm length} \times 1 \text{ cm width}$  for each face, same for all faces since top and bottom face are illuminated from both sides). Thus the total exposed output power is 1.1

W. Based on these values, the number of photons per unit time for each type of light source is calculated by Eq. 4.5 and is presented in Table 4.12:

$$N_p = \frac{P_{Actual}}{E_{Theoretical}} \quad [4.5]$$

**Table 4.12. Number of photons for each type of light source for calculating the efficiency of the reactors**

Light source	$E_{Theoretical}$ Watt-sec/photon	$P_{Actual}$ Watt	No. of photons/sec $N_p = P_{Actual}/E_{Theoretical}$	Condition
UV LED 370	$5.4 \times 10^{-19}$	1.4	$2.7 \times 10^{18}$	Input power
	$5.4 \times 10^{-19}$	0.04	$7.4 \times 10^{16}$	Output power
UV LED 340	$5.8 \times 10^{-19}$	6.2	$1.1 \times 10^{19}$	Input power
	$5.8 \times 10^{-19}$	0.03	$5.1 \times 10^{16}$	Output power
UV Tubes	$5.4 \times 10^{-19}$	60	$1.1 \times 10^{20}$	Input power
	$5.4 \times 10^{-19}$	1.1	$2.0 \times 10^{18}$	Output power

Now to find the efficiency based on the assumption that each photon which is radiated from the source results in generation of  $OH^\bullet$ , which in turn results in degradation of one molecule of methyl orange, an equation to represent number of molecules of methyl orange degraded ( $N_M$ ) as a function of time can be given as:

$$N_M = (C - C_0)M_w V_R N_A \quad [4.6]$$

$$N_M = C_0 (1 - \exp^{-kt})M_w V_R N_A \quad [4.7]$$

where,  $C_0$  is the initial concentration of methyl orange (30 mg/L),  $C$  is the concentration of methyl orange at time  $t$  (mg/L),  $M_w$  is the molecular weight of methyl orange (327

g/mol),  $V_R$  is the volume of reactor (10.8 ml),  $A_N$  is the Avogadro's number ( $6.02 \times 10^{23}$  molecules/mole)

Since for both the reactors, an initial concentration around 30 mg/L is used, for the efficiency calculations, an initial concentration of 30 mg/L has been used in the calculations. The number of molecules in the reactor obtained by using equation [4.7] is divided by the number of photons/sec obtained from the ratio of  $P_{Actual}/E_{Theoretical}$  (Table 4.12). Table 4.13 represents efficiencies calculated based on the input and output powers of LEDs and UV tubes. The input and output power for the prototype reactor are 60 W and 1.1 W, respectively. For the portable reactor, the input and output powers are the sum of input and output powers of individual LEDs, which are 7.6 W and 0.07 W, respectively.

**Table 4.13. Input and output efficiencies as a function of time for prototype and portable reactor**

Time t (min)	C-C <sub>0</sub> (mg/L)	Input Efficiency $\eta_I = tN_M/N_P$ (Input Power) (%)	Output Efficiency $\eta_O = tN_M/N_P$ (Output Power) (%)
PROTOTYPE REACTOR			
5	6.5	4.0E-04	2.2E-02
10	11.6	3.6E-04	1.9E-02
15	15.6	3.2E-04	1.7E-02
20	18.7	2.9E-04	1.6E-02
25	21.2	2.6E-04	1.4E-02
30	23.1	2.3E-04	1.3E-02
PORTABLE REACTOR OPERATED AS DIRECT RECIRCULATION			
60	9.7	5.77E-04	6.06E-02
120	16.3	4.88E-04	5.12E-02
180	20.8	4.17E-04	4.37E-02
240	23.8	3.60E-04	3.78E-02
300	25.8	3.14E-04	3.30E-02
360	27.2	2.77E-04	2.90E-02

Using the input and output power and rate constants for the prototype and portable reactors with direct recirculation, ratios comparing the input to output power and rate constants for the two types of light sources are presented in Table 4.14. Looking at the input power ratio for the UV tubes and UV LEDs, it can be seen that the ratio is 8:1, while the output power ratio is 16:1. When this ratio is compared with the ratio of the rate constants for both reactors for methyl orange degradation under identical conditions, the ratio calculated is 8:1. The input to output power ratio for UV tubes (55:1) is higher than that for the UV LED370 (35:1), while UV LED340 has the highest ratio (207:1), corresponding to higher loss of power due to heat conversion. The reason for higher loss of power in heat is the lower wavelength at which the UV LED340 operates (340 nm) and the corresponding lower efficiency.

**Table 4.14. Comparison of powers and rate constants for methyl orange experiments with different UV light sources.**

<b>Relationship</b>	<b>Ratio</b>
Input power to output power for prototype reactor	55:1
Input power to output power for UV LED340	207:1
Input power to output power for UV LED370	35:1
Input power for prototype reactor to portable reactor	8:1
Output power for prototype reactor to portable reactor	16:1
Rate constant for prototype reactor to portable reactor	8:1

From the power output and rate constant ratios, and Table 4.13, it can be said that the LEDs (operating together) are at least twice as efficient as compared to that of the UV tubes. There could be several reasons for this difference, for example: the output is single wavelength for LEDs as compared to dispersed wavelength for UV tubes, resulting in a highly focused beam on a very small area causing fewer photons being absorbed at the surface of TiO<sub>2</sub>. Also, there could be several reasons for the slower removal rate in the

portable PCO reactor as compared to the prototype reactor; (i) the output power ratio is 1:16 for portable to prototype reactor, while the degradation ratio is 1:8. This indicates that the UV LEDs may not be emitting the required number of photons/sec to generate enough  $\text{OH}^\bullet$ , even though the portable reactor is more efficient (Table 4.13), which as per Cho et al. (2003) are the primary species causing *E. coli* degradation. (ii) the other reason that would hinder the degradation rate is that the LEDs are focused over a very small area and thus they concentrate a high number of photons in that area, resulting in concentrated  $e^- - h^+$  pairs, which would further favor higher  $e^- - h^+$  recombination.

Figure 4.19 shows a comparison for methyl orange degradation with two different UV light sources, (i) Prototype reactor, and (ii) Portable reactor operating as a direct recirculating reactor. Both the reactors were operated under identical conditions, i.e., pH =  $6.0 \pm 0.2$ , Ionic Strength =  $1.72 \times 10^{-2}$  M  $\text{NaClO}_4$  and DO saturated with  $\text{O}_2$ . Figure 4.19 show that both the data sets follow first order degradation kinetics with the rate constant ratio equal to 8:1 for prototype to portable reactor. The prototype reactor can be further used as a reference for reaching the required rate constant in the portable reactor.

From the *E. coli* photocatalytic degradation experiment in the portable reactor, 240 min of HRT is required to achieve a 3  $\log_{10}$  removal. From Table 4.12, the number of photons emitted in 240 min by the UV LEDs is  $1.9 \times 10^{23}$  photons. The results of experiments performed by Dunlop et al. (2002) and Cho et al. (2003) indicate that the first order *E. coli* degradation rate increased linearly with increase in light intensity, while Lee et al. (2002) determined a linear relationship for the photon rate ( $\mu\text{E}/\text{sec}$ , measured using potassium ferrioxalate actinometry) as a function of number of UV lamps (6 W, low pressure mercury lamp).

Using the rate constant values for methyl orange degradation in the portable reactor operated under indirect recirculation configuration and extrapolation, the number of additional UV LED370s can be calculated to achieve any required first order methyl orange degradation rate constant. Use of UV LED370 has been selected based on the input to output ratio which is lower (35:1) than that of UV LED340 (207:1).

Table 4.15 shows the rate constants for methyl orange degradation in the portable reactor under indirect recirculation configuration. Using these data and plotting the rate constant ( $\text{hr}^{-1}$ ) as a function of input power (W) as shown in Figure 4.20, a linear relationship between input power and rate constant for methyl orange degradation illuminated by UV LEDs (340 and 370) operating together can be given as:

$$k_c = 0.09P - 0.41 \quad [4.8]$$

where,  $k_c$  is the first order rate constant ( $\text{hr}^{-1}$ ) for combined LEDs and P is the input power for UV LEDs (Watts) with  $R^2$  equal to 0.9378. The relationship for UV LED370 operating alone is given as:

$$k_i = 0.1P \quad [4.9]$$

where,  $k_i$  is the first order rate constant ( $\text{hr}^{-1}$ ) for UV LED370 operating alone and P is the input power for UV LED370 (Watts) with  $R^2$  equal to 0.9207.

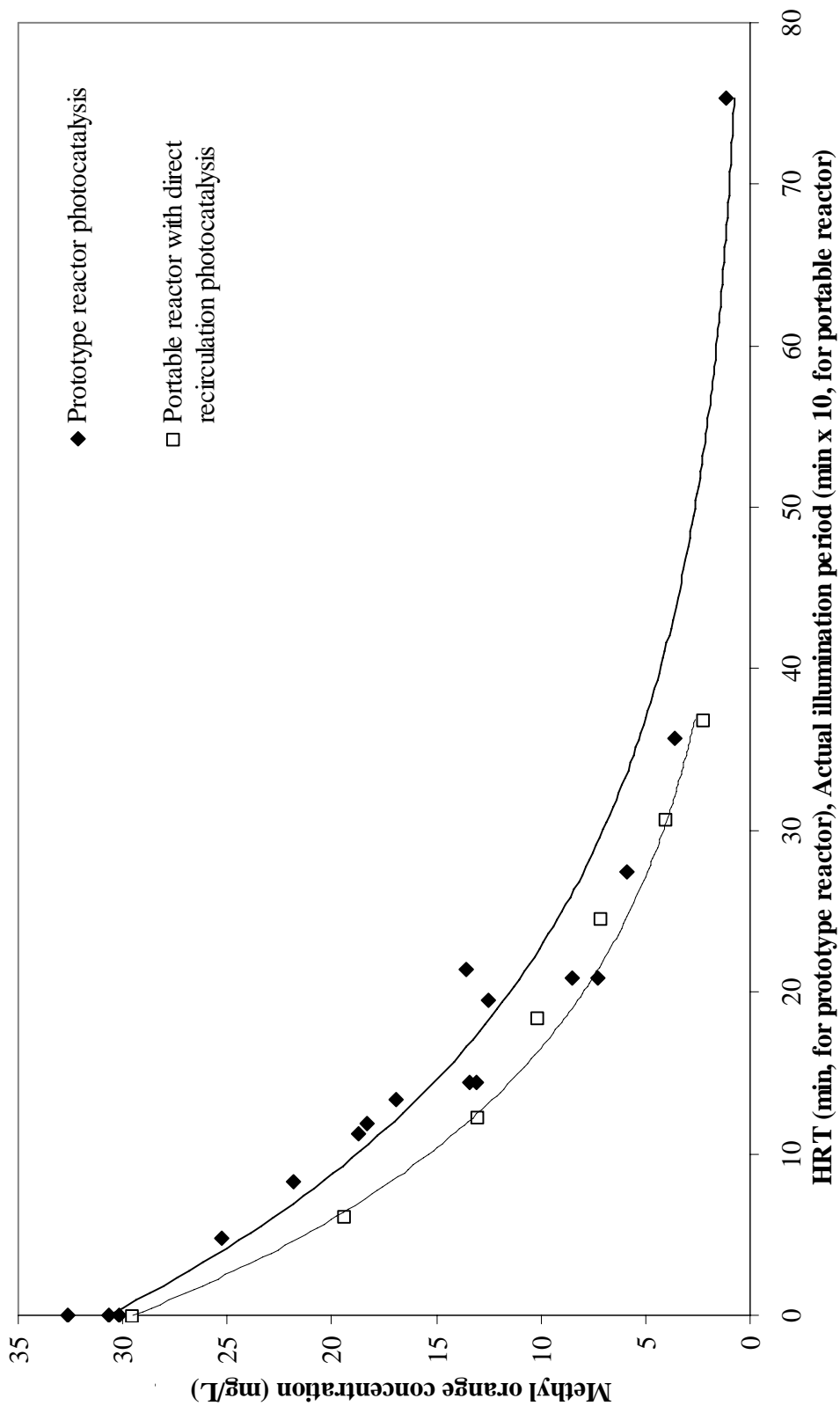
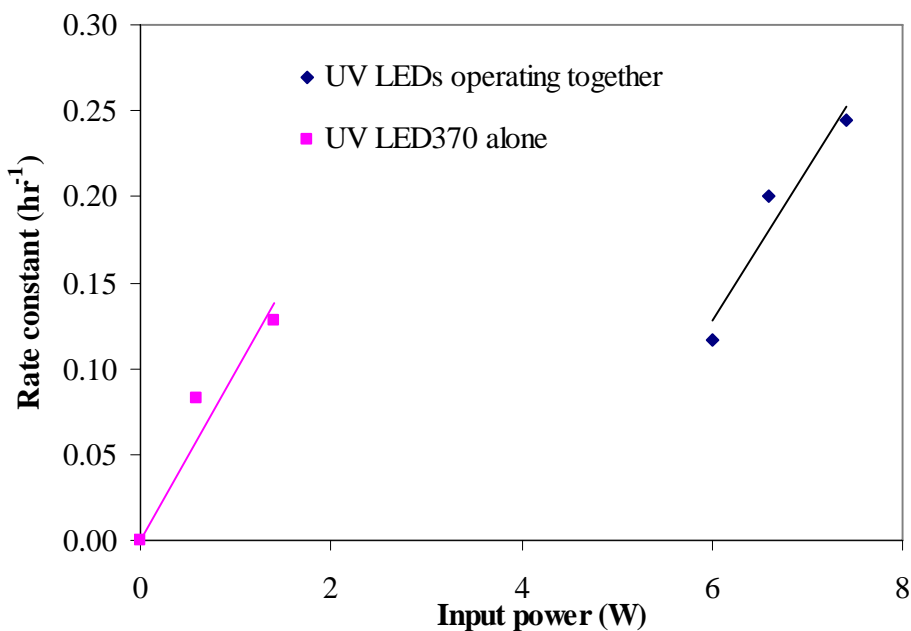


Figure 4.19. Comparison of two reactors with different light sources and power inputs. The HRT (min) on x-axis is for the data of prototype reactor while the illumination time (min x 10) is for the data from the portable reactor

**Table 4.15. Rate constants for methyl orange degradation for portable reactor under indirect recirculation with UV LEDs operated at different input powers. Values in parenthesis represent input powers and rate constants for UV LED370 only.**

Operating conditions	Input power W	Rate constant hr <sup>-1</sup>
12 UV LED340 @ 100 mA each	6.2 (0)	0.12 (0)
12 UV LED340 @ 100 mA + 12 UV LED370 @ 15 mA each	6.8 (0.6)	0.20 (0.08)
12 UV LED340 @ 100 mA + 16 UV LED370 @ 25 mA each	7.6 (1.4)	0.245 (0.12)

From Table 4.14, since UV LED370 are efficient as compared to the UV LED340 in power conversion, using Eq. 4.9, 240 UV LED370's operating at 25 mA each are required to achieve a methyl orange degradation rate of 0.036 min<sup>-1</sup> in a portable reactor operated under indirect recirculation configuration. When the same reactor is operated under direct recirculation the reactor becomes efficient and the rate of methyl orange degradation becomes faster.



**Figure 4.20. First order rate constant for methyl orange degradation in portable reactor operated as indirect recirculation. The rate constant values for UV LED370 operating alone are presented in parenthesis in Table 4.14.**

The ratio of the rate constant for the portable reactor operated under direct recirculation configuration to indirect recirculation configuration remains constant at 1.6 (i.e., 0.39/0.24). Multiplying the rate constant calculated for 240 UV LEDs for the portable reactor operated under indirect recirculation ( $0.036 \text{ min}^{-1}$ ) with the 1.6 factor gives the rate constant for the reactor operated under direct recirculation with 240 UV LEDs, giving  $0.06 \text{ min}^{-1}$ . This degradation rate is fast enough to overcome the flow rate limitations and recirculation can be avoided.

Thus, if the  $0.05 \text{ min}^{-1}$  degradation rate constant for methyl orange in the prototype reactor corresponds to 30 min of HRT for 3  $\log_{10}$  removal of *E. coli*, the  $0.06 \text{ min}^{-1}$  degradation rate constant for methyl orange in portable reactor operated under identical conditions, should result a 3  $\log_{10}$  removal of *E. coli* in 25 min ( $30 \text{ min} \times 0.05 \text{ min}^{-1} / 0.06 \text{ min}^{-1}$ ) of HRT with 240 UV LED370s operating at 25 mA each.

## CHAPTER 5

### CONCLUSIONS AND RECOMMENDATIONS

The increasing concern of providing drinking water for military personnel in hostile areas, even in harshest conditions, and the limited availability of any kind of mobile technology to disinfect water to drinking water standards at low cost led to the current research. The primary goal of this research was to design and construct a portable PCO water decontamination unit to maximize the integration of  $\text{TiO}_2$  into a columnar reactor with UV light emitting diodes (LEDs). The secondary goal was to examine the removal of microbial pathogens (*E. coli*) from unsanitary water conditions using the designed reactor. Even though the use of UV light (254 nm to 375 nm range) has been shown to drive  $\text{TiO}_2$  photocatalysis, the use of UV LEDs with wavelength 340 nm and 370 nm as light sources for  $\text{TiO}_2$  photocatalysis has not been proven to decontaminate drinking water. The entire project was divided into three phases – immobilization of  $\text{TiO}_2$  onto glass beads, optimization of the  $\text{TiO}_2$  coating method and reactor using prototype reactor and design, and construction and testing of the portable reactor for water decontamination. All the objectives were met and the specifics of the conclusions are listed below.

$\text{TiO}_2$  was immobilized on to glass beads by two different methods, the suspension method and the ceramic funnel method with and without etching. The ceramic funnel method reduced the overall coating time to less than 3 hrs as compared to the suspension method which take 24 hrs for coating one layer. Etching the coated glass beads with 0.1 N HCl roughened the catalyst surface and remove any loosely bound  $\text{TiO}_2$ .

Formaldehyde was used as a test pollutant for initial photocatalytic experiments but due to the complex measurement procedure methyl orange was used as the test pollutant for optimizing the reactors (prototype and portable) with experimental conditions,  $\text{pH} = 6.0 \pm 0.2$ , ionic strength =  $1.7 \times 10^{-2}$  M  $\text{NaClO}_4$  and saturated DO, while, *E. coli* was used as a test microbial pathogen for disinfection experiments with  $\text{pH} = 7.0 \pm 0.2$  being the only change in experimental condition.

ESEM micrographs indicated that the coating methods were successful in uniformly coating  $\text{TiO}_2$  onto the glass beads having varying thickness with  $9.9 \mu\text{m}$  as maximum. Due to the supplemental P25 powder the BET surface area increased by a factor of 55 over uncoated glass beads as compared to the increased surface area by factor of 18 without supplemental P25. Further analysis of the coated  $\text{TiO}_2$  mass revealed that the thickness calculated from the mass of coated  $\text{TiO}_2$  was  $2.0 \pm 0.1 \mu\text{m}$ , which supports the ESEM micrograph (Figure 4.6.b) indicating varying thickness. X-ray diffraction analysis for the powder form of  $\text{TiO}_2$  prepared by *Mixture C* and *Mixture F* was dominated by the anatase phase as expected. The calculations for the mass of  $\text{TiO}_2$  coated onto the glass beads resulted in  $3.1 \times 10^{-5}$  g of  $\text{TiO}_2/\text{bead}$  loaded in the column with  $13.1 \text{ m}^2$  as the total catalyst contact surface area in the column.

Due to operating troubles and low catalyst efficiency, optimization of the reactor by changing the configuration from vertical to horizontal reduced failures of column joints and use of a quartz square column resulted in increase in column surface area for higher illumination. Using new sol gel supplemented with  $\text{TiO}_2$  powder to increase the BET surface area was incorporated. Methyl orange degradation for glass beads coated with *Mixture C* by *Method 2* and with *Mixture F* by *Method 3* followed a first order

kinetics with rate constants equal to  $0.018 \text{ min}^{-1}$  and  $0.049 \text{ min}^{-1}$  and  $R^2$  values of 0.9754 and 0.9243, respectively. Thus the increase in rate constant can be attributed to the increased surface area due to the supplemental  $\text{TiO}_2$  added in *Mixture F* and not due to the higher photocatalytic activity of Degussa P25. The increase in surface area is almost linear to the increase in degradation rate (i.e., BET surface area increases by a factor of 3.0 while rate constant increases by a factor of 2.7). The consistency of the coating method was also analyzed by running three different experiments under identical conditions and the data was linearized to calculate a combined rate constant of  $0.05 \text{ min}^{-1}$  with the  $R^2$  value of 0.9248.

After initial design failure using lenses for the construction of the portable reactor, the LEDs were focused directly on the quartz column to achieve maximum illumination. Due to the flow rate limitations the reactor was designed as an indirect recirculation reactor to re-saturate the effluent with DO but since doing so resulted in loss of sample due to evaporation, a direct recirculation reactor was designed. The portable reactor operated in direct recirculation mode (rate constant equal to  $0.39 \text{ hr}^{-1}$  with  $R^2$  value of 0.9815) was more efficient (i.e., by a factor of 1.6) in degrading methyl orange as compared to the indirect recirculation mode (rate constant equal to  $0.24 \text{ hr}^{-1}$  with  $R^2$  value of 0.9418 ).

The results for *E. coli* photocatalytic degradation experiments in the prototype reactor indicated that *E. coli* degradation followed first order degradation kinetics but only after a 10 min lag period. The damage to the cell wall occurs initially with reactive oxygen species (ROS) attack and subsequently peroxidation of the *E. coli* occurs (Kuhn et al. 2003). *E. coli* with damaged cell walls can possibly re-grow and thus result in an

initial lag period. The rate constant for the prototype reactor was calculated to be  $0.29 \text{ min}^{-1}$  and a  $3 \log_{10}$  removal was achieved in 30 mins. Due to inconsistent results for the control experiments in the direct recirculating portable reactor, separate batch experiments in quartz cuvettes were performed. Two sets of experiments were performed which showed that a  $3 \log_{10}$  *E. coli* removal was achieved in 240 mins.

When the two reactors are compared, i.e., prototype and portable reactor with direct recirculation based on the input power, output power and degradation of methyl orange based on first order kinetics, the portable reactor using LEDs as light source was found to be more efficient by a factor of 3 based on output efficiency. When the results of the portable reactor are linearly extrapolated and two different types of LEDs are considered to result in a first order methyl orange degradation, 240 LEDs (UV LED370, 24 pairs with 4 LEDs in series operated at 25 mA each) are required to achieve a  $0.06 \text{ min}^{-1}$  methyl orange degradation rate in the portable reactor with an input power of 21.6 W, and thus eliminating the need of recycling the effluent. Thus, if the  $0.05 \text{ min}^{-1}$  degradation rate constant for methyl orange in prototype reactor corresponds to 30 min of HRT for  $3 \log_{10}$  removal of *E. coli*, the  $0.06 \text{ min}^{-1}$  degradation rate constant for methyl orange in portable reactor operated under identical conditions as prototype reactor should result a  $3 \log_{10}$  removal of *E. coli* in 25 mins of HRT.

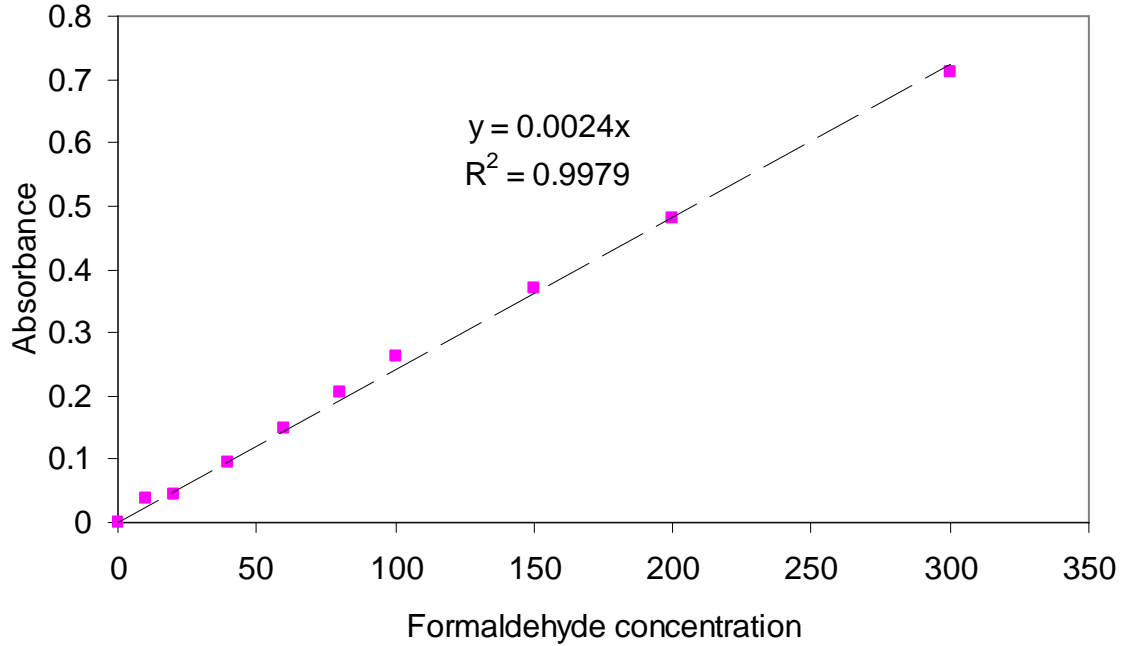
The main scope of the research was to determine whether the LEDs can be used as viable light source for PCO. The promising results of methyl orange degradation and *E. coli* deactivation for the PCO reactor operated with LEDs as light source and the interpretations made will help in further for the development of efficient and low cost

photocatalytic technology. The outcome of current project garners support for use of LEDs as light source in PCO.

Further research should be directed in evaluation of using different types of transition metals like copper, iron, vanadium, silver, platinum and many more as dopants to broaden the adsorption spectra of TiO<sub>2</sub> (Sokmen et al., 2001; Sakthivel et al. 2002; Yu et al. 2002; Zhao et al. 2004; Hou et al. 2006). Also the use of LEDs with higher wall power efficiency (i.e., ratio of output/input power) will result in low power loss due to heat as seen for UV LED370 (1:35) as compared to the UV LED340 (1:207). With higher wall power efficiency, greater number of photons can be delivered to the catalyst surface at low input power, resulting in higher photocatalytic efficiency. Testing the photocatalytic efficiency for different experimental conditions like pH, temperature (for extreme conditions), ionic strength (for brackish water to rain water), DO and turbidity of water (reduce the transmission of light through reactor and higher turbidity can clog the packed bed). Finally, evaluating the disinfection efficiency for pathogens other than *E. coli* is very important, since with the increase or decrease in complexity and density of cell wall the photocatalytic efficiency would also decrease or increase, respectively (Ibanez et al. 2003; Kuhn et al. 2003). Benefit – cost analysis would help in promoting the use of LEDs in PCO as a light source and waiting for the LED technology to develop further will result in reduced cost of LEDs.

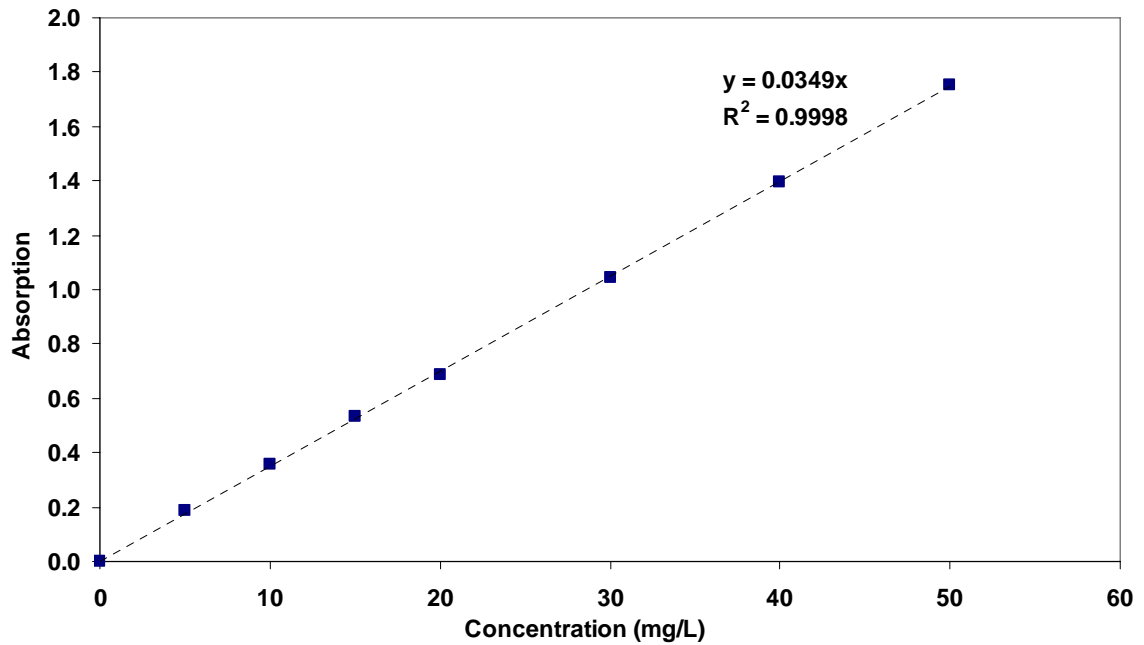
## APPENDIX

### APPENDIX A. Formaldehyde calibration curve using colorimetric method



Formaldehyde calibration curve using Nash reagent at  $\text{pH} = 5.0 \pm 0.2$ , measured at 415 nm wavelength

### APPENDIX B. Methyl orange calibration curve using colorimetric method



Methyl orange calibration curve at  $\text{pH} = 6.0 \pm 0.2$  measured at 510 nm wavelength.

**APPENDIX C.**

**(a) Table for Calculations for TiO<sub>2</sub> coated on glass beads**

Number of Beads	Mass of GB	Mass/bead (g/bead)	Number of Beads	Mass of GB with TiO <sub>2</sub> +Sol	Mass/bead (g/bead)
50	0.0924	0.001848	50	0.0955	0.00191
100	0.1834	0.00182	100	0.184	0.00177
150		0.001783	150		
200	0.3617		200	0.3629	0.001789
250		0.001756	250		0.001813
300	0.5373		300	0.5442	
350		0.001826	350		0.001816
400	0.7199		400	0.7258	
450		0.001817	450		0.001872
500	0.9016		500	0.913	
600	1.0813	0.001797	600	1.1054	0.001924
650	1.1754	0.001882	650	1.1995	0.001882
	Average	0.001816			0.001847
	Standard deviation	0.000036			0.000054
				Difference	
	min	0.001780		0.000031	0.001793
	max	0.001852		0.000017	0.001901

**(b) Table for calculating thickness of coating**

TiO <sub>2</sub> /g of bead = Difference in average value		
3.0875E-05		
Number of beads = Mass of beads/difference		
25205	±1005	
density of TiO <sub>2</sub> g/mm <sup>3</sup>		
0.004		
Volume of TiO <sub>2</sub> mm <sup>3</sup> /bead = TiO <sub>2</sub> /g of bead / density		
0.00771875		
New bead volume (V) = Uncoated bead volume + volume of TiO <sub>2</sub> on bead		
0.704275417		
New Diameter D <sub>C</sub> = (V x 4/π) <sup>1/3</sup>		
1.345749204		
1.104037297		
Thickness of coating x 2 = New diameter - uncoated diameter		0.0040373
Thickness in mm		0.00201865
Thickness in μm		
<b>2.01864838</b>		

**APPENDIX D. Table for calculating flow rate and hydraulic retention time**

Mass of beads	Volume of reactor	Total Length of reactor	Total volume of beads	Net Length of Reactor
g	ml	cm	ml	cm
46	30	30	17.41	26.7
46	30	30	17.41	15.6
Net mass of beads	Actual Volume of beads	Net volume of reactor	Available Volume	
g	ml	ml	ml	
40.25	15.23	26.25	11.02	
23.58	8.92	15.38	6.45	

**APPENDIX E. Table to find number of photons emitted by UV light sources**

$E=hc/\lambda$	$h$ is planks constant = $4.1 \text{ E-}15 \text{ eV-sec}$
	$c$ is velocity of light in vaccum = $3 \times 10^8 \text{ m/s}$
	$1\text{eV} = 1.60218\text{E-}19 \text{ W-sec}$
	$\lambda$ = wavelength of light in m

60W tubes intensity = $2200 \mu\text{W}/\text{cm}^2 = 2.20\text{E-}03$ (at 25 cm, given)			
60W tubes intensity = $22 \text{ m}\mu\text{W}/\text{cm}^2$ (at 2.5 cm)			
4 lights	<b>0.022</b>	<b>W/cm<sup>2</sup></b>	
2 lights	<b>0.011</b>	<b>W/cm<sup>2</sup></b>	
Face area of column = $1\text{cm} \times 25 \text{ cm}$			
Power on one column face $P = 0.011 \text{ W}/\text{cm}^2 \times 1 \text{ cm} \times 25 \text{ cm} = 0.275 \text{ W}$			
On top and bottom face $\frac{1}{2}$ light intensity as compared to column face facing UV lights but receive light from both sides so take $2P_{1/2} = P$			
Total power on all 4 faces = $P + P + 2P_{1/2}(\text{Top}) + 2 P_{1/2}(\text{Bottom}) = 0.275 \times 4 = 1.1 \text{ W}$			

$\lambda$	c	h	$E = hc/\lambda$	P actual	Condition	No. of Photons/sec
m	m/sec	W-sec <sup>2</sup>	W - sec/photon	W		=E/Pactual
3.7E-07	3.0E+08	6.6E-34	5.4E-19	1.4	Input	<b>2.7E+18</b>
3.7E-07	3.0E+08	6.6E-34	5.4E-19	0.04	Output	<b>7.4E+16</b>
3.4E-07	3.0E+08	6.6E-34	5.8E-19	6.2	Input	<b>1.1E+19</b>
3.4E-07	3.0E+08	6.6E-34	5.8E-19	0.03	Output	<b>5.1E+16</b>
3.7E-07	3.0E+08	6.6E-34	5.4E-19	60	Input	<b>1.1E+20</b>
3.7E-07	3.0E+08	6.6E-34	5.4E-19	1.1	Output	<b>2.0E+18</b>

**APPENDIX F. Methyl orange experimental data for prototype reactor**

**(a) For Mixture C & Method 2, Batch 1**

Flow Rate	HRT	Influent	Effluent	C/Co
ml/min	min	mg/L	mg/L	
	0	31.3	31.3	1.00
2.50	4.3	31.3	28.9	0.92
0.91	11.9	31.3	23.9	0.77
0.50	21.6	31.3	21.6	0.69
0.50	21.6	31.3	20.8	0.66
0.45	24.0	31.3	19.7	0.63
0.45	24.0	31.3	19.1	0.61
0.20	54.0	31.3	12.7	0.41

**Batch 2**

Flow Rate	HRT	Influent	Effluent	C/C0
ml/min	min	mg/L	mg/L	
0	0.0	20.3	20.32	1.00
1.47	7.4	20.3	17.5	0.86
1.32	8.2	20.3	17.2	0.84
0.53	20.6	20.5	13.6	0.66
0.53	20.6	20.5	13.8	0.67
0.47	23.0	20.5	12.6	0.62
0.47	23.0	20.5	12.2	0.60
0.15	71.3	20.3	7.2	0.36

**(b) For Mixture D and Method 3**

Flow Rate	HRT	Influent	Effluent	C/C <sub>0</sub>
ml/min	min	mg/L	mg/L	
0.00	0	32.7	32.7	1.00
0.96	11.2	32.7	21.9	0.67
0.96	11.2	32.7	18.7	0.57
0.75	14.4	32.7	13.1	0.40
0.75	14.4	32.7	13.4	0.41
0.52	20.9	32.7	7.2	0.22
0.52	20.9	32.7	8.5	0.26

**(c) For Mixture E and Method 3**

Flow Rate	HRT	Influent	Effluent	C/C <sub>0</sub>
ml/min	min	mg/L	mg/L	
0.00	0	28.9	28.9	1.00
0.81	13.3	28.9	16.0	0.55
0.81	13.3	28.9	15.9	0.55
0.41	26.6	28.9	6.3	0.22
0.41	26.6	28.9	6.3	0.22

**(d) For Mixture F and Method 3 – Batch 1**

Flow Rate	HRT	Conc.	%Deg	Log (C/C <sub>0</sub> )
ml/min	min	mg/L	-	-
-	0	30.7	0	0.0
2.22	5	25.3	18	-0.1
0.9	12	18.3	40	-0.2
0.55	19	12.5	59	-0.4
0.39	27	5.9	81	-0.7
0.3	36	3.6	88	-0.9
0.142	75	1.1	96	-1.4

**Batch 2**

Flow Rate	HRT	Conc.	%Deg	Log (C/C <sub>0</sub> )
ml/min	min	mg/L	-	-
-	0	30.2	0	0.00
1.3	8	21.9	29	-0.14
0.8	13	16.9	45	-0.25
0.5	21	13.5	56	-0.35

**Batch 3**

Flow Rate	HRT	Influent conc	Effluent	Log (C/C <sub>0</sub> )
ml/min	min	mg/L	mg/L	
0.00	0	32.7	32.7	0.00
0.96	11	32.7	21.9	-0.17
0.96	11	32.7	18.7	-0.24
0.75	14	32.7	13.1	-0.40
0.75	14	32.7	13.4	-0.39
0.52	21	32.7	7.2	-0.65
0.52	21	32.7	8.5	-0.58

**(e) For: Mixture F and Method 3, beads used once for photocatalysis experiment, washed and reused.**

Flow Rate ml/min	HRT min	Concentration (mg/L)	C/C <sub>0</sub>
	0.0	28	1.0
1.54	7.0	24.9	0.9
0.54	20.0	16.9	0.6
0.41	26.3	14.6	0.5
0.31	35.0	10.3	0.4

**APPENDIX G. Methyl orange experiments for portable reactor**

**Actual illumination period = (Experiment time x Volume of sample illuminated) / Total volume of the sample running through the reactor**

**(a) For indirect recirculation**

12 led's operating at 340 nm 100 mA each and 15V total 6 on each sides 6.5 inch of length covered 4 parallel circuits each with 3 in series	Influent (mg/L)	Effluent (mg/L)	Experiment period (h)	Actual Illumination Period (h)	C/C <sub>0</sub>
	32.7	32.7	0	0.0	1.00
	32.7	29.3	6	1.8	0.90
	32.7	26.6	7	2.1	0.82
	33.5	27.2	8	2.3	0.81
	34.9	27.4	10	2.9	0.79

12 led's operating at 340 nm 100 mA each 6 on each sides 6.5 inch of length covered	Influent (mg/L)	Effluent (mg/L)	Experiment period (h)	Actual Illumination Period (h)	C/C <sub>0</sub>
	16.3	16.3	0	0.0	1.00
	16.3	13.8	6	1.8	0.85
	16.3	11.9	8	2.3	0.73
	16.3	11.7	10	2.9	0.72

12 led's operating at 100 mA each 6 on each sides 6.5 inch of length covered 12 LED's 370 nm wavelength at 15 mA 4 led's in series with 3 in parallel	Influent (mg/L)	Effluent (mg/L)	Experiment period (h)	Actual Illumination Period (h)	C/C <sub>0</sub>
	16.3	16.3	0	0.0	1.00
	16.3	11.9	6	1.8	0.73
	16.3	10.1	8	2.3	0.62
	16.3	8.9	10	2.9	0.55

**(b) For indirect recirculation with 12 led's operating at 100 mA each 6 on each sides 6.5 inch of length covered 16 LED's 370nm wavelength at 25mA 4 led's in series with 3 in parallel**

Experiment time	Actual illumination period	Actual illumination period	Conc.	C/Co
hr	hr	minx 10	mg/L	-
0	0.0	0	30.7	1.00
10	2.9	18	17.1	0.56
15	4.4	26	12.9	0.42
20	5.9	35	9.3	0.30
25	7.3	44	5.2	0.17

30	8.8	53	2.6	0.08
35	10.3	62	0.3	0.01
40	11.7	70	0.2	0.01

**(c) For direct recirculation with 12 led's operating at 100 mA each 6 on each sides 6.5 inch of length covered 16 LED's 370nm wavelength at 25mA 4 led's in series with 3 in parallel**

HRT	Actual HRT	Actual HRT	Conc.	C/Co
hr	hr	minx 10	mg/L	-
0	0.0	0	29.5	1.00
2.5	1.0	6	19.4	0.66
5	2.1	12	13.0	0.44
7.5	3.1	18	10.1	0.34
10	4.1	25	7.1	0.24
12.5	5.1	31	4.0	0.13
15	6.2	37	2.2	0.07

**(d) Doping With 0.5 g PbCl<sub>2</sub> added to Mixture C**

12 led's operating at 100 mA each 6 on each sides 6.5 inch of length covered 12 LED's 370nm wavelength at 15mA 4 led's in series with 3 in parallel.	Influent (mg/L)	Effluent (mg/L)	Experiment period (h)	Actual Illumination Period (h)	C/Co
	0	15.2	0.0	0.0	0.00
	15.2	8.1	6.0	1.8	-0.63
	15.2	4.6	8.0	2.3	-1.20
	15.2	3.4	10.0	2.9	-1.49
12 led's operating at 100 mA each 6 on each sides 6.5 inch of length covered 8 LED's 370nm wavelength on two sides at 20mA 4 led's in series with 4 in parallel.	Influent (mg/L)	Effluent (mg/L)	Experiment period (h)	Actual Illumination Period (h)	C/Co
	0	15.2	0.0	0.0	0.00
	15.2	8.1	6.0	1.8	-0.63
	15.1	7.0	8.0	2.3	-0.77
	15.2	4.1	10.0	2.9	-1.30

**APPENDIX H. *E. coli* experimental data for prototype reactor**

**(a) Dark control with glass beads coated by Mixture F and Method 3**

Flow Rate (ml/min)	HRT (min)	Initial Count (CFU/100 ml)	Final Count (CFU/100 ml)	C/Co	Log (C/Co)
0.40	27	2.20E+05	1.50E+05		
		2.80E+05	3.00E+05		
		<b>2.50E+05</b>	<b>2.25E+05</b>	9.00E-01	-0.05
0.42	25.7	9.50E+05	8.50E+05		

		1.10E+06	8.00E+05		
		<b>1.03E+06</b>	<b>8.25E+05</b>	8.05E-01	-0.09
		9.50E+05	6.80E+05		
		1.10E+06	7.20E+05		
0.89	<b>12.1</b>	<b>1.03E+06</b>	<b>7.00E+05</b>	6.83E-01	-0.17

**(b) Light control experiment with UV tubes as light source and uncoated beads packed in column**

Flow Rate (ml/min)	HRT (min)	Initial Count (CFU/100 ml)	Final Count (CFU/100 ml)	C/Co	Log (C/Co)
0.60	18	3.00E+06	5.50E+05		
		4.00E+06	3.50E+05		
	<b>18</b>	<b>3.50E+06</b>	<b>4.50E+05</b>	1.29E-01	-0.89
0.49	22.0	6.00E+06	8.50E+05		
		8.00E+06	8.00E+05		
			9.00E+05		
	<b>22.0</b>	<b>7.00E+06</b>	<b>8.50E+05</b>	1.21E-01	-0.92
0.36	30	3.00E+06	2.00E+05		
		4.00E+06	2.00E+05		
	<b>30</b>	<b>3.50E+06</b>	<b>2.00E+05</b>	5.71E-02	-1.24

**(c) Photocatalysis experiment with UV tubes as light source and glass beads coated with Mixture C and Method 2**

Flow Rate (ml/min)	Hydraulic Retention Time (min)	Initial Count (CFU/100 ml)	Final Count (CFU/100 ml)	Log(C/Co)
ml/min	min	CFU/100 ml	CFU/100 ml	
0.37	29	2.0E+05	1.3E+04	-1.2
0.37	29	2.0E+05	1.1E+04	-1.3
0.37	29	2.0E+05	1.8E+04	-1.0
0.33	32	2.5E+06	7.5E+04	-1.5
0.33	32	2.5E+06	1.3E+05	-1.3
0.33	32	2.5E+06	2.0E+05	-1.1
0.33	32	2.5E+06	2.0E+05	-1.1
0.31	34	1.9E+05	8.4E+03	-1.4
0.31	34	1.9E+05	7.8E+03	-1.4
0.31	34	1.9E+05	8.5E+03	-1.3
0.31	34	1.9E+05	9.0E+03	-1.3
0.3	35	1.3E+06	6.8E+04	-1.3
0.3	35	1.3E+06	7.0E+04	-1.3

0.3	35	4.0E+06	2.1E+04	-2.3
0.3	35	4.0E+06	2.2E+04	-2.3

**(d) Photocatalysis experiment with UV tubes as light source and glass beads coated with Mixture F and Method 3**

Flow Rate (ml/min)	HRT (min)	Initial Count (CFU/100 ml)	Final Count (CFU/100 ml)	C/Co	Log (C/Co)
0.86	12.5	2.60E+06	1.00E+06		
		2.80E+06	7.50E+05		
		2.70E+06	8.75E+05	3.24E-01	-0.49
0.71	15.2	8.30E+06	1.50E+06		
		8.70E+06	1.65E+06		
		8.50E+06	1.58E+06	1.85E-01	-0.73
0.55	19.5	3.50E+06	2.00E+04		
		4.50E+06	3.00E+04		
		4.00E+06	2.50E+04	6.25E-03	-2.20
0.46	23.3	3.00E+06	1.00E+04		
		5.00E+06	1.20E+04		
		4.00E+06	1.10E+04	2.75E-03	-2.56
0.42	26.0	1.40E+07	3.00E+04		
		1.20E+07	5.00E+04		
		1.30E+07	4.00E+04	3.08E-03	-2.51
0.41	27.0	3.00E+06	4.00E+03		
		5.00E+06	5.00E+03		
		4.00E+06	4.50E+03	1.13E-03	-2.95
0.35	30.9	1.10E+07	1.50E+04		
		1.30E+07	1.20E+04		
		1.20E+07	1.35E+04	1.13E-03	-2.95
0.34	32.0	5.60E+05	5.00E+02		
		6.00E+05	7.00E+02		
			6.50E+02		
		5.80E+05	6.17E+02	1.06E-03	-2.97
0.25	43.2	1.10E+07	3.40E+02		
		1.40E+07			
		1.25E+07	3.40E+02	2.72E-05	-4.57

**(e) Photocatalysis for *E. coli* in portable reactor with UV LEDs as light source and glass beads coated by Mixture F and Method 3**

<b>Illumination time</b>	<b>Initial Count</b>	<b>Final Count</b>	<b>C/Co</b>	<b>Log (C/Co)</b>	
min	CFU/100ml	CFU/100ml			
300	7.00E+06	4.00E+06	<b>5.17E-01</b>	<b>-0.29</b>	NATURAL DECAY
	7.50E+06	3.50E+06			
	<b>7.3E+06</b>	<b>3.8E+06</b>			
300	1.30E+07	5.50E+06	<b>5.37E-01</b>	<b>-0.27</b>	
	1.40E+07	9.00E+06			
	<b>1.4E+07</b>	<b>7.3E+06</b>			
300	7.0E+06	1.1E+06	<b>1.53E-01</b>	<b>-0.81</b>	Dark Controls
	8.0E+06	1.2E+06			
	<b>7.5E+06</b>	<b>1.2E+06</b>			
300	7.0E+06	8.0E+05	<b>1.13E-01</b>	<b>-0.95</b>	
	8.0E+06	9.0E+05			
	<b>7.5E+06</b>	<b>8.5E+05</b>			
300	6.0E+06	1.0E+04	<b>3.07E-03</b>	<b>-2.51</b>	Lighted Controls
	8.0E+06	3.3E+04			
	<b>7.0E+06</b>	<b>2.2E+04</b>			
300	6.0E+06	8.0E+04	<b>1.14E-02</b>	<b>-1.94</b>	
	8.0E+06				
	<b>7.0E+06</b>	<b>8.0E+04</b>			
300	4.0E+06	4.0E+02	<b>1.11E-04</b>	<b>-3.95</b>	Photocatalysis
	3.2E+06				
	<b>3.6E+06</b>	<b>4.0E+02</b>			
300	4.0E+06	8.0E+02	<b>2.22E-04</b>	<b>-3.65</b>	
	3.2E+06				
	<b>3.6E+06</b>	<b>8.0E+02</b>			

## REFERENCES

- Addamo, M; Augugliaro, V; Paola, A.Di; Lopez, E.G; Loddo, V; Marci, G; Molinari, R; Palmisano, L; Schiavello, M. (2004) "Preparation, Characterization and Photoactivity of Polycrystalline Nanostructured TiO<sub>2</sub> Catalysts," *J. Phys. Chem. B*, 108;3303-3310.
- Ahn, Y.U; Kim, E.J; Kim, H.T, Hahn, S.H. (2003) "Variation of Structural and Optical Properties of Sol-Gel TiO<sub>2</sub> Thin Films with Catalyst Concentration and Calcination Temperature," *Mater. Lett*, 57;4660-4666.
- Arana, J; Nieto, J.L.M; Melian, J.A.H; Rodriguez, J.M.D; Diaz, O.G; Pena, J.P; Bergasa, O; Alvarez, C; Mendez, J.(2004) "Photocatalytic Degradation of Formaldehyde Containing Wastewater from Veterinarian Laboratories," *Chemosphere*, 55;893-904.
- Bao, N; Feng, X; Yang, Z; Shen, L; Lu, X, (2004) "Highly Efficient Liquid Phase Photooxidation of an Azo Dye Methyl Orange over Novel Nanostructured Porous Titanate Based Fiber of Self Supported Radially Aligned H<sub>2</sub>Ti<sub>8</sub>O<sub>17</sub> 1.5H<sub>2</sub>O Nanorods," *Environ. Sci. Technol*, 38;2729-2736.
- Bideau, M; Claudel, B; Dubien, C; Faure, L; Karzouan, H, (1995) "On the Immobilization of Titanium Dioxide in the Photocatalytic Oxidation of Spent Waters," *J. Photochem. Photobiol. A. Chem*, 91;137-144.
- Blake, D.M; Maness, P.C; Huang, Z; Wolfrum, E.J; Huang, J, (1999) "Application of the Photocatalytic Chemistry of Titanium Dioxide to Disinfection and the Killing of Cancer Cells," *Sep. Purif. Methods* 28;1-50.
- Brown, G.T; Darwent, J.R, (1984) "Methyl Orange as a Probe for Photooxidation Reaction of Colloidal TiO<sub>2</sub>," *J. Phy. Chem*, 88;4955-4959.
- Burnside, S.D; Shklover, V; Barbe, C; Comte, P; Arendse, P; Brooks, P; Gratzel, M, (1998) "Self Organization of TiO<sub>2</sub> Nanoparticles in Thin Films," *Chem. Mater*, 10;2419-2425.
- Chen, D.H; Ye, X; Li, K, (2005) "Oxidation of PCE with a UV LED Photocatalytic Reactor," *Chem. Eng. Technol*, 28;1;95-97.

- Cho, M; Chung, H; Choi, W; Yoon, J, (2003) "Linear Correlation Between Inactivation of E. Coli and OH Radical Concentration in TiO<sub>2</sub> Photocatalytic Disinfection," *Water Res*, 30;1069-1077.
- Degan, G; Tomkiewicz, M, (1993) "TiO<sub>2</sub> Aerogels for Photocatalytic Decontamination of Aquatic Environment," *J. Phy. Chem*, 97;12651-12655.
- Demessie, E.S; Gonzalez, M; Wang, Z.M; Biswas P, (1999) "Synthesizing Alcohols and Ketones by Photoinduced Catalytic Partial Oxidation of Hydrocarbons in TiO<sub>2</sub> Film Reactors Prepared by Three Different Methods," *Ind. Eng. Chem. Res.* 38;3276-3284.
- Dijkstra, .F.J; Budwalda, H; Jong, A.W.F; Michorius, A; Winkelmann, J.G.M; Beenackers, A.A.C.M, (2001) "Experimental Comparison of Three Reactor Designs for Photocatalytic Water Purification," *Chem. Engg. Sci*, 56;547-555.
- Dunlop, P.S.M; Byrne, J.A; Manga, N; Eggins, B.R, (2002) "The Photocatalytic Removal of Bacterial Pollutants from Drinking Water," *J. Photochem. Photobiol. A: Chem.* 148;355-363.
- Eaton. A.D; Clesceri, L.S; Greenberg, A.E, (1995) "Standard Methods for Examination of Water and Wastewater," *American Public Health Association*, Washington D.C.
- Guillard, C; Beaugiraud, C.D; Herrmann, J.M; Jaffrezic, H; Renault, N.J; Lacroix, M, (2002) "Physiochemical Properties and Photocatalytic Activities of TiO<sub>2</sub> Films Prepared by Sol Gel Methods," *App. Catal. B: Env*, 39;331-342.
- Hamid, M.A; Rehman, I, (2003) "Preparation of Titanium Dioxide (TiO<sub>2</sub>) Thin Films by Sol Gel Dip Coating Method," *Malay. J. Chem*, 5;1;86-91.
- Halmann, M.M, (1996) "Photodegradation of Water Pollutants," *CRC Press Inc*, Boca Raton
- Hoffman, M.R; Martin, S.T; Choi, W; Bahnemann, D.W, (1995) "Environmental Applications of Semiconductor Photocatalysis," *Chem. Rev*, 5;69-96.

Hou, X.G; Hao, F.H; Fan, B; Gu, X.N; Wu, X.Y; Lui, A.D, (2006) "Modification of TiO<sub>2</sub> Photocatalytic Films by V<sup>+</sup> Ion Implantation," *Nucl. Instr. And Meth. In Phys. Res. B* 243;99-102.

<http://www.edmundoptics.com>

<http://www.epa.gov>

<http://www.pottersbeads.com>

<http://www.roithner-laser.com>

<http://www.s-et.com>

<http://www.thorlabs.com>

Huang, Z; Maness, P.C; Blake, D.M; Wolfrum, E.J," (2000) "Bactericidal Mode of Titanium Dioxide Photocatalysis," *J. Photochem. Photobiol. A. Chem*, 130;163-170.

Ibanez, J.A; Litter, M.I; Pizarro, R.A, (2003) "Photocatalytic Bactericidal Effect of TiO<sub>2</sub> on *Enterobacter Cloacae*. Comparative Study with Other Gram (-) Bacteria," *J. Photochem. Photobiol. A: Chem*, 157;81-85.

Kato, K, (1993) "Photocatalytic Property of TiO<sub>2</sub>, Anchored on Porous Alumina Ceramic Support by the Alkoxide Method," *J. Ceramic Soc. Japan*, 101;245-249.

Kim, D.J; Hahn, S.H; Oh, S.H; Kim, E.J, (2002a) "Influence of Calcination Temperature on Structural and Optical Properties of TiO<sub>2</sub> Thin Films Prepared by Sol-Gel Dip Coating," *Mater. Lett*, 57;355-360.

Kim, J.K; Choi, H.S; Kim, E; Lee, Y.S; Kim, Y.H; Kim, S.W, (2002b) "Comparative Effects of TiO<sub>2</sub>-Immobilized Photocatalytic Supporters on the Bactericidal Efficiency of a Novel Photoreactor," *Biotech. Lett*, 24;1397-1400.

- Kuhn, K.P; Chaberny, I.F; Massholder, K; Stickler, M; Benz, V.W; Sonntag, H.G; Erdinger; L, (2003) "Disinfection of Surfaces by Photocatalytic Oxidation with Titanium Dioxide and UVA Light," *Chemosphere*, 53;71-77.
- Lee, J.C; Kim, M.S; Kim, B.W, (2002) "Removal of Paraquat Dissolved in a Photoreactor with TiO<sub>2</sub> Immobilized on the Glass Tubes of UV Lamps," *Water Res*, 36;1776-1782.
- Lee, J.H; Kang, M; Choung, S.J; Ogiono, K; Miyata, S; Kim, M.S; Park, J.Y; Kim, J.B, (2004) "The Preparation of TiO<sub>2</sub> Nanometer Photocatalyst Film by a Hydrothermal Method and its Sterilization Performance for *Giardia Lamblia*," *Water Res*, 38;713-719.
- Lee, Y.C; Hong, Y.P; Lee, H.Y; Kim, H; Jung, Y.J; Ko, K.H; Jung, H.S; Hong, K.S, (2003) "Photocatalysis and Hydrophilicity of Doped TiO<sub>2</sub> Thin Films," *J. Colloid and Interface Sci*, 267;127-131.
- Legrini, O; Oliveros, E; Braun, A.M, (1993) "Photochemical Process for Water Treatment," *Chem. Rev*, 93;671-698.
- Lisebigler, A.L; Lu, G; Yates, J.T, Jr, (1995) "Photocatalysis on TiO<sub>2</sub> Surfaces; Principles, Mechanisms, and Selected Results," *Chem. Rev*, 95;735-758.
- Maness, P.C; Smolinski, S; Blake, D.M; Huang, Z; Wolfrum, D.J, Jacoby, W.A, (1999) "Bactericidal Activity of Photocatalytic TiO<sub>2</sub> Reaction: Toward an Understanding of its Killing Mechanism," *App. Env. Microbiol*, 65;9;4094-4098.
- Melian, J.A.H; Rodriguez, J.M.D; Suarez, A.V; Rendon, E.T; Campo, C.V; Arena, J; Pena, J.P, (2000) "The Photocatalytic Disinfection of Urban Waste Waters," *Chemosphere*, 41;323-327.
- Mills, A; Le Hunte, S, (1997) "An Overview of Semiconductor Photocatalysis. *J. Photochem. Photobiol. A. Chem*, 108;1-35.
- Nam, W; Kim, J; Han, G, (2002) "Photocatalytic Oxidation of Methyl Orange in a Three Phase Fluidized Bed Reactor," *Chemosphere*, 47;1019-1024.

- Ohko, Y; Tryk, D.A; Hashimoto, K; Fujishima, A, (1999) "Autoxidation of Acetaldehyde initiated by TiO<sub>2</sub> photocatalysis under weak UV illumination," *J. Phy. Chem. B*, 102; 2699-2704.
- Ollis, D.F, (2000) "Photocatalytic Purification and Remediation of Contaminated Air and Water," *Surface Chem. Catal. Chem*, 3;405-411.
- Oppenlander, T, (2003) "Photochemical Purification of Water and Air," *Wiley-VCH Verlag*, Weinheim
- Ryu, C.S; Kim, M.S; Kim, B.W, (2003) "Photodegradation of Alacholor with the TiO<sub>2</sub> Film Immobilized on the Glass Tube in Aqueous Solution," *Chemosphere* 53;765-771.
- Sakthivel, S; Shankar, M.V; Palanichamy, M; Arabindoo, B; Murugesan, V, (2002) "Photocatalytic decomposition of leather dye. Comparative Study of TiO<sub>2</sub> Supported on Alumina and Glass Beads," *J. Photochem. Photobiol. A. Chem*, 148;153-159.
- Smith, R.V; Erhardt, P.W, (1975) "Nash Determination for Formaldehyde in Presence of Bisulfite" *Anal. Chem*, 47;2462-2464.
- Sokmen, M; Candan, F; Sumer, Z, (2001) "Disinfection of E.coli by the Ag-TiO<sub>2</sub>/UV System: Lipidperoxidation," *J. Photochem. Photobiol. A: Chem*, 143;241-244.
- Stumm, W; Morgan, J.J (1996) "Aquatic Chemistry: Chemical Equilibria and Rates in Natural Environment," *Wiley-Interscience*, New York.
- Sun, D.D; Tay, J.H; Tan, K.M. (2003) "Photocatalytic Degradation of E.coliform in Water," *Water Res*, 37;3452-3462.
- Sunada, K; Kikuchi, Y; Hashimoto, D; Fujishima, A, (1998) "Bactericidal and Detoxification Effects of TiO<sub>2</sub> Thin Film Photocatalyst" *Environ. Sci. Technol*, 32;5;726-728.
- Taguchi, T; Siato, Y; Sarukawa, K; Ohno, T; Matsumara, M, (2003) "Formation of New Crystal Faces on TiO<sub>2</sub> Particles by Treatment with Aqueous HF Solution or Hot Sulfuric Acid," *New J. Chem*. 27;1304-1306.

- Vohra, M.S; Davis, A.P, (2000) "TiO<sub>2</sub> – Assisted Photocatalysis of Lead – EDTA," *Water Res*, 34;3;952-964.
- Watts, R.J; Kong, S; Lee, W, (1992) "Sedimentation and Reuse of Titanium Dioxide: Application to Suspended-Photocatalyst Reactors," *J. Environ. Engg*, 121(10);730-735.
- Wei, C; Lin, W.Y; Zainal, Z; Williams, N.E; Shu, K; Kruzic, A.P; Smith, R.L; Rajeshwar, K, (1994) "Bactericidal Activity of TiO<sub>2</sub> Photocatalyst in Aqueous Media: Towards a Solar-Assisted Water Disinfection System," *Environ. Sci. Technol*, 28;5;934-938.
- Wist, J; Sanabria, J; Dierolf, C; Torres, W; Pulgarin, C. (2002) "Evaluation of Photocatalytic Disinfection of Crude Water for Drinking-Water Production," *J. Photochem. Photobiol. A: Chem*, 147;241-246.
- Wu, K.T; Spencer, H.G. (1998) "Sol Formation Rates in Acid Catalyzed Titanium Isopropoxide Water Reaction in Isopropanol," *J. Non-crystalline Solids*, 226;249-255.
- Yu, J.G; Yu, J.C; Cheng, B; Zhao, X.J. (2002) "Photocatalytic Activity and Characterization of the Sol-Gel Derived Pb-Doped TiO<sub>2</sub> Thin Films," *J. Sol-Gel Sci. Tech*, 24;1;39-48.
- Zhao, X.F; Meng, X.F; Zhang, Z.H; Liu, L; Jia, D.Z. (2004) "Preparation and Photocatalytic Activity of Pb-Doped TiO<sub>2</sub> Thin Films," *J. Inorg. Mater*, 19;1;140-146.